Scuola Internazionale Superiore di Studi Avanzati

(SISSA)

Department of Neuroscience

Insights in the Regional Distribution and Physiological Role of the Cellular Prion Protein in the Central Nervous System of Mammalian Organisms

Ilaria Poggiolini

A dissertation submitted for the degree of
Doctor of Philosophy
in Functional and Structural Genomics
December 2012

.

Supervisor:	**Prof. Giuseppe Legname, D. Phil.**
External examiners:	**Prof. Roberto Chiesa, Ph.D.**
	Prof. Giampiero Leanza, Ph.D.

“Fairy tales are more than true;
not because they tell us that dragons exist,
but because they tell us that dragons can be beaten.”

— G.K. Chesterton

ABSTRACT

The cellular form of the prion protein (PrP^C) is a sialoglycoprotein ubiquitously expressed in the central nervous system (CNS) of mammalian species along the neurodevelopment and in the adulthood. The PrP^C localization in the brain has attracted interest because of its involvement in fatal neurodegenerative disorders, denoted as transmissible spongiform encephalopathies. In mammals, PrP^C is expressed early in embryogenesis, and in the adulthood it reaches its highest levels in the neurons of the encephalon and spinal cord. The protein is also found at lower levels in glial cells of the CNS, as well as in almost all peripheral cell types. By combining *in situ* hybridization and immunohistochemical techniques, we show the earliest expression of the protein in mouse hippocampus, thalamus and hypothalamus. In particular, specific white matter fiber tracts in mouse CNS (the hippocampal fimbria, the *stria terminalis*, and the *fasciculus retroflexus*) show the highest expression of the protein. To extend our understanding of varying PrP^C expression profiles in different mammals, we carried out a detailed expression analysis of PrP^C distribution along the neurodevelopment of the metatherian South American short-tailed opossum (*Monodelphis domestica*). No naturally occurring prion diseases have been reported yet for this species. Compared with mice, in opossums we detected lower levels of PrP^C in the white matter fiber bundles of the CNS. This result might offer new insights into a possible involvement of PrP^C in the varying susceptibility to prion diseases for different mammals.

The different distribution of PrP^C in the hippocampal layers of mammals led us to hypothesize a different physiological relevance of PrP^C in this region. To better understand this issue, we used PrP knock-out mice, in which PrP^C is not expressed in the hippocampal strata. We observed that the absence of PrP^C impairs the signaling pathway promoted by Reelin, a protein of the extracellular matrix expressed in the *stratum lacunosum molecolare* and hippocampus of the early postnatal mouse. Overall, our findings suggest a possible role for PrP^C in the modulation of the events triggered by the Reelin-signaling pathway in the developmental mouse hippocampus.

ACKNOWLEDGEMENTS

I wish to thank Prof. Giuseppe Legname for giving me the opportunity to work in his group. He supported me in my professional growth, teaching me how to manage a research project. Remarkably, he encouraged me to always do a further step, either when I did not see the solution. More important, he motivated me with always new scientific open-mind discussions.

I would like to thank Dr Gabriele Giachin for all the support he provided me and for being part of my life.

I wish to thank Dr. M. Righi for his technical assistance in brain dissections and Mr. A. Tomicich for the image acquisitions in the opossum project.

I wish to thank Erica Sarnataro for the proofreading of my manuscripts.

LIST OF PUBLICATIONS

This thesis reports my own experiments and data analysis performed at SISSA or as a result of joint collaborations.

Benvegnù S., Poggiolini I., Legname G. Neurodevelopmental expression and localization of the cellular prion protein in the central nervous system of the mouse. J Comp Neurol. 2010 Jun 1;518 (11):1879-91.

Author's contribution: performed *the in situ* hybridization experiments, analyzed the data and contributed to the writing of the paper.

Poggiolini I., Legname G., *Monodelphis domestica* partial *Prnp* gene for major prion protein. Deposition date: November 22, 2010. EMBL accession number: FR728385.

Author's contribution: cloning and sequencing of the partial Opossum *Prnp* gene.

Poggiolini I., Legname G., Mapping the Prion Protein Distribution in Marsupials: Insights from Comparing Opossum with Mouse CNS. PLoSOne. 2012; 7(11):e50370. doi: 10.1371/journal.pone.0050370. Epub 2012 Nov 29

Author's contribution: performed all the experiments, analyzed and interpreted the data and co-wrote the paper.

TABLE OF CONTENTS

Chapter One

INTRODUCTION

The cellular form of the prion protein (PrP), PrP^C, is a sialoglycoprotein ubiquitously expressed in the central nervous system (CNS) of a wide range of species, form fish to mammals. Several studies based on physiological abnormalities in PrP-knockout mice or in cells derived from them, have suggested the involvement of PrP^C in a plethora of physiological functions including synaptic plasticity, protection against oxidative stress, cell-adhesion, neuronal excitability and neurite outgrowth and maintenance of white matter. However, the underlying molecular mechanisms have not been fully clarified yet. Mapping the regional distribution of PrP^C in different mammals and analyzing its involvement in physiological pathways may help to decipher the physiological role of PrP^C in the CNS. This study might also contribute to explain the toxic phenotypes observed in prion disorders or transmissible spongiform encephalopathies (TSEs), caused by the conversion of PrP^C into a pathogenic isoform called PrP^{Sc}.

1.1 Biogenesis of PrP^C, the cellular prion protein

The mature form of PrP^C is composed of 209 amino acids (aa) (hereafter in human numbering). NMR spectroscopy studies show a predominantly α-helical folded protein with a C-terminal structured domain from residues 128 to 231 [1] and a flexible disordered N-terminal region including a series of octapeptide repeat units [2,3] enriched in histidine (His) residues, which can bind bivalent metal ions such as copper, zinc and manganese [4].

In the endoplasmatic reticulum (ER) the immature form of PrP undergoes some post-translational modifications. The N-terminal signal peptide (residues 1-22) is removed and a

single disulphide bridge is formed between two cysteines (Cys) in the C-terminal. The subsequent cleavage of a carboxy-terminal signal sequence precedes the attachment of the glycosylphosphatidylinositol (GPI) moiety at residue 230. In mouse PrP^C, two N-linked oligosaccharide chains may also be added to asparagines 180 and 196 (corresponding to Asn181 and Asn197 in human numbering). The protein is then trafficked to the Golgi apparatus where the N-linked oligosaccharides are further processed, thus resulting in modified glycosylation to include complex sugar molecules. Following these modifications, PrP is further trafficked to the cell surface, where it preferentially localizes in the lipid raft fractions via the GPI-anchor [5]. The protein is partially endocytosed via clathrin coated-pits. The subcellular localization and processing of PrP^C may also present different topological isoforms of the protein, namely ^{Ctm}PrP and the ^{Ntm}PrP. The former is believed to span the membrane once, with its highly conserved hydrophobic region in the center of the molecule (residues 111-134) as a transmembrane anchor and the C terminus in the ER lumen. The latter spans the membrane with the same transmembrane segment, but with its N-terminal reversed in the ER lumen [6]. Besides the existence of topological isomers of PrP, it has also been observed that part of the protein is proteolitically cleaved by cellular proteases near amino acid residues 110–111, resulting in N-terminal and C-terminal fragments called N1 and C1, respectively [7].

Both N-linked glycosylation sites in all mammalian PrP genes analyzed to date appeared to be conserved. This hints at a functional significance for this post-translational modification. Indeed, depending on the number of glycosylation sites occupied with oligosaccharide chains, PrP can be unglycosylated, monoglycosylated or diglycosylated.

The internalization of PrP^C is still debated, because either raft/caveolae or caveolae-like endocytosis [8], [9,10] as well as clathrin-dependent endocytosis may be occurring [11], [12]. The constitutive endocytosis of PrP^C by clathrin-coated vesicles seems to be influenced by the interaction of the positively charged N-terminal motif KKRPKP with a transmembrane protein [13]. Major questions remain unanswered as to the physiological regulation of the endocytic cycle of PrP^C. This subject requires further investigations, especially because of its possible involvement in physiological PrP^C-mediated signaling mechanisms.

2. PrP^C structure

High-resolution NMR studies of bacterially expressed recombinant (rec) PrP — a model for PrP^C lacking any post-translational modifications — have revealed a folded C-terminal domain and an N-terminal unstructured region. The PrP globular domain is highly conserved among mammals. It consists of two short β-strands and three α-helices, with a disulfide bond bridging α-helices 2 and 3 [1]. The structure of the globular half of the human PrP^C is identical to that of several other mammals. Notably, despite the low sequence identity between mammalian and non mammalian PrP^C, the structural features of PrP^C are remarkably preserved [14].

2.1. The N-terminal unstructured domain

The flexible and disordered N-terminal half of PrP^C (or NH_2-PrP^C) may be divided into four different domains: a first charged cluster (CC1); the octapeptide repeat (OR); a second charge cluster or CC2; and a hydrophobic domain-termed (HD) (Fig. 1.1). Remarkably, several segments of this flexible region are highly conserved in different mammalian species, suggesting their strong functional significance [15,16].

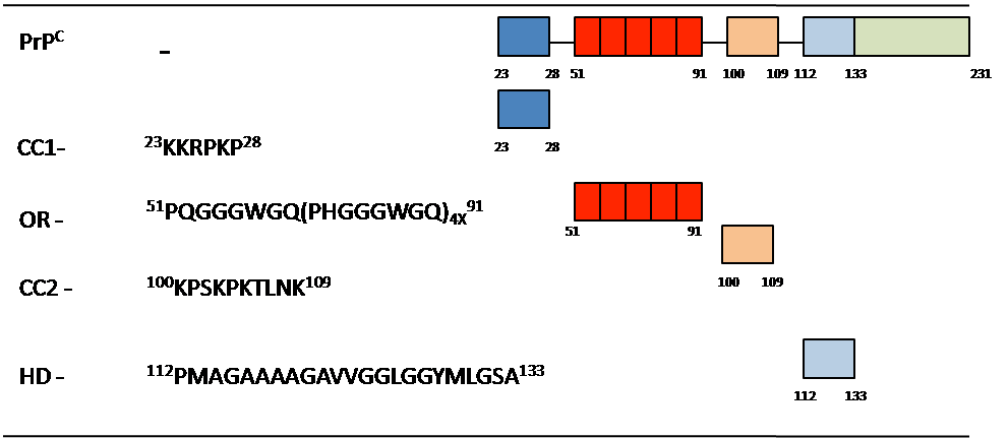

Figure 1.1. The NH_2-PrP^C domains: CC1, OR, CC2 and HD represent the charged cluster 1 (aa 23–28), the octapeptide repeat (aa 51–91), the charged cluster 2 (aa 100–109), and the hydrophobic domain (aa 112–133), respectively.

The presence of an unstructured N-terminal domain qualifies PrP^C as a partially intrinsically unstructured or disordered protein [17]. Intrinsically disordered proteins are characterized by:

1. their function in molecular recognition;
2. their ability to interact with multiple partners including themselves using the same flexible region;
3. their unfolded-to-folded transition upon binding to functional partners [18].

Similarly to other unstructured proteins, PrP^C can bind different ligands. The N-terminal of the recPrP has been shown to bind small unilamellar vesicles containing anionic lipids at pH 7.4 via both electrostatic and hydrophobic interactions [19]. It is also important for nucleic acid binding activity [20]. Furthermore, NH_2-PrP^C has been shown to play a role for several extracellular and transmembrane proteins, namely: stress-inducible protein 1 [21], low-density lipoprotein receptor-related protein 1 [22], neuronal cell adhesion molecules (NCAM) and Aβ oligomers [23]. The binding diversity agrees with PrP^C being involved in different biological processes [24,25]. Many ligands binding to NH_2-PrP^C trigger a rapid internalization of PrP^C, and endocytosis is likely to be an important feature for the physiological function of PrP^C. The combination of binding diversity and ligand-induced

endocytosis supports a role for PrP^C as a broad-spectrum molecular sensor at the cell surface.

2.2. The C-terminal globular domain

The C-terminal domain of PrP^C is characterized by 3 α-helices (H1, H2, H3) and a short, double-stranded, antiparallel ß-sheet (S1, S2) [1]. A disulfide bridge between Cys179 and Cys214 anchors H2 and H3 (Fig 1.2).

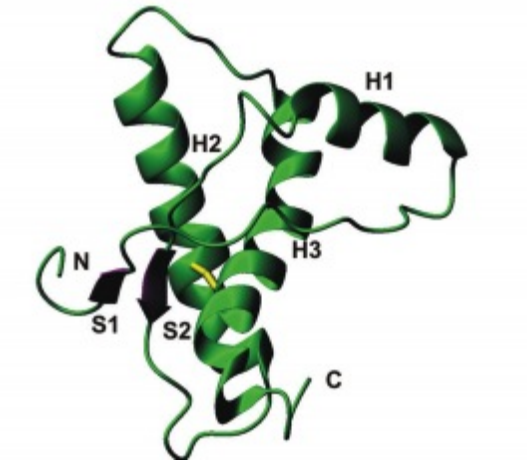

Figure 1.2. Overall fold of PrP^C. Ribbon representation of the C‑terminal structured domain of mouse PrP. The secondary structure elements and the N‑ and C‑termini are labeled. The disulphide bridge is depicted in yellow [Modified from [26]].

The NMR structures of PrP^C from different species have been resolved in an attempt to understanding both the relation to disease-causing mutations and the molecular bases of the so-called specie barrier. Local sequence and structure variations are most prominently localized at the interface between the β_2–α_2 loop (residues 165-175) and in the C-terminal of α_3 helix (residues 215-228) (Figure 1.2). This localization provides insights into these sub-domains of potential importance for pathogenicity and specie barriers to disease

transmission across species. Indeed, while this loop is highly flexible in most species, it shows a well-defined conformation in the PrP structures of Syrian hamster [27], elk [28], bank vole [29], wallaby [30], rabbit [31] and horse [32]. In elk and bank vole PrP, this rigidity was shown to be controlled by a single amino acid substitution, S170N, within the loop, whereas in wallaby, rabbit and horse PrP it correlates with a long-range interaction between residue 166 in the β_2–α_2 loop and residue 225 in the α_3 helix. Different experimental studies suggested that the conformation of the β_2–α_2 loop plays a role in TSE transmission and susceptibility. It has been postulated that mammals carrying a flexible β_2–α_2 loop could be easily infected by prions, whereas prions are not very efficiently transmitted to animals carrying a rigid loop [33]. Notably, horse and rabbit display resistance to prion infections and do not develop spontaneous prion diseases. However, under controlled laboratory conditions, prions are able to adapt and infect species previously believed to be TSE resistant, as was recently reported in rabbits infected by the murine ME7 prion strain using protein misfolding cyclic amplification (PMCA) techniques [34-37]. NMR studies showed that their PrP structures are characterized by a rigid β_2–α_2 loop, and by closer contacts between the loop and α_3 helix. Thus, prion resistance seems to be enciphered by the amino acidic composition of the β_2–α_2 loop, and its long-range interactions with residues in the C-terminal end of α_3 helix [34-37].

3. PrP^C functions in the nervous system

The physiological role of PrP^C is usually disregarded at the expense of its role in TSEs. The high level of PrP^C expression in the CNS and the conserved motifs in its structure suggest that protein may play an important role in cellular function.

3.1. PrP knock-out mice

Molecular cloning of the cDNA encoding the entire open reading frame (ORF) of mouse *Prnp* [38] and the use of homologous recombination has allowed for the generation of mice in which the *Prnp* gene is deleted. All PrP-null animals generated to date have confirmed a tight correlation between the expression of PrP^C and the sensitivity to prion infection. Genetic ablation of PrP^C expression in mice, either prenatally or postnatally, produces relatively little phenotypic effect other than an inability to propagate prions [39].

The first PrP-null mouse strain was generated in a mixed C57BL/6J × 129/Sv(ev) background, by replacing codons 4-187 with a neomycin phosphotransferase (*neo*) expression cassette [40]. These animals, designated $Prnp^{0/0}$ or Zürich I (ZrchI), did not show gross abnormalities in the overall phenotype.

A second line of PrP knock-out mice was produced by interrupting the *Prnp* ORF at position 93 (a Kpn 1 site) and introducing a *neo* cassette [41]. These mice are known as Edinburgh (Edbg) $Prnp^{-/-}$, and are under 129/Ola genetic background. Like the ZrchI, they do not show any developmental alteration.

In sharp contrast with the ZrchI and the Edbg mice, the Nagasaki *Prnp*-ablated mice (Ngsk) develop severe ataxia and Purkinje cell degeneration at advanced ages. In the Ngsk mice, besides the *Prnp* ORF, 0.9 kb of intron 2, 10 bp of the 5'-oncoding region, 0.45 kb of the 3'-noncoding region have also been replaced by the *neo* cassette [42]. Since the observed phenotype is abolished by the reintroduction of *Prnp*, this phenotype was attributed to the absence of PrP^C. The same phenotype has been shown in other knock-out mice such as Rcm0 mice and in Zurich II (ZrchII) mice. In the latter, the *Prnp* ORF, 0.26 kb of intron 2,

10 bp of the 5'-noncoding region, the 3'-noncoding region of exon 3 plus 0.6 kb of the adjacent region were removed [43].

It has been shown that the distinct phenotypes of Ngsk, Rcm0, ZrchII mice are due to the gene deletion approach. In fact it has been shown that ataxia in these animals is caused by overexpression of another protein denominated Doppel (Dpl), a protein encoded by the *Prnd* gene, located at 16 kb downstream of *Prnp*. The ectopic expression of Dpl in ZrchII mice causes ataxia and degeneration of cerebellar granule and Purkinje cells, and its levels are inversely correlated with the onset of the disease [44]. The ectopic expression of Dpl, rather than the deletion of the *Prnp* gene is responsible for neurodegeneration. Notably, the reintroduction of *Prnp* in mice overexpressing Dpl in the brain rescues the phenotype [45]. PrP^C thus counteracts Dpl neurotoxicity, but the mechanism underlying this antagonism is still controversial [46].

3.2. Neurodegeneration in other transgenic mice

Two constructs have been used to generate mice overexpressing PrP^C. The first one was a large cosmid composed of three exons and two introns of the mouse $Prnp^b$ allele (108 Phe, 189 Val). Mice overexpressing PrP^C encoded by this construct develop ataxia, hind limb paralysis, and tremors. The second genetic construct, called *half-genomic* DNA, was derived from the former by deleting intron 2 and replacing exon 3 by the $Prnp^a$ allele (108Leu, 189Thr) and the 18 kb of the 3'-sequence by a 2.2 kb downstream sequence from the $Prnp^a$ locus. Mice carrying the *half-genomic* DNA do not show an obvious phenotype [47]. The half genomic PrP vector was also used to clone deletion mutants of the $Prnp^a$ allele, which were then expressed as transgenes in ZrchI $Prnp^{0/0}$ animals. (Fig 3.1 - modified from [25])

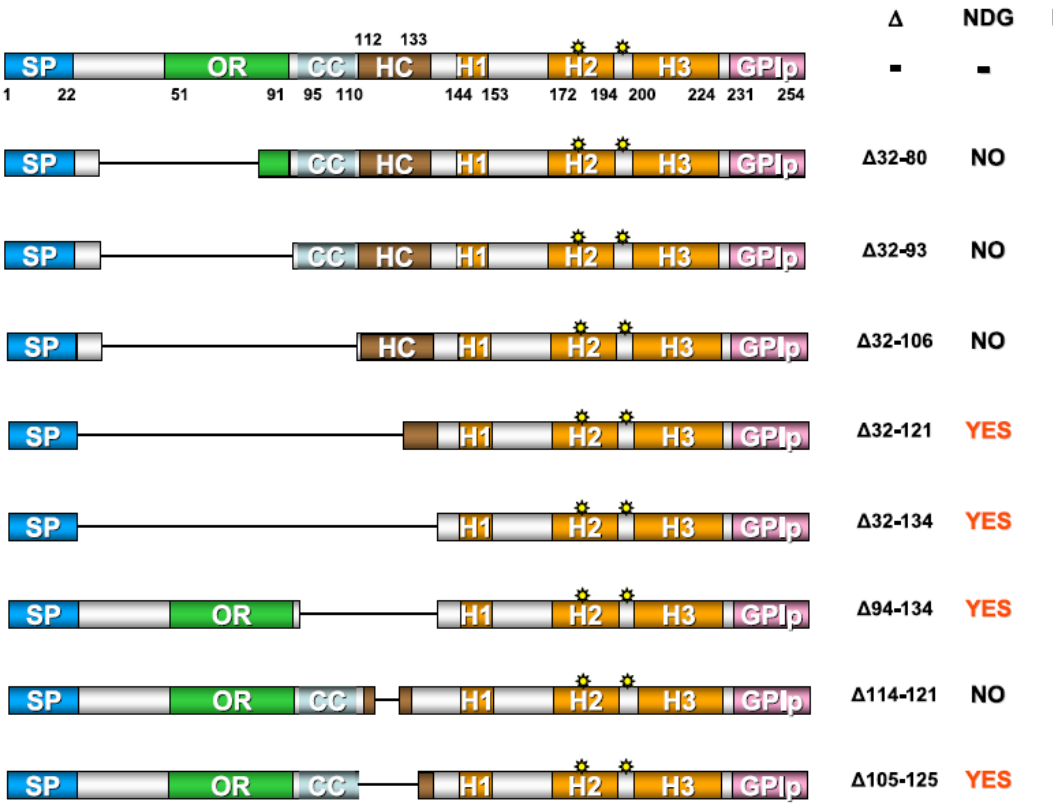

Figure 3.1. PrP^C deletion mutants expressed in *Prnp*$^{0/0}$ mice and their neurodegenerative phenotypes. The wild-type (WT) PrP^C molecule with major domains annotated is shown at the top. Deleted domains are replaced by a solid black line and the deleted amino acids are indicated to the right of each diagram (Δ). The presence or absence of neurodegeneration (NDG) is indicated [25].

It has been shown that deletion of aa 32–121, or 32–134, leads to both severe ataxia and apoptosis in the cerebellum of relatively young animals. This phenotype is rescued by introducing one copy of a WT *Prnp* gene [48].

Mice expressing $PrP_{\Delta 32\text{-}134}$ and mice overexpressing Dpl share a similar phenotype suggesting that the Dpl and $PrP_{\Delta 32\text{-}134}$ may promote the same kind of neurodegeneration. However, overexpression of Dpl leads to massive degeneration of Purkinje cells, whereas $PrP_{\Delta 32\text{-}134}$ causes degeneration in the granule cell layer [42].

Mice expressing Dpl or one of the truncated forms $PrP_{\Delta 32\text{-}121}$ or $PrP_{\Delta 32\text{-}134}$ are characterized by severe demyelination and axon loss in the spinal cord and in the cerebellar white matter.

The oligodendrocyte-specific expression of PrP^C can rescue leukodystrophy but not cerebellar granule cell degeneration [49].

Interestingly, two-week-old mice expressing truncated $PrP_{\Delta 105\text{-}125}$ are characterized by cerebellar atrophy, severe loss of cerebellar granule cells, gliosis and astrocytic hypertrophy. Mice expressing $PrP_{\Delta 94\text{-}134}$ showed a lethal phenotype which was rescued dose-dependently either by WT PrP^C or a PrP^C lacking all octarepeats. Mice with the $PrP_{\Delta 114\text{-}121}$ deletion did not show a particular phenotype and the expression of this smaller mutation ameliorated the phenotype caused by truncated $PrP_{\Delta 32\text{-}134}$ but worsened the degenerative effect of $PrP_{\Delta 94\text{-}134}$. Several mechanisms have been proposed to elucidate how the truncated forms of PrP^C induce degeneration. Baumann et al. suggest that dimers of truncated $PrP_{\Delta 32\text{-}134}$ would trap a putative PrP^C receptor in a dominant-negative form and thus hamper signals for myelin maintenance. The presence of the octarepeat region in the $PrP_{\Delta 94\text{-}134}$ can generate a more stable dominant-negative form of the receptor, leading to a more severe pathology than the truncated $PrP_{\Delta 32\text{-}134}$ [50]. Alternatively, the higher affinity of the truncated $PrP_{\Delta 105\text{-}125}$ compared with that of $PrP_{\Delta 32\text{-}134}$ for a putative PrP^C receptor causes a more severe neurodegeneration. The putative PrP^C receptor may show an altered conformation in presence of the centrally truncated PrP^C leading to neurotoxic signals [51]. Furthermore, in PrP^C null background mice $PrP_{\Delta 105\text{-}125}$ causes cerebellar degeneration [51] whereas $PrP_{\Delta 114\text{-}121}$ does not. This suggests that these two truncated PrP may exert different activities.

3.3. Marsupials as a model organism in prion biology

The sequence identity of PrP^C among mammals suggests an essential physiological role. Defining the function of PrP^C is also a prerequisite for understanding TSEs, or prion diseases, as they are attributed to the post-translational conversion of PrP^C into a misfolded, pathogenic form denoted prion or PrP^{Sc} [52]. A still controversial aspect in TSEs is the different ability of prions to infect some mammalian species and not others. Although it has been recently demonstrated that under forced laboratory conditions rabbits are not resistant to prion infection, so far no naturally occurring TSEs have been reported in rabbit, horse or any marsupial species. A possible explanation for this argues that the PrP^C primary sequence, together with local structural variations within the C-terminal globular domain, might account for prion resistance in different mammals. However, little is known about the regional distribution of PrP^C in the CNS of mammalian species that seem resistant to TSEs. Differences in PrP^C expression in mammalian species, for which no naturally occurring TSE has been reported, may shed new light on different susceptibility to these maladies [33].

Several animals have been used to study neurodegeneration and pathology of the human CNS. For instance, marsupials have been used to investigate developmental white matter damage, a brain pathology associated with several long-term neurological disorders [53].

3.3.1. The *Monodelphis domestica*

The metatherian mammal South American short-tailed opossum (*Monodelphis domestica*) (hereafter Op) has been used as animal model in biomedical research. The laboratory Op is used in a broad range of research programs focused on development, physiology and disease susceptibility. This animal model is used in developmental studies mainly because of the rudimental stage of development of the newborn pups, which resemble 11- or 12-day-old mouse embryos [54,55]. In the newborn Op pup the CNS is still at an embryonic stage [54], because its development is completed during postnatal life, thus making experimental studies less invasive. Figure 4.1 shows the Op at different developmental stages.

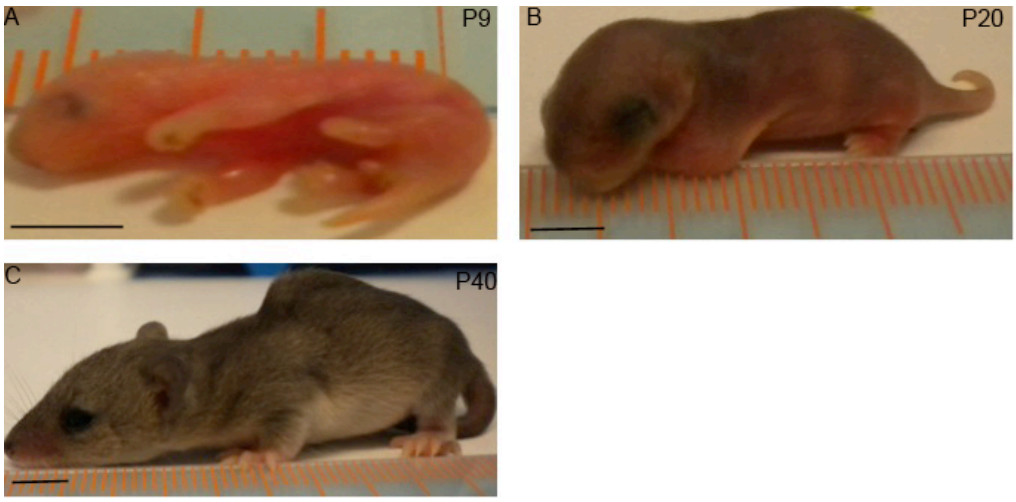

Figure 4.1. The *Monodelphis domestica* at different development stages. (A-C) pups 9 (P9), 20 (P20) and 40 days (P40) after birth. Bars: 1 cm.

The Op is the first metatherian species whose genome has been sequenced, providing insights into the evolution and organization of mammalian genomes [56]. The strategic importance of the Op genome sequence accrues from both the unique phylogenetic position of marsupials, which distinguish them from other mammalian species. Owing to their close relationship, marsupials and placentals share fundamentally similar genetic structures and molecular processes. However, during their long evolutionary separation, these mammals have developed distinctive anatomical, physiologic, and genetic features that hold tremendous potential for examining relationships between the molecular structures of mammalian genomes and the functional attributes of their components [57]. Judging from the multiple nuclear sequence, the most closely related mammalian lineages are Methateria and Eutheria, which diverged from their common mammalian ancestor ~173-190 million years ago (Fig. 4.2).

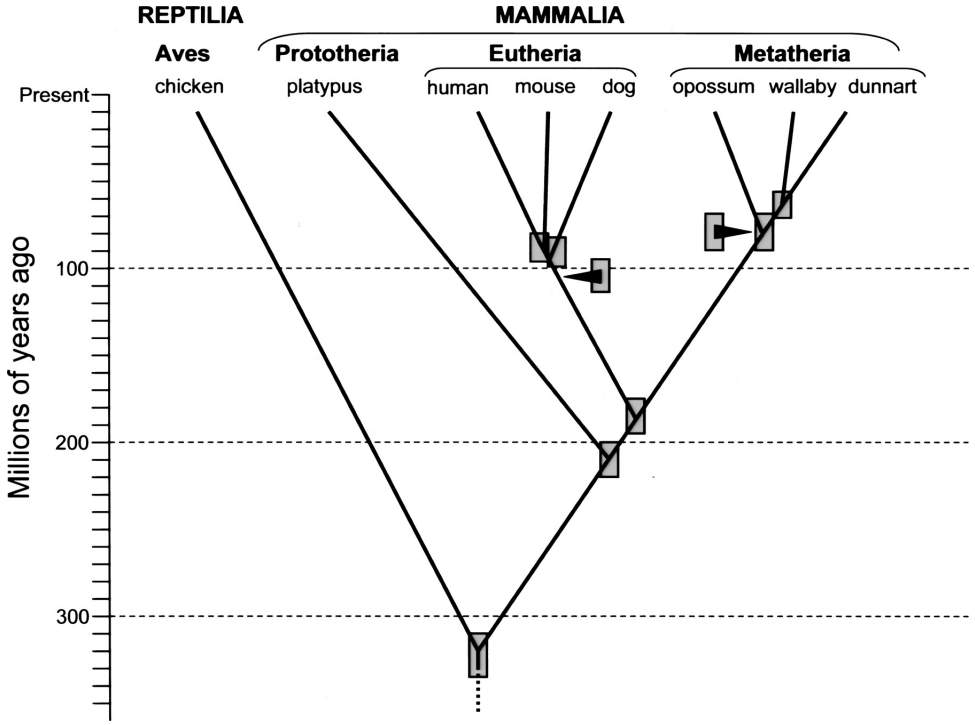

Figure 4.2. Phylogenetic splitting topology and approximate ages for mammalian divergences. Shaded boxes indicate approximate ranges for divergence date. Approximate dates for the earliest (deepest) divergences among extant species within the eutherian and metatherian lineages are indicated by arrowheads. As for the branching points, the shaded boxes associated with arrowheads indicate approximate range estimates for these basal divergence dates. (From [57]).

Because of their close evolutionary position, marsupial and placental mammals share similar genetic structures and molecular processes, reflecting elemental and ancient mammalian characteristic. Each group has then developed its own unique morphologic and physiologic features on these elemental patterns. Due to its peculiar position in the phylogenetic tree, the methaterian Op has developed unique features that retain an extraordinary potential for understanding the CNS physiology. Furthermore, its small size, ease of care and the non-seasonal breeding make Op a suitable laboratory animal model [58].

4. CNS Cellular Processes Influenced by PrP^C

The PrP^C has been hypothesized to be involved in numerous physiological functions including neuronal cell survival, neurite outgrowth, synapses formation and function, and maintenance of myelinated fibers (Figure 4.3).

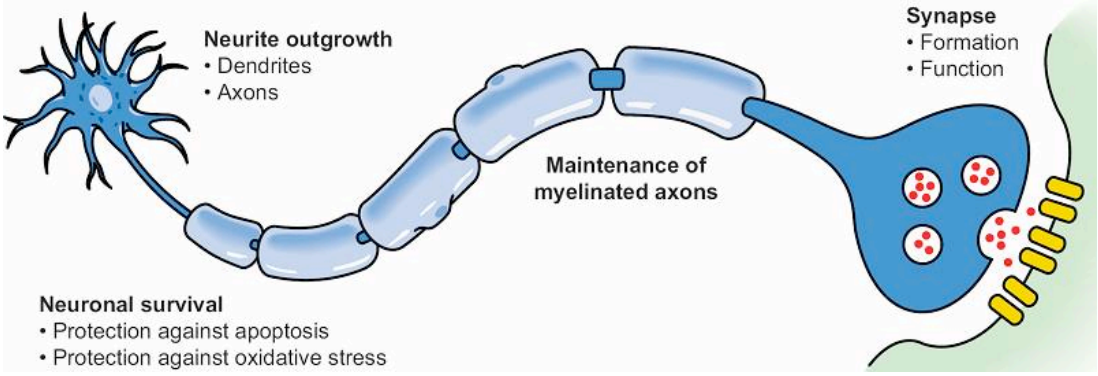

Figure 4.3. Schematic representation of CNS processes influenced by PrP^C. [59]

In vitro and *in vivo* studies have shown that PrP^C has a survival-promoting effect on neuronal and non-neuronal cells that is mainly mediated by antiapoptotic or antioxidative mechanisms [60].

4.1. Anti-apoptotic function

Studies on human primary neurons have shown that PrP^C potently inhibits Bax-induced cell death. The deletion of four octapeptide repeats of PrP (PrPΔOR) and familial D178N and T183A PrP mutations completely or partially eliminate the neuroprotective effect of PrP^C. PrP remains antiapoptotic despite truncation of the GPI anchor signal peptide. This indicates that the neuroprotective form of PrP does not require the abundant, cell surface GPI-anchored PrP [61].

In post-ischemic rodent brain, PrP^C expression increases in a time-dependent manner [62]. In addition, overexpression of PrP^C transduced by adenovirus-mediated gene transfer could

reduce ischemic injury and improve neurological dysfunction after cerebral ischemia in rats [62]. The post ischemic caspase-3 activation is enhanced in PrP^C knock-out mice and the increased activation of ERK1/2, STAT-1 and JNK 1/-2 suggests a possible role for PrP^C in signaling pathway [63]. Furthermore, the reduced levels of phospho-Akt in the gray matter suggest an impairment of the antiapoptotic phosphatidylinositol 3-kinase/Akt pathway in mice lacking PrP^C.

4.2 Protection against oxidative damage

Several lines of evidence suggest an antioxidative effect for PrP^C. Studies in primary cerebellar granule neuron cultures exposed to hydrogen peroxide have shown that PrP^C knock-out neurons are significantly more susceptible than WT neurons after 6 and 24 hours of exposure [64]. *In vivo* studies have shown that in presence of PrP^C the activity of the Cu/Zn superoxide dismutase is higher than in absence of PrP^C. The latter condition is characterized by high Mn superoxide dismutase activity [65]. Experiments with recombinant chicken and mouse PrP^C, as well as immunoprecipitated PrP^C, have shown a PrP^C-dependent SOD activity that was abolished by deletion of the octapeptide-repeat region. This has suggested an enzymic function for PrP^C, dependent on copper intake and consistent with its cellular distribution [66]. However this issue is very controversial. [67,68].

Mithocondria are involved in both oxidative stress and the induction of apoptosis. Studies in scrapie-infected hamsters have reported a decreased activity of Mn-SOD compared to controls, possibly ascribable to an increasing oxidative stress in the mitochondria of the infected brain. This hypothesis is supported by a high level of lipid peroxidation and low levels of ATPase and cytochrome c oxidase activity in the infected cerebral mitochondria [69]. In an inbred line of mice, in tissues that normally express PrP at moderate-to-high levels, ablation of PrP^C resulted in reduced mitochondrial numbers, unusual mitochondrial morphology, and elevated levels of mitochondrial manganese-dependent superoxide dismutase antioxidant enzyme [70].

4.3. PrP^C at synapses

The putative role of PrP^C in neuronal cellular communication derives from its localization both in the pre- [71] and postsynaptic structures [72]. Using a sensitive post-embedding immunogold electron microscopy method in the brain of variant Creutzfeldt-Jakob disease patients, PrP-gold labeling has been found predominantly in the presynaptic domain of synapses [73,74]. This suggests that synaptic pathology is a major event in spongiform encephalopathy, with loss of GABAergic neurons as the first detectable neuropathological change. Presynaptic bouton loss (an alteration accompanied by abnormally aggregated vesicles) is also observed, but only at the terminal stage of disease. This is associated with a significant decrease in the stimulated [3H]-GABA release from synaptosomes and with the accumulationof PrP^{Sc} [75]. Alterations may also be attributed to PrP^C loss of function, since hippocampal slices from PrP-null mice have weakened GABA receptor-mediated fast inhibition and impaired long-term potentiation [76]. The circadian rythm and sleep homeostasis alteration reported in PrP^C-null mice may also be related to synaptic dysfunction [77] and impaired hippocampal-dependent spatial learning [78].

PrP^C has also been found in the neuromuscular junction, namely enriched in subsynaptic endosomes [79]. In a mouse phrenic-diaphragm preparation, nanomolar concentrations of PrP^C induce a very striking potentiation of the acetylcholine release. The effect was mainly pre-synaptic with an increased amplitude of the miniature end-plate currents, probably calcium dependent [80].

Taken together, these data suggest that PrP^C modulates neuronal excitability and synaptic activity, which probably forms the neural basis for some of the systemic brain functions attributed to PrP^C.

4.4. Neurite outgrowth

Mounting evidence indicates that PrP^C may act as a recognition molecule or as an adhesion molecule. NCAM, the 67-kDa laminin receptor (LR), the 37-kDa laminin receptor precursor (LRP) and the extracellular matrix glycoprotrein laminin are believed to be interactors of PrP^C [81], [82,83], [84].

Since these molecules play pivotal roles in cell proliferation, neuronal cell survival, and differentiation, it has been proposed that the specific interaction between PrP^C and some of these molecules could have different consequences for neurite outgrowth, neuronal cell survival, and differentiation via some signaling transduction pathways including p59Fyn kinase, cAmp/protein kinase A (PKA), protein kinase C (PKC) and MAP kinase activation[85], [86]. Both *cis* and *trans* interactions between NCAM at the neuronal cell surface and PrP^C promote recruitment of NCAM to lipid rafts, and thus regulate activation of fyn kinase, an enzyme involved in NCAM-mediated signaling. *Cis* and *trans* interactions between NCAM and PrP promote neurite outgrowth. When these interactions are disrupted in NCAM-deficient and PrP-deficient neurons or by PrP antibodies, NCAM/PrP-dependent neurite outgrowth is arrested. This indicates that PrP is involved in nervous system development and cooperates with NCAM as a signaling receptor.

Loss- and gain-of-function experiments have shown that PrP^C levels correlate with differentiation of multipotent neural precursors into mature neurons *in vitro.* They have also shown that PrP^C levels positively influence neuronal cellular differentiation in a dose-dependent manner. PrP^C also increases cellular proliferation *in vivo*. In the subventricular zone of the olfactory bulbs (SVZ), PrP^C overexpresser mice have more proliferating cells compared with WT or knock-out mice. In the hippocampal dentate gyrus (DG), PrP^C overexpressor and WT mice have more proliferating cells compared with knock-out mice, indicating that PrP^C plays an important role in neurogenesis and differentiation [87].

5. Molecular mechanisms mediating PrP^C function

PrP^C interacts with different partners, hence it relates to a variety of signaling pathways.

5.1. Signaling

Like the other raft-associated proteins, PrP^C may be involved in different signaling pathways. Experiments in the 1C11 cell system aimed at studying PrP^C in relation to the onset of neuronal cellular functions and within an integrated neuronal context have shown that coupling of PrP^C with the tyrosine kinase Fyn is closely related to the maturation of the cells in a caveolin-dependent manner [88]. This finding suggests that caveolin mediates the signaling triggered by engagement of PrP^C in cells that express both proteins. This process may thus require an intermediate component. NCAM, whose engagement induces phosphorylation of Fyn, is a candidate PrP^C-binding transmembrane signaling protein [89]. Biochemical and co-immunoprecipitation experiments have found that DRMs from growth cones show different NCAM species and that caveolae segregate from phosphorylated Fyn [90].

It has been hypothesized that the cross-linking of PrP^C to Fyn promotes a rearrangement of membrane rafts through lateral movement of distinct domains, and that the interaction with NCAM may couple PrP^C with Fyn on the cytoplasmatic leaflet of the plasma membrane [91].

Experiments with PrP^C-binding peptide in retinal explants from neonatal rats or mice have shown that PrP^C activates both cAMP/protein kinase A (PKA) and ERK pathways. It also partially prevents cell death induced by anisomycin (ANI) in explants from WT rodents, but not in those from PrP^C-null mice. This result indicates that PrP^C may function as a trophic receptor, whose activation leads to a neuroprotective state [92]. In support of this hypothesis, cell surface binding and pull-down experiments have shown that recPrP binds to cellular STI1 (stress-inducible protein 1), and co-immunoprecipitation assays strongly suggest that both proteins are associated *in vivo*. Moreover, PrP^C interaction with STI1 induces neuroprotective signals that rescue cells from apoptosis [21]. Protection of

hippocampal neurons in culture by hop/STI1 can also be blocked by a PKA inhibitor [85]. Interestingly, in PrP knock-out retinal explants from neonatal rats or mice the basal levels of both cAMP and PKA are higher than in PrP WT samples, arguing for a compensatory effect for PrP^C ablation [93]. The induction of neurite outgrowth and neuronal cell survival by *trans*-interacting PrP^C in cerebellar granule cells can be blocked by a PKA inhibitor. Yet it has no effect on axon outgrowth induced by recPrP upon embryonic hippocampal neurons in culture [94].

In $1C11^{5\text{-HT}}$ cells the antibody-mediated ligation of PrP^C, concomitant with agonist stimulation of 5-HT receptors, disturbs the couplings of all three serotoninergic receptors present on $1C11^{5\text{-HT}}$ cells by affecting the potency or dynamics of G-protein activation by agonist-bound serotonergic receptors. The PrP^C-dependent modulation of 5-HT receptor couplings critically involves a PrP^C-caveolin platform implemented on the neurites of $1C11^{5\text{-HT}}$ cells during differentiation [95]. Despite this evidence, the adenylyl cyclase family includes both transmembrane and soluble forms, which can be regulated by other factors such as calcium and calmodulin [96]. PrP^C-dependent activation of the cAMP-PKA pathway may be mediated by either voltage-gated or store-operated calcium-channels at the plasma membrane. Alternatively, PrP^C may modulate this pathway interacting with transmembrane forms of adenylyl cyclase.

PrP^C expression has also been linked to activation of the ERK pathway. In the neuroblastic layer of the developing retina, a peptide that binds residues 113–128 of the mouse (114–129 human) PrP^C (the PrR peptide) induces a neuroprotective response *in vitro,* activating both the cAMP/PKA and the ERK signaling pathways. Interestingly, inhibition of PKA activity blocked the effect of the PrR peptide, whereas inhibition of the ERK pathway potentiated the PrP^C-mediated neuroprotection [92]. In PrP-null retinae and in hippocampal neurons, basal ERK phosphorylation has been found to be higher than in the WT controls, hinting at a compensatory response for the ablation of the *Prnp* gene. Since ERK phosphorylation can be prevented by blocking the activity of NADPH oxidase, which also follows PrP^C cross-linking, the production of reactive oxygen species (ROS) may be an intermediate step in the PrP^C activation of ERK. In both serotoninergic and noradrenergic

1C11-derived cells, recruitment of the tyrosine kinase Fyn appears to be a prerequisite for both NADPH oxidase activation and ERK1/2 phosphorylation [97]. The idea of an additional NADPH oxidase-independent pathway is drawn from the observation that in the differentiated 1C11 derivatives, the pharmacologicals inhibition of NADPH does not completely block ERK1/2 phosphorylation.

The exposure of PrP^C fusion proteins in a mouse monocyte/macrophage cell line is accompanied by an increase in cellular tyrosine phosphorylation, as a result of activated signaling pathways including phosphorylation of ERK(1/2) and Akt kinase [98]. Taken toghether these results indicate that the ERK signaling pathway is activated by both the recruitment of PrP^C at the cell surface and exposure to extracellular PrP^C. This activation may be secondary to various upstream events.

In differentiated 1C11 cells, the antibody cross-linking promotes Fyn phosphorylation [99] and the inhibition of Fyn by PP2 inhibits, in turn, ERK activation [97]. Adding purified recPrP to rat fetal hippocampal neurons in culture influences axon elongation. This effect is blocked by inhibitors of protein kinase C (PKC) and of Src kinases, including p59Fyn. On the other hand, inhibitors of phosphatidylinositol 3-kinase show only a partial inhibition, suggesting that signaling cascades involving these kinases are candidates for transduction of recPrP-mediated signals [94]. In contrast, immunofluorescence confocal microscopy observations of cerebellar granule cells have established that Fyn with PrP^C are present within the same cell and are mostly not colocalized [100]. Moreover, adding exogenous PrP fusion proteins to monocyte/macrophage cell line P388D-1 — in which a high basal phosphorylation level of fyn kinase has been found — does not remarkably change phosphorylation level of fyn kinase after stimulation with PrP-Fc. Notably, PrP-Fc resulted in phosphorylation of the non-receptor tyrosine-kinase Syk and Pyk2, as well as the adaptor protein Cbl [98].

Several studies describe the activation of the Protein kinase C (PKC) by PrP^C. In membrane detergent-resistant fractions, PrP and PKC have been detected in the immunoprecipitate obtained with anti-GAP43 or anti-PrP antibody at 4°C [100] and in rat hippocampal primary cultures. Inhibitors of protein kinase C (PKC) have blocked the effect of recPrP on axon elongation [94]. Consistent with a possible role for PrP^C in immune function, PrP

knock-out splenocytes have displayed defects in upstream or downstream mechanism(s) that modulate PKCα/β phosphorylation. This in turn may affect PrP capacity to regulate splenocyte mitosis [101]. However the link between PrP^C and PKC is not fully clarified.

The relationship between PrP^C expression and induction of phosphatidylinositol 3-kinase (PI 3-kinase) activity has also been investigated [100]. This kinase plays a pivotal role in neuronal cell survival and apoptosis and, like PrP^C, it is also associated with lipid microdomains. Both mouse neuroblastoma N2a cells and immortalized murine hippocampal neuronal cell lines expressing WT PrP^C had significantly higher PI 3-kinase activity levels than their respective controls. Moreover, PI 3-kinase activity was found to be elevated in brain lysates from WT mice, as compared to PrP-knockout mice. Recruitment of PI 3-kinase by PrP^C was shown to contribute to cellular survival toward oxidative stress by using 3-morpholinosydnonimine (SIN-1) and serum deprivation. Both PI 3-kinase activation and cytoprotection by PrP^C appeared to rely on copper binding to the N-terminal octapeptide of PrP^C [102]. In other studies, PrP^C deletion impaired the antiapoptotic PI3K/Akt pathway by reducing postischemic phospho-Akt expression, followed by enhanced postischemic caspase-3 activation. PrP^C deletion also aggravated neuronal injury after both transient and permanent cerebral ischemia *in vivo* [103]. Nonetheless, authors did not rule out the possibility that additional pathways (e.g., MAPK/ERK19) or molecular events mediating necrotic cell death (e.g., poly(ADP-ribose)polymerase [PARP] activation) may also contribute to enhanced ischemic brain injury in absence of PrP^C.

5.2. Trafficking of PrP^C

PrP^C is expressed on the cell surface and endocytosis is hypothesized to function as a way to control its related cellular signaling.

5.2.1. PrP^C endocytosis

Like the other GPI-anchored proteins, in PrP^C the lack of intracellularly oriented amino acid sequences indicates that it cannot interact directly with adaptor proteins necessary for clathrin-mediated endocytosis. However, the presence of GPI-anchored proteins in lipid rafts may be important for their endocytosis [104]. In particular, some GPI-anchored proteins are colocalized with caveolae or caveolin-1. Caveolae are markers of 'flask-shaped' or 'omega-shaped' membrane invaginations, which present no clathrin coat . It has been proposed that localization of GPI-anchored proteins at caveolae or caveolae-like domains may be triggered by antibody cross-linking [105].

A number of studies have detected the expression of PrP^C or PrP^{Sc} from cultured cells in caveolae-like organelles, based on their resistance to solubilization by certain detergents at 4°C, isolation by flotation in sucrose gradients and also copurification with markers for DRMs [106,107]. The observation that PrP^C is found in DRMs and that perturbation of cholesterol synthesis or drugs that bind to cholesterol changes PrP^C trafficking, it was suggested that, similarly to some GPI-anchored proteins, mammalian PrP^C and PrP^{Sc} might be internalized independently of clathrin [106]. However, many of the drugs used for determining raft association have variable effects on cellular cholesterol levels. Therefore, it is still unclear whether caveolae-mediated endocytosis is involved in PrP^C trafficking in neuronal cells. Interestingly, chPrP, a chicken homologue of mammalian PrP^C, has been shown to constitutively cycle between the cell surface and an endocytic compartment, with a transit time of approximately 60 min in cultured neuroblastoma cells, and its endocytosis is mediated by clathrin-coated pits [11]. The internalization of chPrP was observed to drop by 70% after neuroblastoma cells incubation in hypertonic medium — a treatment that inhibits endocytosis by disrupting clathrin lattices. This led to the hypothesis that, unlike other GPI-anchored proteins, PrP^C is internalized by clathrin-coated pits [11]. In addition, in primary cultured neurons and in the N2a neural cell line, PrP^C has been shown to be

rapidly and constitutively endocytosed. While still on the cell surface, PrP^C leaves lipid 'raft' domains to enter non-raft membrane, from which it enters coated pits [13].

The use of GFP–tagged PrP^C to examine PrP trafficking [108] (PrPc on the road: trafficking of the cellular prion protein. Marco A. M. Prado, 2004) has suggested that clathrin- and dynamin-mediated endocytosis is one of the main pathways for the internalization of the PrP^C, although clathrin-independent mechanisms may also participate in its internalization. The same experimental paradigm has also shown that the protein is found in both the Golgi and the recycling endosomial compartment. Perturbation of endocytosis with a dynamin I-K44A dominant-negative mutant has altered the steady-state distribution of the GFP-PrP^C, leading to the accumulation of fluorescence in unfissioned endocytic intermediates [109]. Further immunoelectron microscopy experiments have shown that, in neurons, PrP^C is present in endosomes containing transferrin [13]. Together, these results suggest that at least one of the pathways for PrP^C internalization involves classical endosomes. In contrast, cryoimmunogold electron microscopy studies on the localization and internalization of PrP^C in CHO cells have shown a caveolae-dependent endocytic pathway that was not observed for other GPI-anchored proteins [10]. These results indicate that there are different routes for the internalization of PrP^C (clathrin- or non-clathrin-mediated endocytosis) although increasing evidence supports the importance of classical endosomal organelles containing distinct Rab proteins.

5.2.1.1. Copper-dependent PrP^C endocytosis

Over the past few years, it has become clear that the PrP binds copper *in vivo*, and the interaction between PrP^C and copper requires the highly conserved, N-terminal octarepeat domain. In 1997 Brown *et al*., showed that brain extracts from PrP knock-out mice have lower copper content than WT mice, and they also exhibit reduced copper metalloprotein activity [110]. However this result was not further confirmed. Indeed, in 2000 Waggoner and collaborators have demonstrated that brain Copper content and Cuproenzyme activity do not vary with PrP^C expression levels leading to the suggestion that PrP^C is not the primary carrier responsible for entry of copper into the brain via the blood-brain or blood-CSF barriers or for uptake of the metal into neurons from the extracellular space [67].

Experiments with GFP-PrP^C have shown that PrP^C is internalized in response to Cu^{2+}, and it accumulates in the perinuclear region of organelles. The internalization of GFP-PrP^C appears to be specific to the interaction of Cu^{2+} with GFP-PrP^C, as the N-terminal mutants are not internalized under the same condition [111]. However, it is still unclear whether the steps involved in Cu^{2+}-induced PrP^C endocytosis are the same for constitutive internalization of the protein.

5.3 PrP^C and cell adhesion

Different studies have highlighted the function of PrP^C as adhesion or recognition molecule. In cultured hippocampal neurons, PrP^C promotes survival by mediating their adhesion and it triggers their phenotypic modifications by interacting with the extracellular matrix glycoprotein laminin (LN) [112]. In the PC-12 cell line, the PrP^C–LN interaction is involved in the neuritogenesis induced by NGF plus LN and the binding site resides in a carboxy-terminal decapeptide from the γ-1 LN chain [82].

PrP^C has also been shown to co-localize with the 37-kDa laminin receptor precursor (LRP) and with its mature 67-kDa form termed high-affinity laminin receptor (LR) on the plasma membrane fractions of N2a cells [83]. *In situ* crosslinking of N2a cells has allowed for the identification of the neural cell adhesion molecule (N-CAM) as PrP^C-interacting protein [84]. This latter is recruited by PrP^C into lipid rafts, activating Fyn kinase and promoting cell adhesion and neurite outgrowth [89] (Fig. 5).

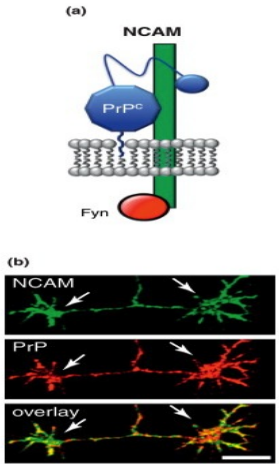

Figure 5. PrP^C interaction with neural cell adhesion molecule (NCAM). (a) Schematic illustration of the interaction between PrP^C and NCAM leading to the activation of Fyn. (b) PrP^C partially colocalizes with NCAM along neurites and in growth cones (arrows) of cultured hippocampal neurons. (Modified from [113]).

PrP^C has also been involved in the proteolysis of the contactin-associated protein (Caspr). PrP inhibits the extracellular matrix Reelin-mediated shedding of Caspr from the cell surface, thereby increasing surface levels of Caspr and potentiating the inhibitory effect of Caspr on neurite outgrowth [114].

Further evidence for a role of PrP^C in the modulation of cell adhesion via signaling derives from studies in zebrafish embryos [115]. Zebrafish contain duplicated PrP genes, *PrP-1* and *-2*, which play different roles during distinct developmental stages. *PrP-1* and E-cadherin interact genetically to control distinct cell morphogenetic movements required for zebrafish gastrulation. In this model, also the accumulation of PrP at cell contact sites was shown to be concomitant with the activation of Src-related kinases, the recruitment of reggie/flotillin microdomains, and the reorganization of the actin cytoskeleton.

5.4 Role of PrP^C in neuronal excitability

The synaptic distribution of PrP^C in the hippocampus [72] — where many kinds of ion channels are concentrated — has led to hypotesize a possible involvement of PrP^C in their regulation and in neuronal excitability. Hippocampal slices from PrP null mice have weakened $GABA_A$ (γ-aminobutyric acid type A) receptor-mediated fast inhibition and impaired long-term potentiation [76]. The neurophysiological evaluation of double transgenic mice generated using the Cre–loxP system has showed a significant reduction the after hyperpolarization potentials (AHPs) in hippocampal CA1 cells depleted of PrP^C. This observation has reinforced the idea of a direct role for PrP^C in the modulation of neuronal excitability [116]. Patch-clamp studies of Ca^{2+}-activated K^+ currents in cerebellar Purkinje cells in the slice preparation of $Prnp^{0/0}$ mice have shown a significant correlation between PrP^C expression in Purkinje cells and the maximal amplitude of TEA-insensitive Ca^{2+}-activated K^+ currents. Moreover they have shown reduced current amplitudes in $Prnp^{0/0}$ mice and a rescue of the phenotype in transgenic mice where PrP^C had been reintroduced [117]. Animals lacking PrP^C expression have resulted more susceptible to seizures induced by various convulsant agents than WT controls, probably as hyperexcitability leads to excitotoxicity [118]. This observation might be linked to the aberrant activation of the NMDA subtype of ionotropic glutamate receptors (NMDARs) observed in PrP knock-out mice [119]. Coimmunoprecipitations from PrP^C WT mouse hippocampal homogenates of PrP^C and the NR_2D subunits of the NMDARs have shown the close association of these two proteins. This interaction may serve to silence the activities of NR_2D-containing NMDARs [119].

PrP^C-deficient mice have also been shown to have an increased sensitivity to kainate-induced seizures *in vivo* and *in vitro* in organotypic slices. This sensitivity is cell-specific because interference experiments to abolish PrP^C expression have increased susceptibility to kainate in PrP^C-expressing cells [120]. Other studies have described the association between PrP^C and the group I metabotropic glutamate receptors (mGluR1 or mGluR5), which is able to transduce cellular signals on Laminin γ1 peptide binding to PrP^C [121].

Patch-clamping experiments to directly test for a connection between PrP^C molecules carrying neurotoxic deletions in the central region (ΔCR PrP) and ion channel activity have

shown the generation of spontaneous currents when expressed in a variety of different cell types [122]. Remarkably, similar currents were induced by several different point mutations in the central region, which are linked to familial prion diseases in humans. This suggests that common structural domains control both the functional activity of PrP^{C} and its ability to be converted to PrP^{Sc} [123].

6. PrP^C and Reelin

The expression of PrP^C on the cell membrane makes it a potential candidate for a ligand uptake, cell adhesion and recognition molecule or a membrane-signaling molecule. PrP^C has been shown to interact with the contactin-associated protein (Caspr). This adhesion molecule is required for the formation of axoglial paranodal junctions surrounding the nodes of Ranvier in myelinated axons [124]. PrP^C prevents Caspr from shedding at the cell surface and result in an inhibitory modulation of neurite outgrowth in neurons, which is counterbalanced by the proteolytic activity of Reelin [114].

6.1. Reelin

6.1.1. Reelin structure and processing

Reelin is a large (>400 kDa) extracellular glycoprotein, which is secreted by several neurons, particularly, in the embryonic cortex, by Cajal–Retzius cells. Defective Reelin is the cause of the reeler brain malformation in mice [125,126] and of a peculiar type of lissencephaly in man [127]. In Reeler mice, neurons are generated in ventricular zones (VZ) and initially migrate as in normal animals. However, unlike normal cells, Reeler neurons form defective architectonic patterns. Whereas normal cortical neurons form a dense, radially and laminarly organized cortical plate (CP) in which maturation proceeds from inside to outside, Reeler neurons form a loose CP in which they are oriented obliquely and the gradient of maturation is almost inverted.

Reelin gene (Reln) is localized to chromosome 7 in man [128]. On SDS-PAGE, Reelin appears as several protein bands, ranging from 410 to 330, 180 kDa, and several smaller fragments [129],[130,131]. Figure 6 schematizes the domain structure organization of Reelin.

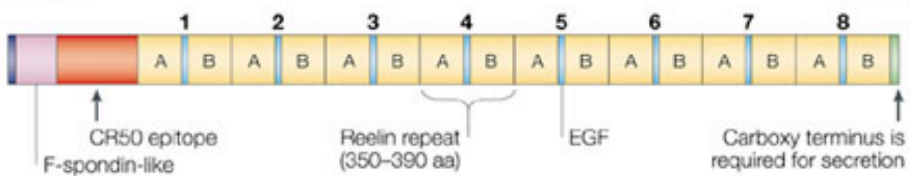

Figure 6. Modular structure of the Reelin molecule. Reelin contains a cleavable signal peptide at the amino terminus, followed by a region of similarity to F-spondin, a secreted protein produced by floor plate cells that controls cell migration and neurite outgrowth. The most striking feature of Reelin is the presence of eight internal repeats comprising aa 350–390. These so-called Reelin repeats contain two related subdomains, A and B, separated by a stretch of 30 amino acids harbouring an epidermal growth factor (EGF)-like motif. A region rich in arginine residues at the carboxy terminus is required for secretion. Modified from [132].

Human Reelin is 94.8% identical to the mouse protein at the amino acid level, indicating strong functional conservation [128]. It is a modular protein composed of a signal sequence, an F-spondin-like region, nine sequentially concatenated repeat units of ~380 amino acids, and a C-terminal basic tail region. Each of the eight Reelin repeats contains a central epidermal growth factor (EGF) module flanked by two homologous subrepeats of 150-190 amino acids. The EGF-like module is ubiquitous among extracellular proteins, but the two subrepeats are unique to Reelin and do not show any sequence similarity to other protein families. A Reelin fragment composed of central repeats 3–6 recapitulates most of its functions in cortical development [133,134]. Reelin is cleaved *in vivo* at two sites approximately located between repeats 2 and 3 and between repeats 6 and 7. This process did not occur in *Reln*$^{rl\text{-}Orl}$ mutant mice in which Reelin is not secreted. It can also be prevented in explant cultures by brefeldin treatment, thus suggesting that this process takes place extracellularly or in a postendoplasmic reticulum compartment. Further Reelin cleavage can be inhibited by zinc chelators known to inhibit metalloproteinases, and has been shown to be insensitive to inhibitors of matrixins, neprilysin, meprin, and peptidyl dipeptidase A, suggesting that the processing enzyme belongs to a different enzyme family

[135]. An epitope known as the CR-50 is localized near the N-terminus [136] and is composed of aa 230–346 of Reelin glycoprotein. This epitope is essential for Reelin–Reelin electrostatic interactions that produce a soluble string-like homopolymer, composed of up to 40 or more regularly repeated monomers, which form *in vivo*. Reelin mutants lacking the CR-50 epitope fail to form homopolymers and are therefore unable to transduce the Reelin signal [137]. *In vitro*, after purification, Reelin undergoes rapid self-degradation and the major 140-kDa fragment has an enzymatical activity, since it has been shown to bind the FP-Peg-biotin stronger than full-length Reelin. These data argue that the proteolytic processing of Reelin is functionally important, and that full activity of Reelin might require degradation of the 400-kDa full-length precursor to generate smaller, more active isoforms. The observation that fibronectin and laminin are rapidly degraded by purified Reelin and that fibronectin degradation is inhibited by inhibitors of serine proteases and by monoclonal antibody CR-50 suggests that Reelin has a specific serine protease activity. The proteolytic activity of Reelin on adhesion molecules of the extracellular matrix and/or receptors on neurons may explain how Reelin regulates neuronal cell migration and synaptic plasticity [131].

6.1.2. Reeler mice

The reeler mouse is one of the best-known spontaneously occurring mutants in the research field of neuroscience. This animal model has been used to understand mammalian brain development. The reeler mutant mouse was first described over 50 years ago. It is a spontaneously arising mutant that displays behavioral abnormalities such as ataxia, tremor, and Reelin gaits, which may be caused by cerebellar malformation [138]. In these mutants the migration of many neurons is abnormal, resulting in disrupted cellular organization of brain laminated structures such as cerebellum, cortex and hippocampus [139]. Differently from the cerebellum of a normal mouse, the Reeler one is smaller, its surface is occupied by a thin, quasi-normal cerebellar cells with many malpositioned Purkinje cells, which aggregate into a central cellular mass. The granular cells in the Reeler form a layer beneath the molecular one, with a lower cell density than in the normal counterpart [138]. In Reeler mice, the distinct laminar structure of the hippocampus proper (i.e. Ammon’s horn) and

dentate gyrus (DG) is disrupted (Fig. 7). The radial glial scaffold, which is presumed to be important for neuronal cell migration, is not present in Reeler hippocampus [140]. In the dentate gyrus of the adult Reeler, the number of newly generated neurons is lower than in the WT controls, whereas GFAP-positive astrocytes increase, suggesting that the balance of neurogenesis and gliogenesis is regulated by Reelin in the adult brain [141].

At embryonic stage (E) E12.5 and E14.5, prominent expression of Reelin by Cajal-Retzius cells is detectable just beneath the pial surface of the cerebral cortex corresponding to the marginal zone or the future layer I [142]. Autoradiographic analysis of brains that received tritiated thymidine at specific stages during development can reveal the temporal and spatial assembly of cells. This approach has revealed that cortical neurons in the mouse are generated between E10 to E18 and that the 6 layers of the cerebral cortex assemble in an inside-out sequence [143]. These studies have shown that, in addition to morphological and physiological characteristics, neurons positioned within specific cortical layers also share a common birth date. The Reeler cerebral cortex violates this fundamental plan of cortical assembly [144]. Layer I is not discernible in the mutant, and the position of cells comprising other layers is relatively inverted. Importantly, all major morphological cell classes are present in the Reeler cortex, and cohorts of neurons comprising specific layers are generated on schedule [145]. The neuronal classes in Reeler cortex fail to align in an inside-out fashion like their counterparts in the normal cortex. In Reeler, neurons born relatively late during corticogenesis reside in deep layers beneath the older neurons [145]. These comparative studies have shown that the Reeler mutation affects the positioning of neurons within specific layers (Fig. 8).

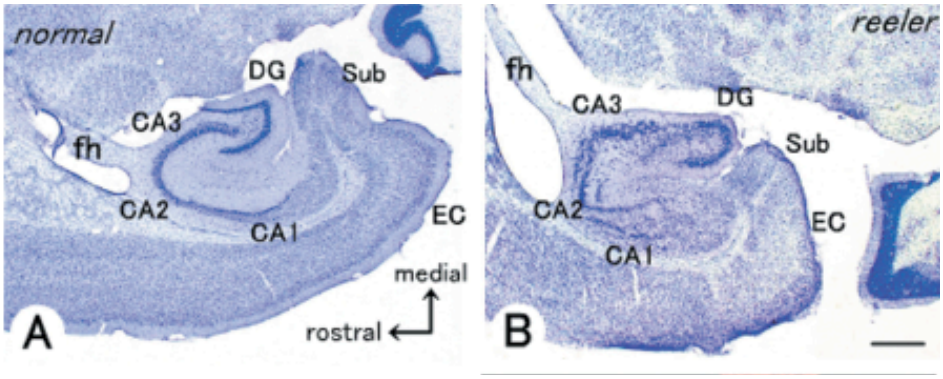

Figure 7. Horizontal sections through the hippocampal formation show cytoarchitecture of the normal (A) and Reeler (B) mice. A, B: The distinct laminar structure of the hippocampus proper (i.e. Ammon's horn) and dentate gyrus (DG) of the normal mouse (A) is disrupted in those of the Reeler mouse (B). Modified from [138].

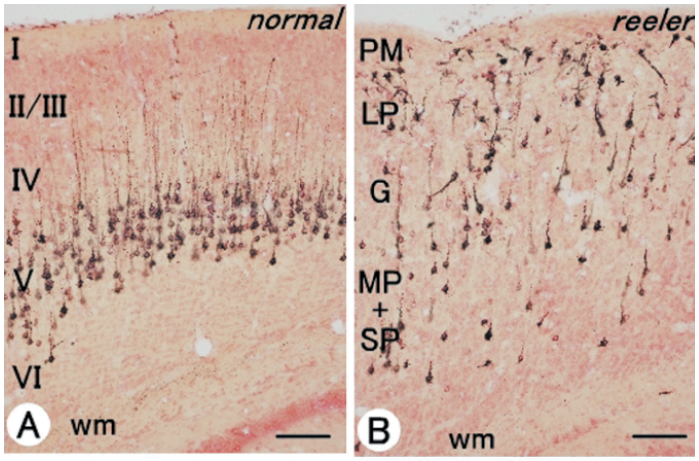

Figure 8. Retrogradely labeled corticospinal tract (CST) neurons in the motor cortex of normal (A) and Reeler (B) mice A, B: CST neurons in the motor cortex are retrogradely labeled by injecting horseradish peroxidase (HRP) in the spinal cord 2 days before death. HRP-labeled neurons accumulate in layer V of the normal cortex (A), whereas they are scattered throughout the radial axis of the reeler cortex (B). Modified from [138].

6.1.3. The molecular basis of Reelin signal transduction

Using genetic and biochemical approaches, several studies by different laboratories have shown the existence of a linear signalling pathway for Reelin [146,147]. Reelin signals through its binding to the very-low-density lipoprotein receptor (VLDLR) and APOE receptor 2 (ApoER2) which in turn activate the cytoplasmic adapter protein disabled 1 (DAB1) by tyrosine phosphorylation (Fig.9).

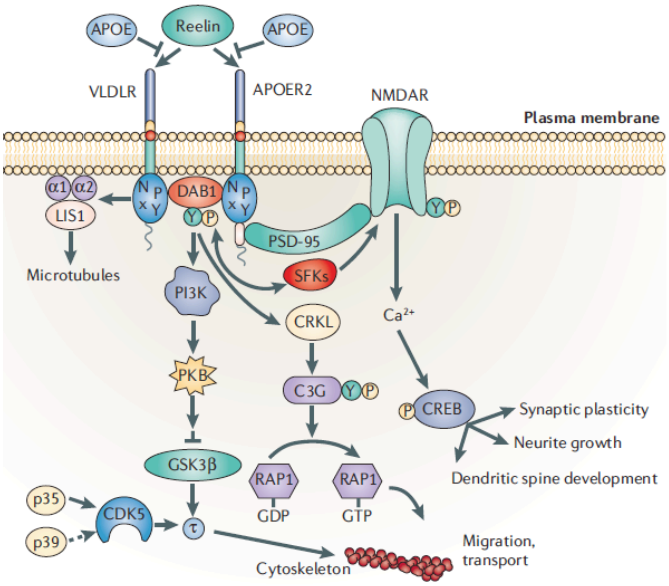

Figure 9. Schematic representation of the Reelin-signaling pathway in neurons. The high affinity Reelin binding to the two lipoprotein receptors, ApoER2 and VLDLR, induces the feed-forward activation of Dab1, a cytoplasmatic interactor protein that specifically recognizes the NPxY motifs present in the cytoplasmatic tails of both receptors. The clustering of Dab1 activates SRC family tyrosine kinases (SFKs), which enhance the phosphorylation levels of Dab1 and, in turn, promote the activation of phosphatidylinositol-3-kinase (PI3K) and subsequently protein kinase B (PKB). PKB activation inhibits the activity of glycogensynthase kinase 3β (GSK3β). As a result, phosphorylation of τ is reduced, promoting microtubule stability. ApoER2 associates with postsynaptic density protein 95 (PSD-95), an abundant scaffolding protein in the PSD, through an alternatively spliced exon. This interaction is crucial for the coupling of the

Reelin signaling complex to the NMDA (Nmethyl-d-aspartate) receptor (NMDAR). Reelin-activated SFKs tyrosine phosphorylate the NMDAR on NR2 subunits, resulting in the potentiation of NMDAR-mediated Ca^{2+}influx. Elevated intracellular Ca^{2+} can activate the transcription factor cyclic AMP response element binding protein (CREB), thereby potentially initiating the expression of genes that are important for synaptic plasticity, neurite growth and dendritic spine development. Modified from [148].

Binding to the receptors, Reelin induces Dab1 tyrosine phosphorylation by Src-family kinases such as Src and Fyn [149,150]. Phosphorylated Dab1 subsequently interacts with other proteins known to be important for the regulation of neuronal cell migration including lissencephaly protein 1 [151] and phosphatidylinositol 3-kinase (PI3K) [152]. Activation of PI3K leads to further downstream signaling including activation of Akt and alterations in glycogen synthase kinase 3ß (GSK3 ß) one of the main kinases that phosphorylates the microtubule-stabilizing protein τ (tau) [153].

The recruitment of ubiquitin ligases to phosphorylated DAB1 promotes its polyubiquitylation and possibly also monoubiquitylation, which could mediate the phosphorylation-dependent endocytosis of the entire Reelin signalling complex. The signal is terminated with Reelin being targeted to the lysosome and DAB1 being degraded by the proteasome, and the receptors recycle back to the membrane [154-156].

6.1.4. Involvment of the Reelin pathway in synaptic functions

The principal signalling of Reelin does not act only on microtubules during development, but is also used in the synapse to regulate NMDA receptor activity through the phosphorylation of intracellular tyrosine residues. During development, Reelin is produced in abundance by Cajal–Retzius neurons at the surface of the developing neocortex [157], but these cells eventually disappear and Reelin expression is maintained by a subset of GABA (γ-aminobutyric acid)-containing interneurons that originate from the medial ganglionic eminence [158]. Studies with VLDLR and ApoER2 knock-out mice have shown that both receptors can bind Reelin with the same affinity and only the lack of both can rensemble the Reeler phenotype [147]. Electrophysiological studies in VLDLR- and ApoER2 knock-out mice have also shown that not only both receptors must function in concert to increase synaptic plasticity in response to Reelin, but also that there is a highly regulated physiological function for Reelin in the control of synaptic transmission, memory and learning [159]. A physiological role of Reelin-signaling in learning and memory by modulating NMDA receptor functions is directly evidenced by the observation that Reelin mediates tyrosine phosphorylation of the cytoplasmic domains of the NMDA receptor, NR2A or NR2B, and potentiates calcium influx through NMDA receptors in primary WT

cortical neurons but not in Dab1 knock-out neurons or in cells in which Reelin binding to its receptors is blocked by a receptor antagonist [160]. In particular ApoER2 at the synapses seems to be involved in the regulation of the NMDA receptors by tyrosine phosphorylation of its cytoplasmatic domain and the coupling of both can occur through extracellular as well as intracellualr interactions [161], [160,162]. The presence of amino acids encoded by an exon in the intracellular domain of ApoER2 has been reported to enhance LTP.

The poor performance in learning and memory tasks by mice constitutively lacking the exon reinforces the hypothesis that the alternative splicing of ApoER2 can control the modulation of NMDA receptor activity, synaptic neurotransmission and memory by Reelin [161].

6.1.5. Involvement of the Reelin pathway in neuropathology

The Reelin signalling pathway has been related to some neurological and neuropsychiatric disorders that afflict the adult brain. This hypothesis is supported by the prominent role for Reelin and APOE receptors in the control of synaptic functions and plasticity. The reduction of *RELN* mRNA in postmortem brain tissues from schizophrenia patients and in bipolar postmortem brain tissues is considered among the most consistent molecular findings in these diseases [163]. A decreased expression of Reelin mRNA by hippocampal Cajal–Retzius cells has also been correlated with the extent of migration defects in the dentate gyrus of patients with temporal lobe epilepsy. This suggests that Reelin is required for normal neuronal lamination in humans, and that deficient Reelin expression may be involved in migration defects associated with temporal lobe epilepsy [164]. Reeler mutants have also been to shown to have profound sensory defects. They manifest a significant reduction in mechanical sensitivity and a pronounced thermal hyperalgesia (increased pain sensitivity) compared with control mice, indicating that Reelin-signaling is an essential contributor to the normal development of central circuits that underlie nociceptive processing and pain [165].

Furthermore, Reelin expression and processing is altered in several amyloid conditions. In particular, alterations in Reelin-mediated signaling have been suggested to contribute to neuronal dysfunction associated with Alzheimer's disease (AD). Experiments with aged

Reelin-deficient transgenic AD mice have shown an age-related Reelin aggregation and a concomitant reduction in Reelin-mediated signaling which plays a proximal role in synaptic dysfunction associated with amyloid-beta deposition. This effect is sufficient to enhance Tau phosphorylation and tangle formation in the hippocampal formation of those mice [166].

7. PrP^C in neurodegeneration

The conversion of PrP^C in the abnormal isoform PrP^C is the causative agent of the TSEs including Creutzfeldt-Jakob disease (CJD) [167]. According to the seeding-nucleation model, during prion propagation in the brain the pre-existing or acquired PrP^C oligomers catalyze the conversion of PrP^C molecules into PrP^{Sc} fibrils. Their breakage releases more PrP^C seeds for the conversion process [168]. However, the means by which prions damage the CNS remain unknown.

The observation that PrP^C is a mediator of amyloid-β-oligomer-induced synaptic dysfunction has led to hypothesize a connection between prions and AD [23]. However this issue is still controversial, since several groups failed to reproduce this finding *in vivo* or *in vitro* [169-171].

As for other protein aggregation diseases, PrP^{Sc} oligomers are the major component of infectious prion particles. The intracerebral inoculation of prions in PrP-deficient mice previously grafted with neural tissue overexpressing PrP^C, has shown that the grafts accumulate high levels of PrP^{Sc} and infectivity, and develop the severe histopathological changes characteristic of scrapie [172]. Moreover, substantial amounts of graft-derived PrP^{Sc} migrated into the host brain. Even 16 months after inoculation no pathological changes were seen in PrP-deficient tissue, not even in the immediate vicinity of the grafts. Therefore, in addition to being resistant to scrapie infection, brain tissue devoid of PrP^C is not damaged by exogenous PrP^{Sc}. This indicates that PrP oligomers and fibrils are not toxic *per se*.

Considering that PrP^C is an extracellular GPI-anchored protein, it is still unclear how it transmits signals across the membrane during the infection. Although PrP^C seems to

interact both with NMDA and GABA receptor subunits, how this interaction might be involved in neurodegeneration ([119], [173,174]) is still unknown. It has been hypothesized that neurodegeneration might be due to the aberrant regulation of protein biogenesis and topology at the endoplasmic reticulum [175]. ^{Ctm}PrP and cytosolic PrP (cyPrP) have been reported to interact with and disrupt the function of Mahogunin (Mgrn), a cytosolic ubiquitin ligase whose loss causes spongiform neurodegeneration. In particular, the transient or partial exposure of PrP to the cytosol leads to inappropriate Mgrn sequestration and this, in turn, contributes to neuronal dysfunction and disease [176]. Some interstitially shortened PrP^C mutants have been described as highly neurotoxic, thus leading to the hypothesis that PrP^C may oligomerize and those interstitial deletion mutants of PrP^C may form transmembrane pores [46]. In particular the expression in transfected cells of PrP $\Delta_{105-125}$ can provoke large, spontaneous ionic currents, which are produced by relatively non-selective, cation-permeable channels or pores in the cell membrane and can be silenced by overexpression of WT PrP, as well as by treatment with a sulfated glycosaminoglycan [122]. However, these kinds of currents have not been recorded in cultured cerebellar granule neurons expressing $PrP_{\Delta 105–125}$, raising the question whether such pores suffice to induce cell-autonomous death.

The intracerebral inoculation of large amounts of prions in PrP^C knock-out mice have shown that prions can be physiologically cleared in a very efficient manner [39]. Both in prion infected cultured mouse neuroblastoma cells (ScN2a) PrP^{Sc} [177] and in mouse brain the half-life for PrP^{Sc} is of about 1.5 days [178]. The prominent clearing mechanism seems to be prion phagocytosis. How microglia can possibly recognize prions as edible is nevertheless still unclear. The existence of additional clearance mechanisms has been postulated in neuroectodermal-infected cells. Indeed, when depleted of PrP^C post-infection, neurons show a reversal of early prion pathogenesis, which may suggest an ability to clear prions [179].

8. Aims of the research

Although PrP^C has been established as an absolute requirement for the prion pathology [179], the precise physiological function of PrP^C is still an open question.

To gain more insights in the physiological role of PrP^C, we carried out a detailed PrP^C expression analysis in the neurodevelopmental mouse brain by means of *in situ* hybridization and immunohistochemistry.

We set out to test whether this pattern of PrP^C expression was maintained in other mammalian species for which not naturally occurring prion diseases have been reported so far. To this end we analyzed the PrP^C expression pattern in the metatherian South American short-tailed opossum (*Monodelphis domestica*) (Op). We tested different immunofluorescence protocols but none of them apparently work for the detection of PrP^C in the Op coronal brain section. To overcome this technical issue we mapped the regional distribution of PrP^C by immunohistoblot.

The different PrP^C distribution in the brain regions of Op compared with mouse finding led us to hypothesize a different physiological implication for the expression of PrP^C in these regions. To test the effect of PrP^C ablation in the hippocampus we decided to use PrP^C knock-out mice. In particular we tried to understand how PrP^C may contribute to the normal physiological function of the CNS studying a possible functional connection between PrP^C and the Reelin-signaling pathway in the neonatal mouse hippocampus

Chapter Two

MATERIALS AND METHODS

2.1. Animals

All experiments were carried out in accordance with European regulations [European Community Council Directive, November 24, 1986 (86/609/EEC)] and were approved by the local veterinary service authority. FVB WT, and FVB *Prnp*$^{0/0}$ mice [180] were used in the experiments. Animals were obtained from the colony maintained at the animal house facility of the University of Trieste, Italy. Animals were staged by systematic daily inspection of the colony for newborn litters. P0 corresponds to the day of birth [181]. Each experiment was performed at least in triplicate. Mice and Op pups were decapitated. Mice (at P30) and Op adults (at P45, P50, and P75) were killed by cervical dislocation. For histoblotting, brains were rapidly harvested, immediately covered in powdered dry ice and included in the embedding medium OCT (Optimal Cutting Temperature).

2.2. Histology

CNS specimens were fixed in 4% paraformaldehyde-PBS overnight at 4°C, cryoprotected in 30% sucrose-PBS and cut coronally at 20 μm. Cryosections were mounted on Fischer SuperFrost Plus slides and subsequently processed for immunohistochemistry.

2.3. Immunohistochemistry

Slides were thawed at room temperature for one hour. After two washes with PBS 1X-Triton X100 0.03%, sections were blocked with blocking solution: PBS 1X-Triton X100 0.03%, normal goat serum (NGS) 10% and bovine serum albumin (BSA) 5% for 1 hour at RT. Slides were then incubated with primary antibodies diluted in blocking solution at 4°C. After 16 hours they were washed 3 times for 5 minutes with PBS 1X-Triton X100 0.03% and then incubated for 1 hour with secondary antibodies, diluted in blocking solution. After

3 washes of 5 minutes each, the nuclei were stained with DAPI diluted 1:1000 in PBS1X. Slides were then extensively washed with PBS1X, mounted with Vectashield (Vector Laboratories, Burlingame, CA), and analyzed under Leica fluorescence microscope. All data are representative of at least three independent experiments. The same exposure times were used for acquiring images from both WT and *Prnp* knock-out brain slices. Images were not modified other than to balance brightness and contrast with GIMP software (see section 2.6.7).

2.3.1. Antibodies for immunofluorescence

The following antibodies were used: 1:400 Anti-Reelin, a.a 164-496 mReelin, clone G10 (MAB5364, Millipore), recombinant anti-PrP^C humanized (HuM) Fab D18 antibody was purchased from InPro Biotechnology (S (South San Francisco, CA; ABR-0D18) was used to a final concentration of 2 μg/mL.

2.4. Nissl staining

Twenty-micrometer fixed frozen cryostat sections, mounted on slides, were air-dried for 60 minutes, stained in 0.1% cresyl violet (Sigma at 40°C for 7 minutes) and then rinsed in distilled water. Slides were soaked in 95% ethyl alcohol for 5 minutes and dehydrated in 100% alcohol for 5 minutes. Before mounting on glass slides with resin medium (Eukitt, Bio-Optica) slides were cleared twice in xylene for 5 minutes.

2.5. *In situ* hybridization

Twenty-μm-thick cryosections were cut and collected on slides (Menzel Gläser SuperFrost Plus) and then stored at -80°C. Sections were dried at room temperature for 2 hours and fixed in 4% PFA in PBS 1X at room temperature for 10 minutes, washed in PBS 1X, treated with 18 mg/mL Proteinase K (Roche, Nutley, NJ) at 30°C for 15 minutes, washed in glycine 4 mg/mL, PBS 1X, and fixed once more in 4% PFA-PBS1X for 10 minutes, washed, incubated in 0.1 M thriethanolamine pH 8.0 with acetic anhydride (0.03%), and washed again. Slides were then dried at room temperature and hybridized overnight at 55°C with 1.5 μg/mL digoxigenin (DIG)-labeled probe in hybridization solution: 50% formamide, salts10X pH 7.2 [NaCl 3M, Tris HCl 0.1M, NaH2PO4 0.1M, 2% Ficoll 400

(Sigma), 2% polyvinyl pyrrolidone (Sigma)], DTT 2M (Sigma) in 10 mM sodium acetate pH 5.2, polyadenilic acid (Sigma) 10 mg/mL, ribonucleic acid (Sigma) 9.2 mg/mL, transfer type x–SA (Sigma) 7 mg/mL, 10% dextran sulfate (Sigma). After hybridization, slides were washed in 5X SSC-β-mercaptoethanol at room temperature for 30 minutes. Then they were washed in 50% formamide-1X SSC-β-mercaptoethanol at 65°C for 30 minutes, several times in the NTE solution (5M NaCl, 1M Tris-HCl pH 8.0, 0.5 M EDTA pH 8.0) at RT, then in 2X SSC and 0.2X SSC. Slides were put in a humidified chamber with buffer B1 (1M Tris-HCl pH 7.5, 5 M NaCl), blocked in HI-FBS (heat-inactivated fetal bovine serum)-B1 (10:90) for 60 minutes. Each slide was treated with 1:1,000 anti-DIG (Roche) in HI-FBS-B1, covered with a parafilm coverslip, and incubated overnight at 4°C. Chromogenic-stained slides were washed several times with buffers B1 and B2 (0.1 M Tris-HCl pH 7.5, 0.1 M NaCl, 50 mM MgCl2 pH 9.5) and stained with NBT 3.5 µL (Roche)-BCIP 3.5 µL (Roche) in 4 mL B2. After 10 minutes the reaction was observed under the microscope and stopped when the transcript signal level was detectable. Slides were then washed several times in buffer B1, then in PBS 1X. Slides were mounted with one 20 µL drop of PBS 1X 30% glycerol solution and a glass coverslip, sealed with enamel, and stored at 4°.

2.5.1. *In situ* probes cloning and synthesis

Primer sequences were designed in order to clone the complete 765-basepairs-long coding sequence (CDS) of mouse (*Mus musculus*) *Prnp* gene in pGEM–T vector (Promega, Madison, WI): 5'-TCA TCC CAC GAT CAG GAA GAT GA-3'; 5'-ATG GCG AAC CTT GGC TAC TG-3'. Sense and antisense probes were transcribed in vitro with SP6 and T7 RNA Polymerase (Promega) in the presence of DIGUTP RNA Labeling Mix (Roche), then stored at -80°C. The efficiency of labeling was checked and confirmed by Northern blot assay, which revealed a single band at the expected base pairs number.

2.6. Histoblots

The histoblot technique was performed according to protocols by Taraboulos et al. [182] with a few modifications. Briefly, uncoated microscope slides (Menzel-Glaser, Madison, WI) carrying 20 µm-thick brain serial coronal sections were pressed onto a nitrocellulose

membrane wetted in lysis buffer (0.5% sodium deoxycholate, 0.5% Nonidet P-40, 100 mM NaCl, 10 mM EDTA, 10 mM Tris-HCl, pH 8.0), incubated for one hour at room temperature in 0.1 M NaOH and rinsed 3 times for 1 minute in TBST 1X (50 mM Tris HCl, 150 mM NaCl, 0.1% Tween20, pH 7.4). Blots were blocked for 90 minutes in 5% non-fat dry milk-TBST 1X. They were incubated overnight at 4°C with the primary antibody anti-PrP^C humanized Fab D18 [177] purchased from InPro Biotechnology (South San Francisco, CA; ABR-0D18) and used at a final concentration of 1 μg/mL. This antibody shows high affinity for the region encompassing residues 133 to 152 (in Mo numbering), which is highly conserved in different mammals. Membranes were extensively washed in TBST 1X and incubated for one hour with secondary antibody diluted in blocking mix. The signal was achieved using SIGMAFAST™ 3,3'-Diaminobenzidine tablets (Sigma) according to the protocols of the supplier. All data are representative of at least three independent experiments.

2.7. Western blotting analysis of PrP^C

Total brains or different brain regions were dissected using a stereomicroscope (Nikon SMZ 800) and immediately frozen in liquid nitrogen. Tissues were homogenized in RIPA buffer (150 mM NaCl, NP-40 1%, sodium deoxycholate 0.5%, SDS 0.1%, 50 mM Tris, pH 8.0) with Glass/Teflon Potter Elvehjem homogenizers and spun at 1000 g at 4°C for 5 minutes. The total protein amount was determined using the BCA Protein Assay Kit (Thermo Scientific Pierce). Fifty μg of total protein was then electrophoresed through 10%–SDS polyacrylamide gels and transferred to nitrocellulose membranes. Membranes were probed with monoclonal antibody Fab D18 and developed by enhanced chemiluminescence (Amersham ECL Western Blotting Systems, GE Healthcare). Band intensity was quantified with the UVI Soft software (UVITEC, Cambridge).

2.8. Immunoprecipitations and Immunoblots of Tyrosine-phosphorylated proteins

Immunoprecipitations were carried out using the PureProteome Protein A Magnetic Bead System (Millipore). Briefly, total brain or P1 mouse hippocampus was homogenized in ~3% w/v of ice-cold IP Lysis Buffer (Pierce Thermo Scientific) with 2X Protease Inhibitor Cocktail (Roche), 2% Phosphatase Inhibitor Cocktail 3 (Sigma), 2% Phosphatase Inhibitor

Cocktail 2 (Sigma), 20 mM Na Orthovanadate. Samples were sonicated 3 times for 5 seconds at 4°C and then left on ice for 30 minutes to allow for the complete lysis. Cellular debris and nuclei were removed centrifuging samples at 20'000 g for 20 minutes at 4°C. The supernatant was then transferred into a clean tube and the protein concentration was determined by BCA (Thermo Scientific Pierce). Two hundred micrograms of total protein extracts were then incubated with 2 µg of the capture antibody for 2 hours at 4°C with continuous mixing. Fifty microliters of the beads suspension were used for each reaction. The pre-formed antibody-antigen complex was added to the beads and then incubated for 2 hours at 4°C with continuous mixing. The beads were extensively washed with 500 µL of 0.1% Tween 20-PBS 1X and then resuspended in 30 µL of 2X Sample Buffer (0.1 M TrisHCl pH 6.8, 4% SDS, 20% glycerol, 8 M Urea, 0.2 M DTT, 0.004% bromophenol blue) and boiled for 10 minutes at 95° C. Samples were then electrophoresed on 10%–SDS polyacrylamide gels and transferred to nitrocellulose membranes. To detect Tyrosine-phosphorylated proteins, the blots were blocked for one hour at room temperature using Bløk - PO Noise Cancelling Reagent (Millipore) and incubated for 16 hours at 4°C with the primary antibody diluted 1:500 in the blocking mix. To remove the residual primary antibody, the membranes were washed 3 times for 5 minutes each in TBST 1X , incubated for 45 minutes at room temperature with 1:10'000 Protein A HRP conjugate (Upstate (Millipore)) diluted in blocking mix and then washed several times in TBST 1X. Millipore enhanced chemiluminescence reagent was used to enhance the chemiluminescence in Western blot.

2.8.1. Coimmunoprecipitation of ApoER2-PrP

Immunoprecipitations were carried out using the PureProteome Protein A Magnetic Bead System. Briefly, 100 µL of the bead suspension was washed three times with 500 µL of PBS. Two hundred micrograms of samples, diluted in PBS, were then added to the beads and incubated at room temperature for 30 minutes with constant mixing. The depleted samples were collected and incubated with 2 µg of Anti-ApoER2 antibody [EPR3326] (ab108208, Abcam) or 2 µg of normal Rabbit IgG (12-370, Millipore) for 4 hours at 4°C with constant mixing. The preformed antigen- antibody complex was then incubated with 50 µl of pre-washed beads for 20 minutes at room-temperature with constant mixing. Beads

were then washed 3 times for 5 minutes each with PBS 1X- Tween 0.5% and twice with PBS 1X-Tween 0.1%. The washed beads were then resuspended in 30 µl of loading buffer, boiled at 95°C for 7 minutes and loaded onto a 10% acrylamide gel.

2.8.2. Antibodies for immunoprecipitation and immunoblot

The following primary antibodies were used in immunoprecipitation: 1 µg Anti-phosphotyrosine, clone 4G10 (05-321X, Millipore), 1 µg normal Rabbit IgG (12-370, Millipore), 1 µg Dab1 (H-103) (sc-13981, Santa Cruz Biotechnology). The following primary antibodies were used in immunoblot: 1:1000 Anti-Reelin, a.a 164-496 mReelin, clone G10 (MAB5364, Millipore), 1:500 Dab1 (H-103) (sc-13981, Santa Cruz Biotechnology), 1:1000 Anti-phospho-GSK3 (Tyr279/Tyr216), clone 5G-2F (05-413, Millipore), 1:1000 Anti-VLDL Receptor antibody [1H10] (ab75591, Abcam), 1:1000 Anti-ApoER2 antibody [EPR3326] (ab108208, Abcam).

Chapter Three

RESULTS

The results are presented in chronological order.

3.1. PrP^C expression detected throughout the developmental mouse brain

The overall distribution of PrP^C in the mouse brain was analyzed by immunohistochemistry in coronal brain sections of E14.5, E18.5, P1, P4, P7, P9, and adult mice. Starting from E18.5, the hippocampus showed the highest level of PrP^C immunoreactivity, in particular at the *stratum lacunosum-molecolare* (Fig. 10 A-B), a layer rich in synapses from hippocampal interneurons and from external inputs, such as the enthorinal cortex [183].

Starting from E18.5 a strong and well-defined PrP^C immunoreactivity (IR) was also observed in white matter structures such as the fimbria (Fi) of the hippocampus (Fig. 10 C-H) and the *stria terminalis* (St), the nervous output of the amygdala up to thalamic nuclei [184].

In the thalamus, PrP^C signal was also detected in white matter fiber bundles, such as the fornix, the anatomical continuation of the hippocampal fimbria, and in the *fasciculus retroflexus* (or habulointerpeduncolar tract), with a net increase in IR along neurodevelopment (Fig. 11 A-H). The specificity of PrP^C expression for particular brain white matter tracts could be appreciated by the complete lack of PrP^C IR of the mammillothalamic tract (Fig. 11 A-C). As for the fimbria of the hippocampus and the *stria terminalis*, PrP^C IR was first observed at E18.5 and it progressively increased during development for the fornix (Fig. 11 I-M) and for the *fasciculus retroflexus* (Fig. 11 N-P).

However, in $Prnp^{0/0}$ mice we did not observe any drammatic alterations in the size or morphology of any of these structures.

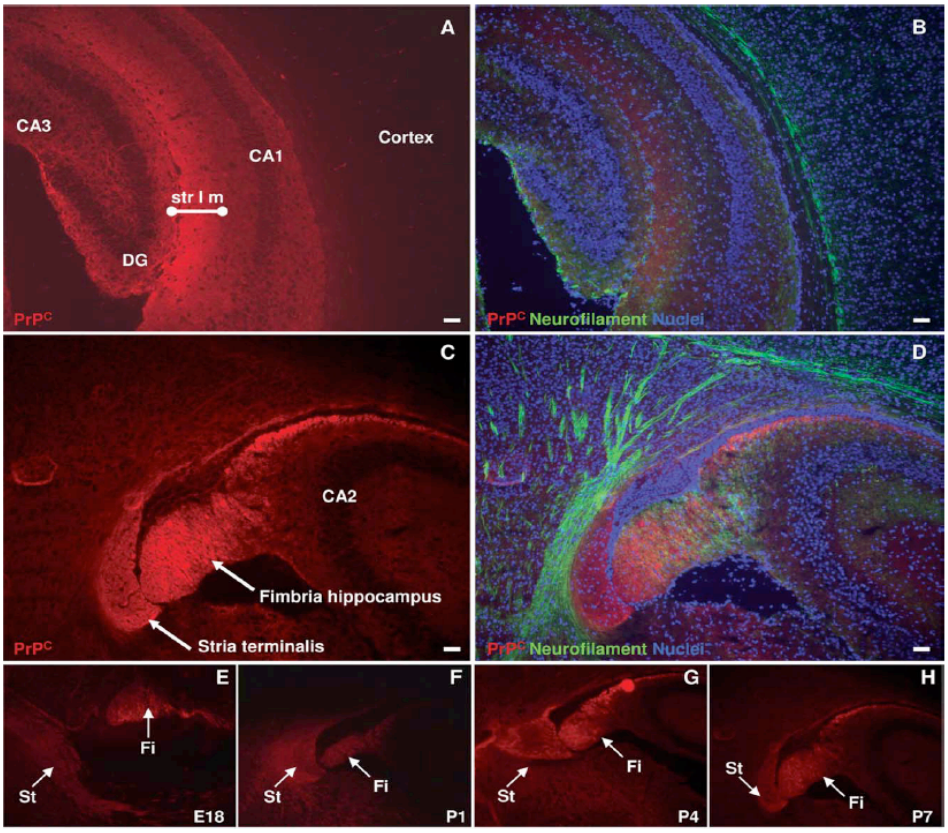

Figure 10. PrP^C expression in the hippocampus during development. A-B: At P7 PrP^C (in red) was detected throughout the hippocampus, and in particularly high levels in the *stratum lacunosum-molecolare* (str l m). A merged image is shown in B (PrP^C, in red; neurofilament, in green; nuclei signals in blue). C-H: PrP^C was specifically and highly expressed by the fimbria (Fi) of the hippocampus and the *stria terminalis* (St) at P7 (C,D). The PrP^C expression level in Fi and St was high also at embryonic stages (E18.5), and it progressively increased during postnatal development: P1 (F), P4 (G), and P7 (H). Scale bars: 50 µm.

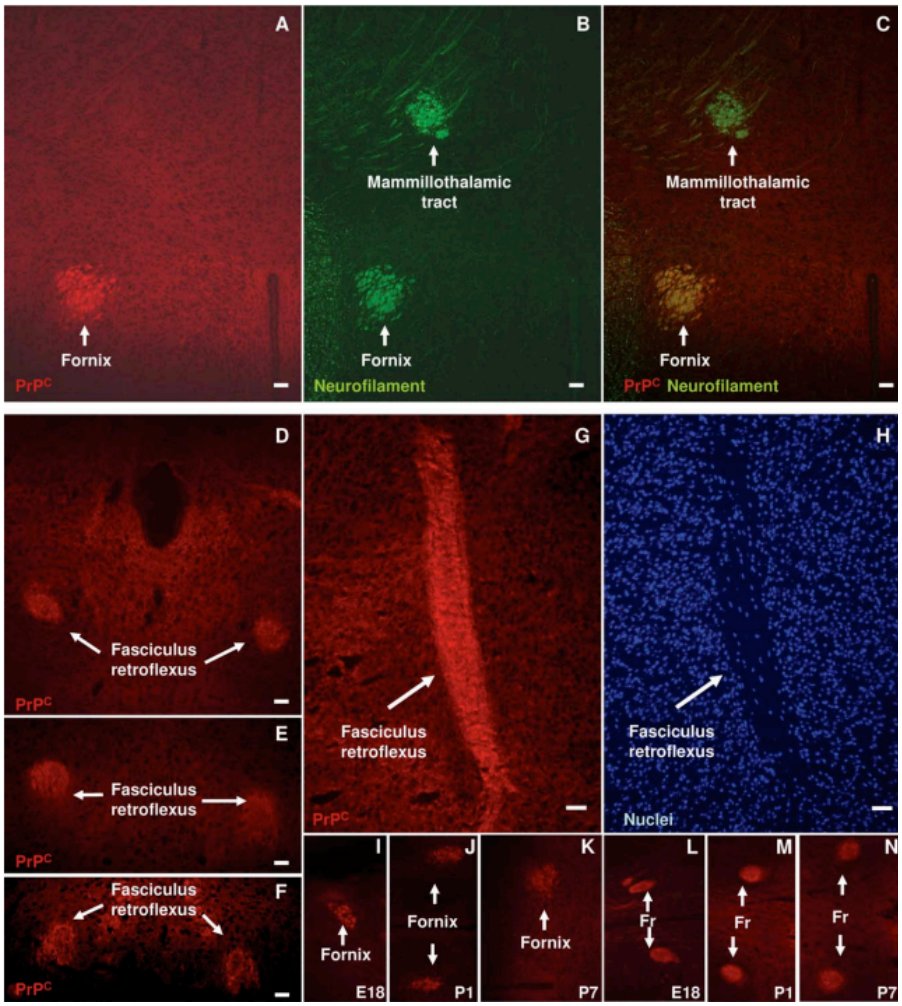

Figure 11. Thalamic expression of PrP^C during development. Immunohistochemical staining for PrP^C (in red; A, C, D–G, I–N) and neurofilament (in green; B,C). A merged image is shown in (C). A–C: At P7 PrP^C was detected in the thalamus, with abundant and specific expression in fornix (A). The specificity of PrP^C expression by this structure was highlighted by the counterstaining of neurofilaments, which labeled both the mammillothalamic tract and the fornix (B). Only the fornix showed colocalization of PrP^C and neurofilament signals (in yellow; C). D–H: At P7, PrP^C expression was detected also specifically in the *fasciculus retroflexus* (or habenulointerpeduncular tract). The *fasciculus retroflexus* expressed PrP^C throughout its length, with clear boundaries, highlighted by coronal (D–F) or longitudinal (G) PrP^C staining. Counterstaining of nuclei (in blue; H) highlighted the low number of nuclei in this white matter structure. I–N: Developmental PrP^C expression by the fornix and the *fasciculus retroflexus* (Fr). Both structures showed a

progressively increasing level of expression of the protein during development, starting from E18.5 (fornix and Fr, respectively; I,L), to P1 (respectively, J,M) until P7 (respectively, K,N). Scale bars: 50 μm.

3.2. *Prnp* gene expression detected throughout the developmental mouse brain

The *Prnp* gene expression was analyzed in the cortex, in the hippocampus and in the olfactory bulbs of the developmental mouse brain by *in situ* hybridization. Between E14.5 and E16.5 noticeable labeling was detected in brain regions known to have a highly active cellular proliferation, namely the ventricular zone (VZ) of the neocortex in the lateral ventricles (Fig. 12 A-B) and the neuroepithelia of the third ventricle (IIIv) (Fig.12 I-L). PrP mRNA signal was also detected underneath the marginal zone (MZ) in the superficial cortical plate (CP), where newborn neurons were. At P1 the signal spanned the entire CP (Fig. 12 C-D), whereas at P7 it was mainly restricted to the superficial CP, where the youngest neurons were (Fig. 12 E-F). At P7, the signal in the subventricular/ependymal zone (SVZ/E) and in the subplate zone (SP) was observed to decrease, whereas it increased in the outer layers of the cortex (layers 6-2) (Fig. 12 E-F). At P1 *Prnp* was detected in the SVZ/E layer of the neocortex, in which the neurogenesis persists throughout the animal's adult life, suggesting a possible involvement of PrP^C in the cellular proliferation control along development [87]. However, a pulse of 5-bromo-2-deoxyuridine (BrdUrd) has shown that at E14.5 PrP^C is expressed close to the proliferative region but not in the BrdUrd positive cells, hence suggesting that PrP^C might not be directly involved in cell proliferation (Fig. 12 G)

At P7 a strong *Prnp* gene expression was detected in the CA1 and in the DG of the hippocampus (Fig. 13).

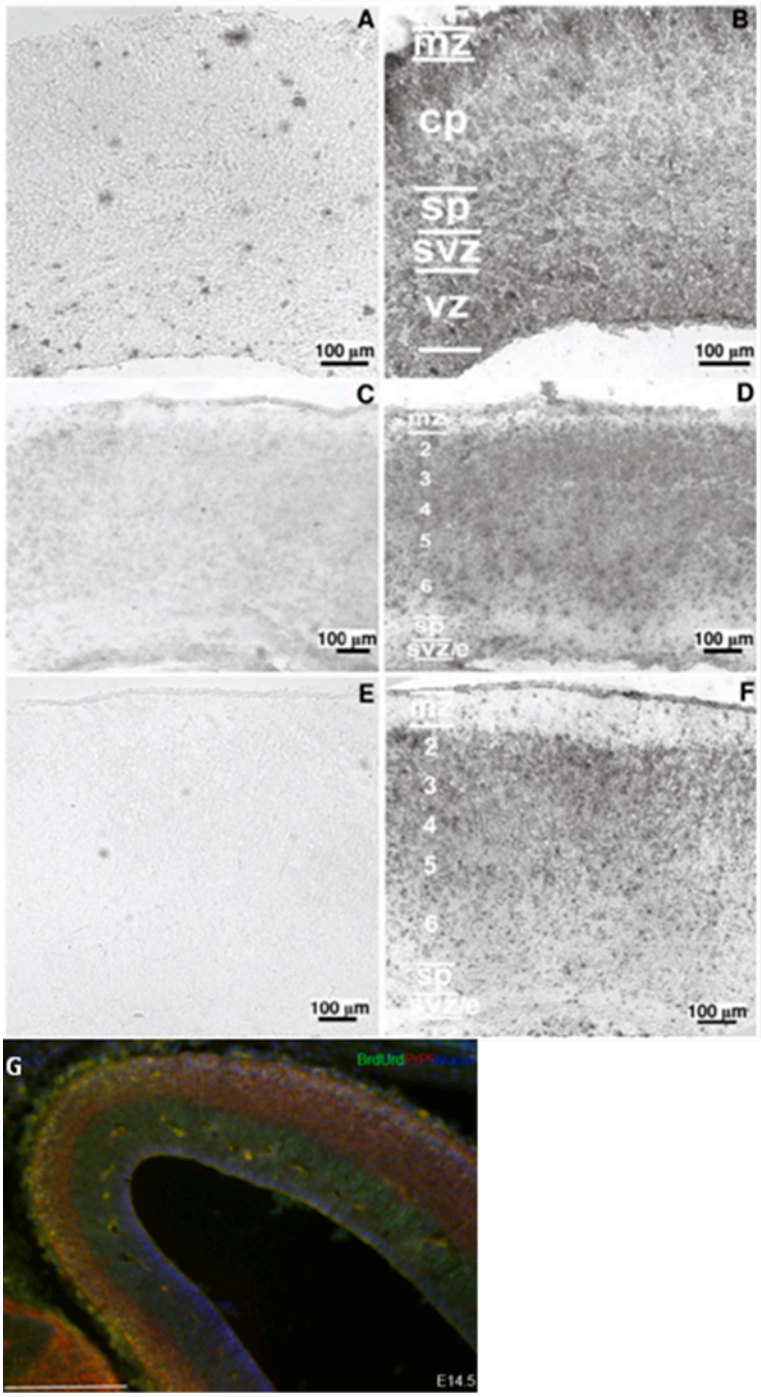
A
B
mz
cp
sp
svz
vz
100 µm
C
D
2
3
4
5
6
E
F
G
BrdUrd
E14.5

Figure 12. *Prnp* and PrP^C expression in the developmental mouse neocortex. A-B: In situ hybridization of E14.5 brain coronal sections. A: No positive cells were detected in the neocortex area using negative sense probe. B: Positive antisense probe detected Prnp in the ventricular zone (VZ). *Prnp* signal seemed to be underneath the marginal zone (MZ) and in the superficial cortical plate (CP). A less intense signal was observed in the subventricular zone (SVZ) and in the subplate zone (SP). C-D: In situ hybridization of P1 brain coronal section. The antisense probe (D) showed signal for *Prnp* spanning the entire CP (layer 6-2). Negative control sense probe showed specificity of the signal in (C). E-F: Expression pattern of *Prnp* gene in the cortex layers of P7 postnatal stage. The positive signal of *Prnp* (F) was mainly concentrated on the superficial CP, whereas it progressively decreased in the subventricular/ependymal zone (SVZ/E) and in the subplate zone (SP). No signal was detected with the sense probe (E). (G) At E14.5 PrP^C is not expressed in proliferating cells. (Scale bar: 119 μm).

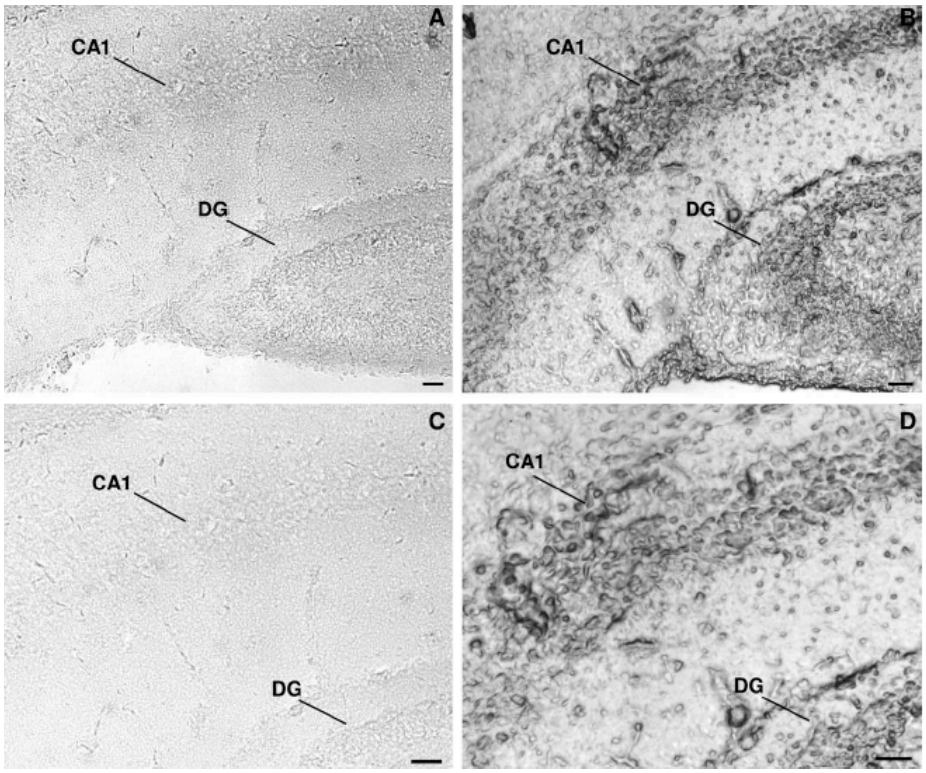

Figure 13. Expression of *Prnp* in the postnatal hippocampus. (A-D) *In situ* hybridization of P7 mouse hippocampal coronal section. (A-B): *Prnp* signal was detected in the CA1 and in the DG cells in the hippocampus. (A) No signal was detected using the sense probe. (C-D) Higher magnification of the CA1 pyramidal cells, indicating a clear perinuclear staining of *Prnp* expression (D). (C) No signal was detected with the negative sense probe. Scale bars = 50 μm.

3.3. PrP^C expression in the Op brain is developmentally regulated

PrP^C protein extracts from adult mouse (Mo) PrP knock-out ($PrP^{-/-}$), PrP WT ($PrP^{+/+}$) and adult Op brains were compared in Western blot (Fig. 14A). The expected di- (~37 kDa), mono- (~30 kDa) and un- (~27 kDa) glycosylated forms were detected by Fab D18 monoclonal antibody both in $MoPrP^{+/+}$ and Op lanes. No signal was detected in the lane loaded with the $MoPrP^{-/-}$ sample, confirming the specificity of the D18 antibody. Although all the lanes were loaded with the same amount of total protein, the lower intensity of Op PrP signal compared to $MoPrP^{+/+}$ signal might be due to a lower affinity of the antibody for the Op PrP than for the $MoPrP^{+/+}$. Alternatively, these results might indicate a lower PrP^C expression in adult Op than in mouse brain.

Starting from Op P1 to P45, a predominance of the diglycosylated and monoglycosylated forms of the protein was observed in Western blot. A minor band corresponding to the unglycosylated form of the protein was observed at ~27 kDa (Fig. 14 B).

The PrP^C expression from P10 to P70 was also evaluated in the thalamus, olfactory bulbs, cortex and hippocampus (Fig. 14 C). In all these regions an increase in PrP^C expression was observed until P50. In adulthood the expression of PrP^C decreased slightly or remained at plateau. At P75, an incremental tendency in PrP^C signal was observed in the olfactory bulbs.

3.4. Regional expression of PrP^C in Op brain coronal sections

Since PrP^C signal was not detectable by immunofluorescence staining performed following well-established protocols (Fig.15) described in the literature (Table 1), we investigated the regional distribution of PrP^C in the Op brain at P15, P20, P37 and P70 by histoblot. After the cortico-cerebral neurogenesis was completed [181] at P15 and at P20 strong PrP^C immunoreactivity (IR) was present in the hippocampus, in the thalamus and in the neocortex. In the hippocampus, a signal was observed in the parenchyma but not in the pyramidal layer of Ammon's Horn (CA1-CA3) nor in the granule cell layer of the dentate gyrus (DG) (Fig. 16 A-B). At P37 (Fig. 17 A-B) a dense PrP^C signal was observed in gray matter structures such as thalamus, cortex and hippocampus. In the latter, PrP^C

immunostaining was deep in the *stratum radiatum* and in the *stratum oriens*. As observed at P20, the signal was virtually absent in the pyramidal cells of the CA and in the granule cells of the DG. In the hilar region, immunoreactivity (IR) was minimal. PrP^C signal was detected around the dorsal and the lateral part of the thalamus (Fig. 16 A), encompassing structures involved in the communication between thalamus and cortex [185].

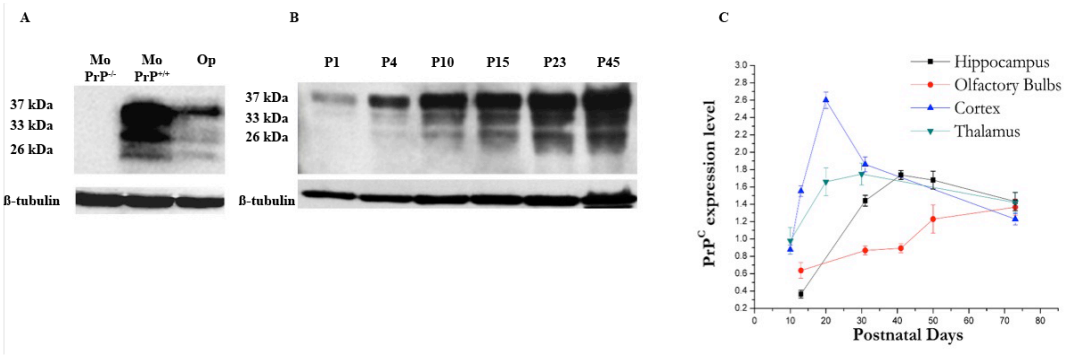

Figure 14. Confirmation of antibody specificity and developmental expression of PrP^C in Op brain. (A) Western blotting of Op, $MoPrP^{+/+}$, and $MoPrP^{-/-}$ whole brain homogenates confirmed the specificity of the PrP^C signal. The blot was reprobed with the ß-tubulin antibody to demonstrate the equal loading of the samples (50 µg per lane). (B) Western blot analysis of equal amounts of total Op brain homogenate (50 µg per lane) at different stages of neural development showed a major electrophoretic band at 37 kDa. ß-tubulin was used as loading control. (C) Western blotting of indicated Op brain regions at different developmental stages showed a relevant change in PrP^C expression during postnatal development. Each data point represents the mean absorbance ±SEM of 3 females from different litters. All the absorbance values were normalized against ß-actin.

Antigen retrieval methods	Antibodies used
	Fab D18, Saf61
10 mM sodium citrate, 0.05% Tween, 1 mM EDTA, pH 6. Samples boiled for 20 minutes in a microwave	Fab D18, Saf61
10 mM sodium citrate, 0.05% Tween, 1 mM EDTA, pH 6. Samples boiled for 25 minutes in autoclave	Fab D18, Saf61
2.3% Na metaperiodate in water+ 1% Na borohydrate in Tris 0.1 M pH 7.5	Fab D18, Saf61
2.3% Na metaperiodate in water+ 1% Na borohydrate in Tris 0.1 M pH 7.5+10 mM sodium citrate pH 6.0 microwave	Fab D18, Saf61
Ethanol 100% pretreatment	Fab D18, Saf61
Pre treatment of sections with 1% SDS in PBS 1X	Fab D18, Saf61

Table 1: Antigen retrieval methods tested to detect PrP^C in the opossum CNS. Different antigen retrieval techniques were tested to uncover the PrP^C antigenic site in the opossum. FabD18 or Saf61 antibodies, previously tested in western blot, did not give a specific PrP^C signal in immunofluorescence.

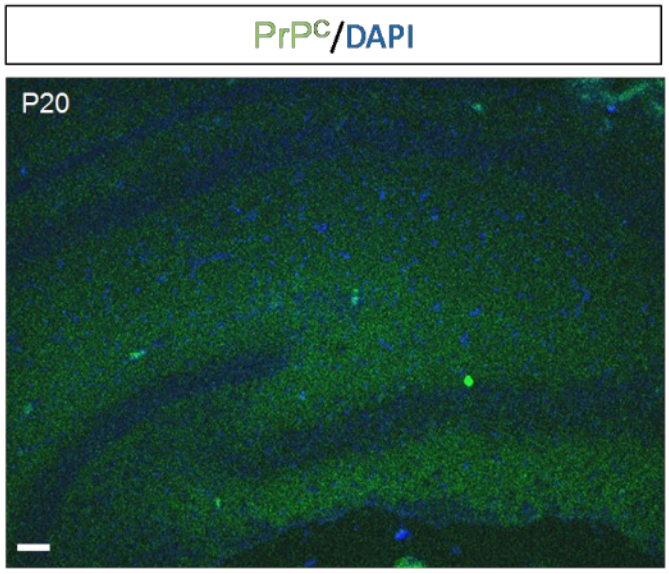

Figure 15 Immunohistochemical staining of P20 opossum brain shows no specific expression of PrP^C in the hippocampus. PrP^C (in green) and nuclei (blue) were stained, and no PrP^C immunoreactivity was detected (Bar: 50 μm).

The PrP^C signal was also evaluated at P70, after the time of weaning [186]. A low IR was observed in white matter structures such as the internal and the external capsule (Fig. 18 B). In the hippocampus, the strongest signal was detected in the *oriens* and in the *radiatum* strata. A less intense signal was detected in the *stratum lacunosum molecolare* (Fig. 18 C). The expression pattern profile observed in the Op hippocampus is similar to that in Syrian Hamster [186].

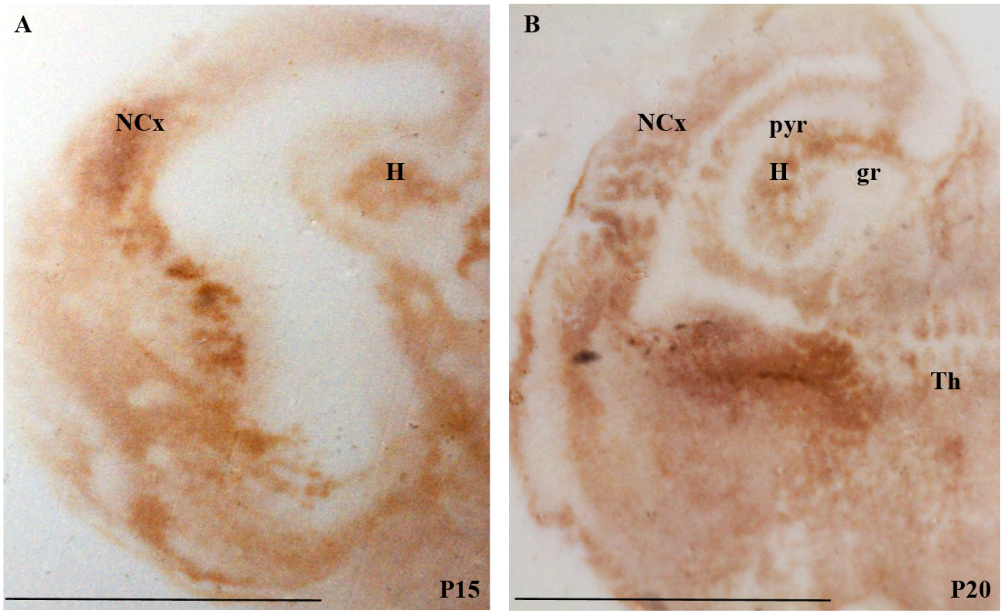

Figure 16. PrP^C expression in histoblots of P15 and P20 Op brains. (A-B) In coronal sections of P15 and P20 Op brains, a PrP^C signal was detected in the thalamus (Th), in the neocortex (NCx) and in the hippocampus (H). The pyramidal layer (pyr) and the granule cell layer (gr) of the hippocampus were not stained by PrP^C. (Bars: A-B 4 mm).

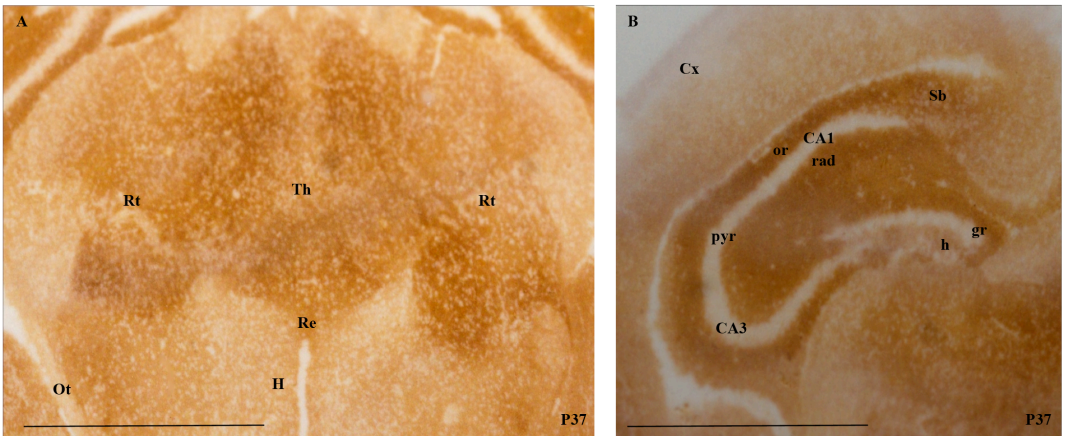

Figure 17. PrP^{C} expression in P37 Op coronal brain sections. (A-B) Coronal sections in the caudal diencephalon from P37 Op were stained for PrP^{C} in the thalamus (Th) and in the parenchyma of the hippocampus. In the ventral thalamus, a strong IR was observed in the *reticular nucleus* (Rt) and in the *nucleus reuniens* (Re). No IR was detected in the optic tract (Ot). In the hypothalamus (H) the IR was lower than in the Th. (B) A strong PrP^{C} signal was observed in the *stratum oriens* (or) and in the *radiatum* (rad) of the hippocampus. A low PrP^{C} signal was found in the hilar region (h) of the hippocampus, while the pyramidal (pyr) and the granule (gr) cell layers of the CA1-CA3 and of the DG were devoid of immunostaining. (Bars: 1 mm).

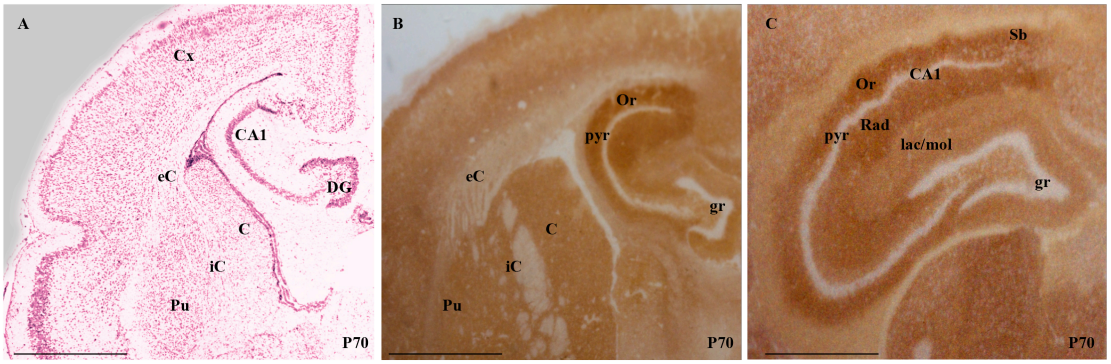

Figure 18. Coronal section of adult Op (P70) (A-C). In (A) the coronal section was Nissl-stained. In adult Op (B) a strong signal was predominantly present in the hippocampus. Marginal signal was also detected in the caudate nucleus (C), in the internal capsule (iC) and in the Putamen (Pu). A very residual signal was observed in the external capsule (eC). In (C) the specific distribution of PrP^{C} in the different hippocampal layers was analyzed. Staining in the *lacunosum* and *moleculare* (lac/mol) was lower than in the *oriens* (Or) and in the *radiatum* (Rad). PrP^{C} IR was also observed in the *subiculum* (Sb) the main output of the hippocampus. (Bars: 0.5 mm).

3.5. PrP^{C} expression in mouse brain coronal sections detected by histoblot

Histoblots of P30 PrP WT ($PrP^{+/+}$) mouse brain coronal sections were immunostained to measure differences in PrP^{C} localization between Op and Mo (Fig. 19 A-B). The lack of signal in P30 PrP knock-out ($PrP^{-/-}$) coronal sections (Fig. 19 C-D) confirmed the specificity of the D18 antibody signal. Ponceau staining was performed to ensure the presence of the brain section on the nitrocellulose membrane. The pattern of PrP^{C} distribution in P30 $PrP^{+/+}$ Mo was detected in many structures throughout the brain (Fig. 19 A-B). At P30 strong IR was observed in the *alveus*, a thalamo-limbic structure of fornix fibers surrounding the *stratum oriens* that contains the axons of pyramidal neurons. As observed with the immunofluorescence staining, a well-defined PrP^{C} signal was present in the *stratum lacunosum-molecolare* (Fig. 19 A). Strong labeling of the white matter fiber bundles was particularly evident at the level of the corpus callosum — the major interhemispheric fiber bundle in eutherians — and in the anterior commissure, also involved in interhemispheric communication [187]. Within the limbic system, a signal was also detected in the hippocampal *fimbria,* in its continuation, the fornix and in the

hippocampus. In the neocortex, staining was detected in a region adjacent to the ependymal layer.

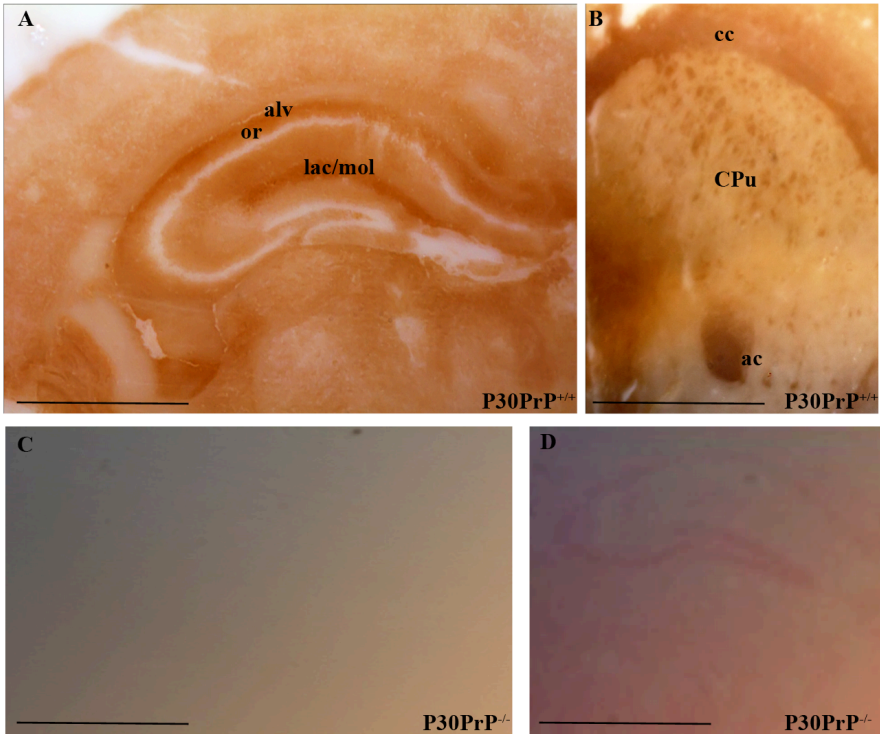

Figure 19. Histoblot of P30 $PrP^{+/+}$ and $PrP^{-/-}$ mouse brain. (A) At P30 a well-defined PrP^{C} signal was present in the hippocampal *stratum lacunosum molecolare* (lac/mo) and in the *alveus* (alv) lying just deep to the *stratum oriens* (or). (B) In the septum-caudatum, PrP^{C} signal was detected predominantly in white matter fiber bundles, such as the anterior commissure (ac) and the *corpus callosum* (cc). The dark dots observed in the caudate-putamen (CPu) are fiber fascicles cut on end. (C) At P30, the lack of staining in $PrP^{-/-}$ Mo coronal section confirmed the signal specificity. (D) The presence of the brain section on the nitrocellulose membrane was confirmed by Ponceau staining. (Bars: A-D 0.5 mm).

3.6 Efficiency of Op substrate in supporting the amplification of Op PrP PK-resistant from different prion sources

Although prion diseases have not been reported in the Op so far, the differential expression profile might account for a different susceptibility to prions in general or to diverse prion strains in particular, as well as for a different pattern of PrP^{Sc} accumulation and propagation between placentals and marsupials. To gain more insights into this issue, serial automated PMCA (saPMCA) experiments were performed in collaboration with Prof. J. Castilla in Bilbao, using different scrapie inocula in adult Op brains. Normal Op brain homogenates were seeded *in vitro* with scrapie mouse adapted prion strains (RML, 22L), scrapie, chronic wasting disease (CWD), and bovine spongiform encephalopathy (BSE) adapted in sheep. Normal Op brain homogenates were then subjected to serial automated PMCA (saPMCA) in an attempt to assess their ability of generating Op PrP^{res}. Seeded samples from round 10 and the unseeded sample were digested with 100 μg/mL of proteinase K (PK) and analyzed by Western blot using the mouse polyclonal antibody 506A. This preliminary experiment indicated that the only *inoculum* able to cross the Op barrier is the BSE adapted in sheep (Fig. 20).

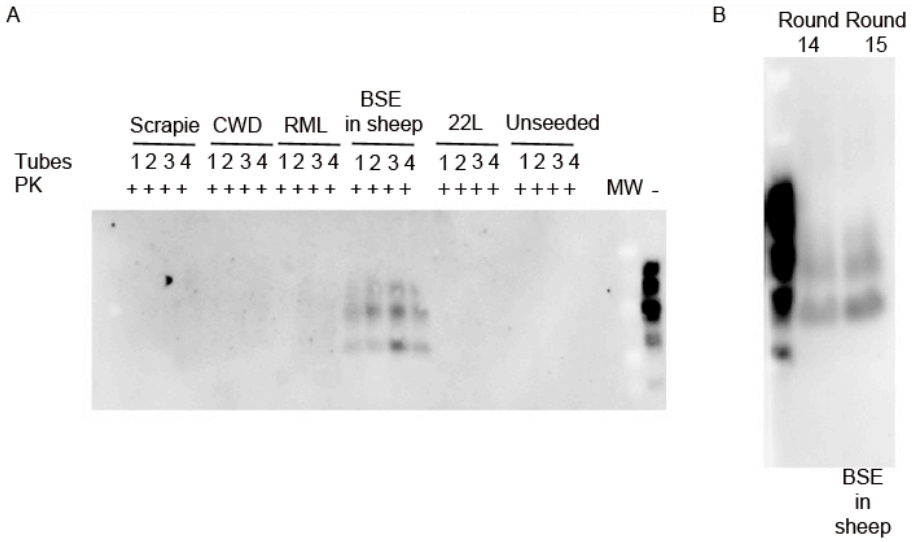

Figure 20. PMCA generation of PK-resistant OpPrP. (A-B) Using only normal Op brain homogenate as a substrate for PMCA, PrP^{C} was efficiently converted to Op PK-resistant PrP only when seeded with strains originating from BSE in sheep. (A) Op brain homogenates seeded with different prion strains (mouse: RML, 22L, scrapie, mule deer:

CWD, cattle: BSE, sheep) or unseeded (*de novo*) were subjected to saPMCA. Seeded samples and the unseeded sample from round 10 were tested for proteinase K (PK) resistance and analyzed by Western blot. (B) Normal Op brains seeded with BSE adapted in sheep shows PK resistance at round 14 and 15 of PMCA. Normal brain homogenate was used as control.

3.7. PrP^C and Reelin expression in the mouse hippocampus

In different eutherian species, PrP^C preferentially localizes in specific hippocampal layers. In the adult the strongest immunoreactive strata are the *oriens* and the *radiatum*, whereas in mouse PrP^C specifically localizes in the *stratum lacunosum-moleculare*.

In an attempt to explain the differences in PrPC distribution in the hippocampus of mouse and Op, we focused on proteins that are localized in this area and share similar functions to PrP^C in the hippocampus. Among all the proteins that are expressed in this region our investigation focused on Reelin, a large extracellular matrix protein that plays an important role in regulating neural migration and synaptogenesis during development [188]. Reelin and Reelin mRNA have been detected in the *stratum lacunosum molecolare* [181] of mouse and Op hippocampi. To gain more insights in this issue we decided to analyze the effect of PrP^C ablation in the Reelin signaling pathway using PrP^C knock-out mice as no PrP^C is expressed in their hippocampal layers.

The distribution of Reelin was analyzed in the hippocampus of P3 mouse PrP WT and P4 mouse PrP knock-out by immunohistochemistry (Fig. 21 and Fig. 22). In both genotypes, Reelin preferentially localizes in the *stratum lacunosum molecolare*, where PrP^C IR is high in the PrP WT genotype.

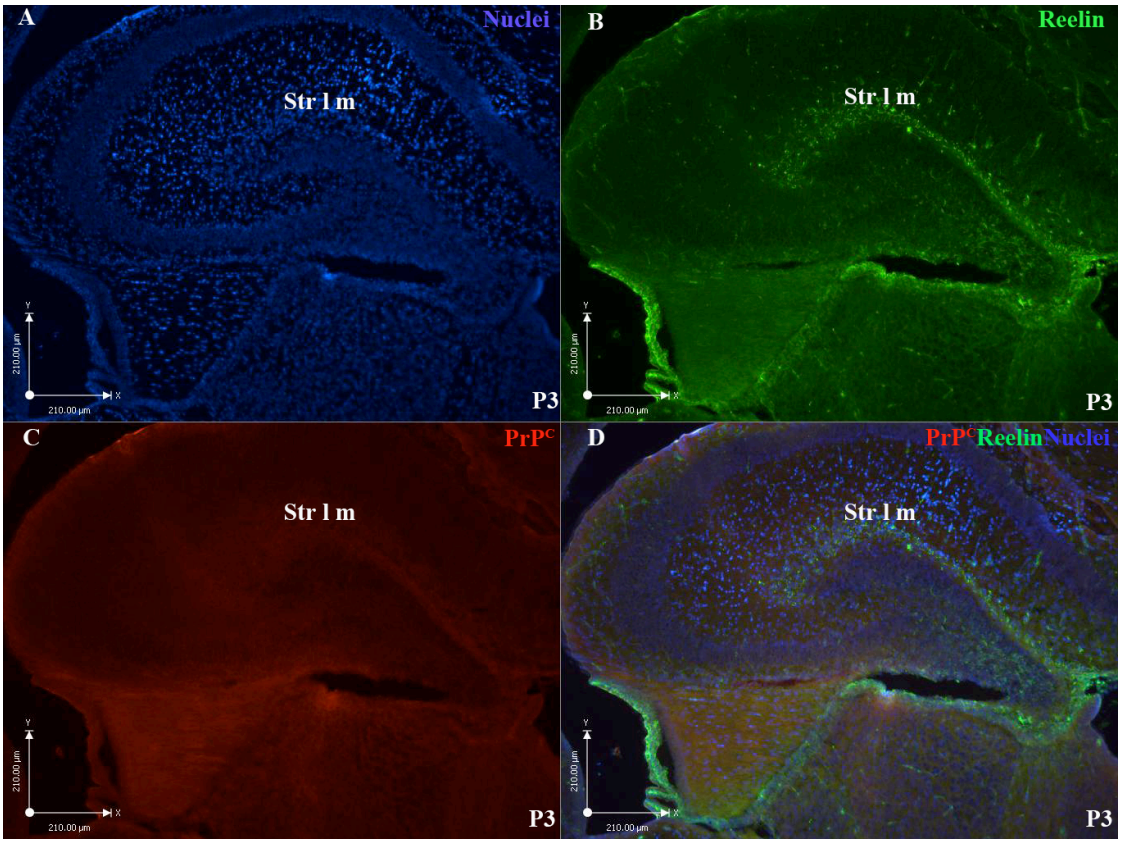

Figure 21. PrP^C and Reelin expression in the $MoPrP^{+/+}$ hippocampus. Immuohistochemical staining for PrP^C (red; C) and Reelin (green; B). A merged image is shown in (D). (A-D) At P3, PrP^C and Reelin were detected in the *stratum lacunosum molecolare* (Str l m) of the hippocampus. (Bars: 210 µm).

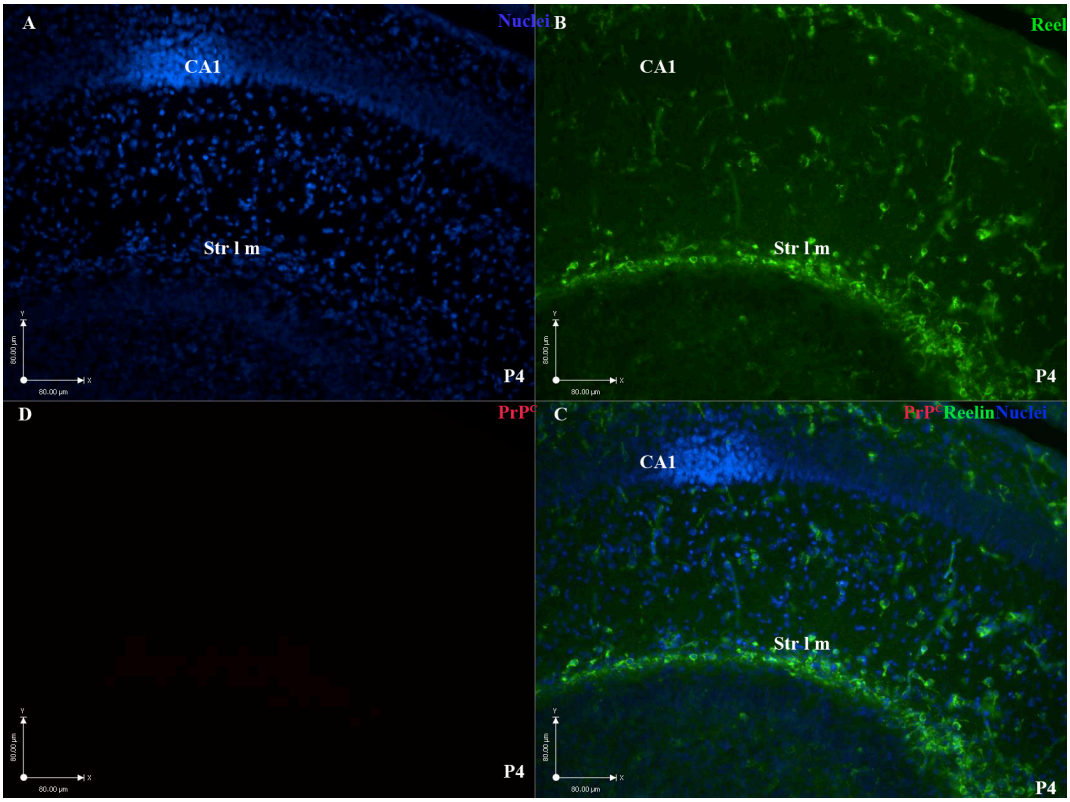

Figure 22. Reelin expression in MoPrP KO hippocampus. (A) DAPI staining of mouse hippocampus in coronal section. (B, D) In the early postnatal PrP KO mouse hippocampus, Reelin IR was detected in the *stratum lacunosum moleculare* (Str l m). (C) No PrP^C immunostaining was observed. (A-D Bars: 80 µm).

3.7.1 Reelin-signaling is enhanced in the hippocampus of early postnatal PrP-deficient mice

PrP^C is highly expressed in the developing brain and it is involved in physiological events in which the Reelin-signaling pathway plays a key role. Therefore, we tested whether PrP deficiency is accompanied by changes in levels of Reelin in the early postnatal brains of PrP knock-out *versus* WT. Western blot analysis with a Reelin N-terminus antibody showed several Reelin isoforms, with the most intense band migrating at ~460 kDa, ~140 kDa and ~70 kDa (Fig. 21 A). Although the levels of full-length Reelin were unchanged between PrP WT mice and PrP KO mice, an increase in the isoforms at ~140 kDa and ~70 kDa was found in PrP-deficient samples (*$p<0.05$, $n\geq4$, paired *t* test) (Fig. 23 A-B). Interestingly, when PrP is overexpressed (Fig. 23 C lanes 7 and 8), independent of the constructs, there seem to be less Reelin (in the 460 kDa and ~150 kDa bands). Lane 7 was loaded with a brain homogenate derived from PrP(ΔSTE) mice which are constructed by deleting the stop transfer effector sequence (STE). Mice with this mutation overexpress PrP^C and can generate almost uniquely the secretory PrP^C (^{Sec}PrP) conformation [189]. Lane 8 was loaded with a brain homogenate of a PrP(KH>II) mouse. This transgenic mouse contains amino acid substitutions lysine and histidine to isoleucines at positions 110 and 111, in the stop transfer effector sequence. It over-expresses PrP^C and favour the ^{Ctm}PrP conformation whith the COOH-terminus in the lumen and the NH_2-terminus in the cytosol [189].

To analyze the involvement of PrP^C in the Reelin-signaling pathway, we compared the levels of PrP^C in Reelin-deficient mice (Reeler) and in Reelin WT mice (Reelin WT). Remarkably, levels of PrP^C were increased in Reeler compared with Reelin WT mice (Fig. 23 D), further supporting a possible relationship between Reelin and PrP^C.

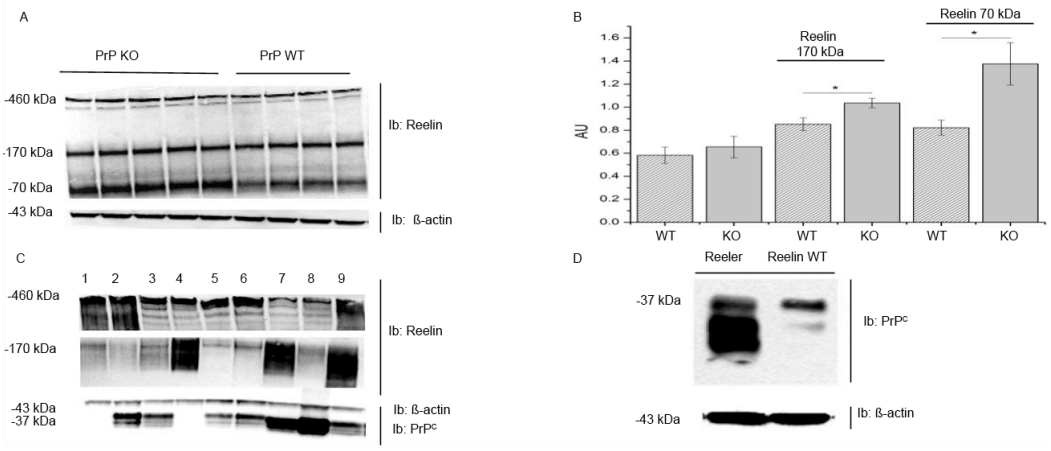

Figure 23. The expression of 140 kDa and 70 kDa Reelin isoforms increased in PrP-deficient mice whereas PrP^C expression increased in Reelin-deficiet mice. (A-B) PrP KO and PrP WT hippocampi were probed by Western blot with an antibody against the Reelin N-terminus. Note increased levels of the ~140 kDa and of the ~70 kDa forms of Reelin in PrP KO *versus* PrP WT samples. ß-actin was used as loading control. (B) The graph shows the quantification of the blots (mean±SEM, n≥4). The levels of each Reelin isoform were normalized to ß-actin. *p<0.05, paired t test. (C) To confirm that the expression of Reelin fragments was increased in absence of PrP^C we probed different brain samples from PrP WT and PrP KO mice with a different genetic background with an antibody against the Reelin N-terminus and against PrP^C. ß-actin was used as loading control. Samples were loaded as follows: (1) FVB PrP KO; (2) FVB PrP WT; (3) FVB PrP WT; (4) FVB PrP KO; (5) C57/B6; (6) SvEv 129 PrP WT; (7) PrP(ΔSTE); (8) PrP (KH>II); (9) Ola129. Lines (1-4) were loaded with FVB mice from different animal houses to confirm that our results were not due to the genetic background of the $Prnp^{0/0}$ strain maintained by inbreeding. (D) Reeler and Reelin WT brain samples were probed by Western blot with antibodies against PrP. ß-actin served as loading control.

Since PrP knock-out mice have no overt phenotype [190], we set out to test whether an impairment in the expression of downstream components of the Reelin-signaling pathway may mask the phenotype of PrP^C deficient mice or may it help to explain some subtle differences described in the literature.

Reelin signals by binding to two transmembrane receptors, apolipoprotein E receptor 2 (ApoER2) and very-low-density lipoprotein receptor (VLDLR) [189]. To a certain extent, both receptors can compensate for each other, and only the loss of both receptors results in the Reelin ko phenotype, which is characterized by gross defects in the architecture of the laminated structures [191], such as the cerebellum, the cortex and the hippocampus.

Although both VLDLR and ApoER2 are members of the low-density lipoprotein family, they differ in a number of ways, including structural differences, expression patterns, alternative splicing, and binding of extracellular and intracellular proteins. Subcellularly, VLDLR is present in non-lipid raft fractions, whereas ApoER2 is found in lipid raft fractions of cell membranes [191]. We therefore analyzed the different expressions of both Reelin receptors in the hippocampus of PrP knock-out and PrP WT mice. The overall expression of both receptors does not differ between the two genotypes (Fig. 24 A-B). Because PrP and ApoER2 are both localized in the lipid raft compartments, we wondered whether they may form a complex. Hence, we immunoprecipitated ApoER2 from hippocampus homogenates and analyzed immunoprecipitates with an antibody against PrP. PrP coimmunoprecipitated with ApoER2 (Fig. 24 C), thus indicating that the two proteins are associated in the hippocampus. Both VLDLR and ApoER2 have short cytoplasmatic tails that contain an NPxY motif to bind Dab1 (Disabled binding protein 1), an intracellular adapter protein expressed in cells that respond to the Reelin signal. Dab1 contains five Tyr residues and phosphorylation of these residues, in response to the binding of Reelin to lipoprotein receptors, is necessary for Dab1 function [192]. It has been shown that Dab1 is a target for the fibrillar PrP (106-126) or PrP^{res}-induced oxidative stress both *in vitro* and in inoculated hamsters [193]. We therefore measured the levels of total Dab1 and Tyr-phosphorylated Dab1 (pDab1) in the hippocampus of early postnatal PrP KO and PrP WT mice (Fig.25 A-D). We immunoprecipitated lysates with anti-Dab1 and anti total phospo-

tyrosine antibodies and we probed for Dab1. We found that Tyr-phosphorylated Dab1was increased in PrP KO mice (*p<0.05, n=3, paired t test) (Fig. 25 C-D), despite total Dab1 was expressed to a similar degree in both genotypes (Fig. 25 A-B).

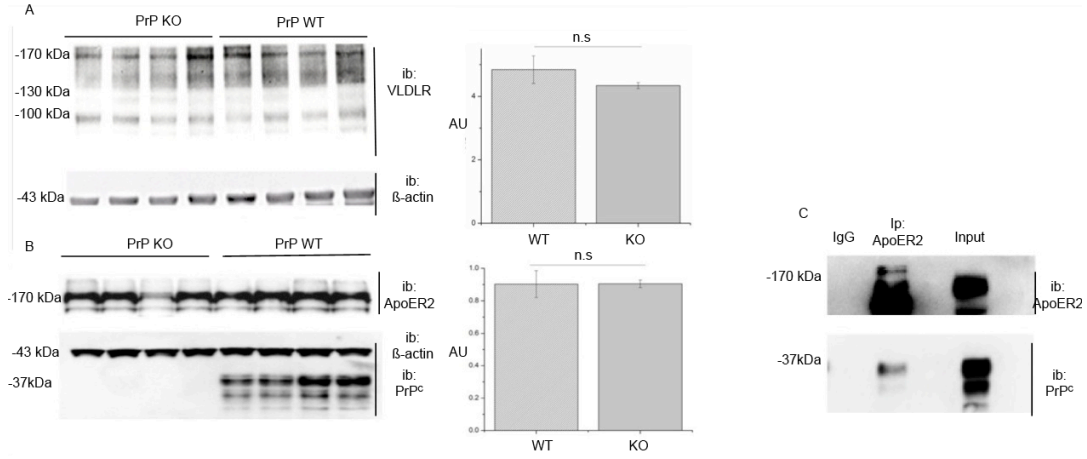

Figure 24. ApoER2 and VLDLR expression in the hippocampi of PrP KO and PrP WT mice. (A-B) Hippocampus homogenates of P1 PrP KO and PrP WT mice were immunoblotted with antibodies against ApoER2 or VLDLR. Diagrams show quantitation of both receptors normalized against ß-actin. Note that the amount of both receptors is similar in the hippocampi of both genotypes. (C) ApoER2 immunoprecipitates from $PrP^{+/+}$ and $PrP^{-/-}$ hippocampi were immnunoblotted with PrP antibody. IgG served as control. Hippocampus homogenates (inputs) were also probed for ApoER2 and PrP.

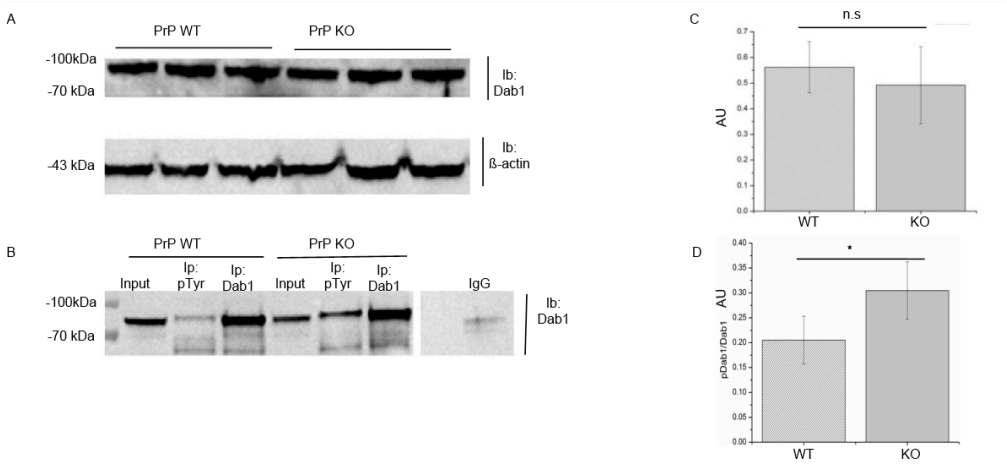

Figure 25. PrP$^{-/-}$ mice have an increased level of pDab1 but not total Dab1. (A,C) Hippocampus homogenates from PrP knock-out and PrP WT mice were blotted for total Dab1. The histogram represents the quantitative results of total Dab1 in both genotypes normalized against ß-actin (mean±SEM, n=3). (B, D) PrP knock-out mice have increased pTyr Dab1 compared to WT mice. The graph in (D) shows the ratio of tyrosine phosphorylated Dab1 normalized to total immunoprecipitated Dab (mean±SEM, n=3).

Phosphorylated Dab1 subsequently interacts with other proteins including lissencephaly protein 1 [151] and phosphatidylinositol 3-kinase (PI3K) [152]. Activation of PI3K leads to further downstream signaling including activation of Akt and alterations in glycogen synthase kinase 3β (GSK3β) and tau [153]. GSK-3 activity is increased by phosphorylation of a tyrosine residue, Tyr-216 in GSK-3β and Tyr-279 in GSK-3α, located in the kinase domain. This phosphotyrosine is important because its dephosphorylation diminishes activity [194] [195]. Phosphorylated DAB1 inhibits GSK3β, a kinase known to phosphorylate Tau protein at multiple sites. The analysis of the gene expression profile in the hippocampi of early postnatal PrP knock-out and WT mice showed that in absence of the *Prnp* gene, the expression of GSK3β was downregulated [196]. Furthermore, it has been reported that in cultured neurons the addition of the prion peptide (PrP 106-126) increases the activity of GSK3 and is accompanied by the enhanced phosphorylation of some microtubule-associated proteins, including tau and microtubule-associated protein 2 [197]. We next investigated whether the levels of total GSK3β and phosphorylated GSK3β were affected in the early postnatal hippocampi of our animal models (Fig. 26).

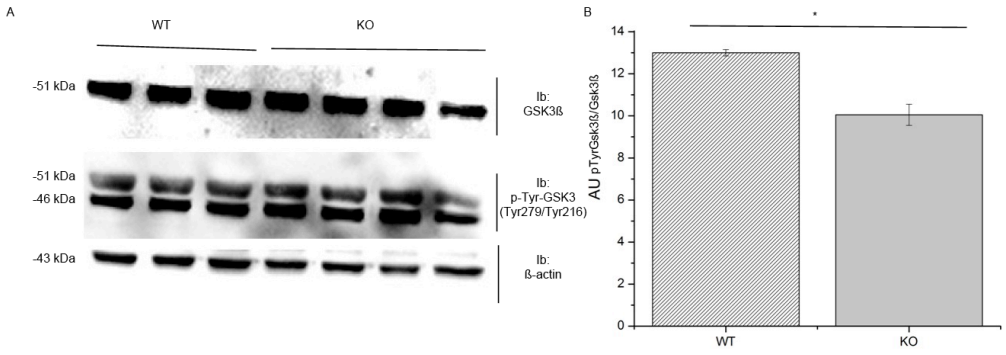

Figure 26. PrP WT mice have higher levels of GSK3β phosphorylated on Tyr216 than PrP KO mice. (A) Total hippocampus homogenates were prepared from 3 P1 PrP WT mice and 4 PrP knock-out mice as described above. Thirty micrograms of protein were loaded in each lane and immunoblotted for indicated proteins. (B) Quantification data obtained from the densitometric analysis of total GSK3β, GSK3β phosphorylated on Tyr 216 (51 kDa) and β-actin.

In agreement with an increased activation of Dab1 in PrP knock-out mice, we found that the ratio between GSK3β phosphorylated on Tyr 216 and total GSK3β normalized on β-actin was significantly higher in newborn mice expressing PrP^C compared with the knock-out counterparts (*p<0.05, n≥3, paired *t test*).

Chapter Four

DISCUSSION

Over the last twenty years, the pattern of PrP^C expression profile in the CNS of placental mammals such as mouse (Mo) and Syrian Hamster (SHa) has been extensively investigated. In this work we described a detailed analysis of PrP^C expression in the developmental mouse CNS, both at protein and at mRNA level. To check whether this expression pattern was maintained in other species, we focused our analysis on the metatherian South American short-tailed opossum (*Monodelphis domestica*) (Op). The most striking difference observed between the two species was the different localization of PrP^C in the white matter. The lower PrP^C signal in Op white matter structures argues for a lower expression of the protein by glial cells and neuronal axons. Athough prion diseases have not been reported in the Op so far, the differential expression profile might account for a different susceptibility to prions in general or to diverse prion strains in particular, as well as for a different pattern of PrP^{Sc} accumulation and propagation between placentals and marsupials. We also found that in different mammals PrP^C localizes in different hippocampal layers. In the mouse, PrP^C is preferentially localized in the synapse-rich *stratum lacunosum molecolare*, whereas in the Op the strongest immunoreactive layers are the *oriens* and the *radiatum*. This finding suggested that PrP^C might play a different regulatory role in the synaptic activity of different mammals. This function might be mediated by other proteins that are localized in the same hippocampal layer and share functions similar to that of PrP^C in the hippocampus. In particular we decided to focus our analysis on the Reelin-signaling pathway, which plays a pivotal role in synaptogenesis during development [198].

4.1. PrP^C and *Prnp* expression in the developmental mouse brain

By *in situ* hybridization we identified PrP^C mRNA expression in two layered brain structures, the cortex (Fig. 12) and the hippocampus (Fig. 13). In the former, we described *Prnp* gene expression at E14.5 in the VZ, a proliferative brain area underneath the MZ where the newborn neurons are. The MZ is the outermost layer of the cerebral cortex. MZ cells are known to orchestrate the development of the cortical layers and contribute to the GABAergic interneurons in the cerebral cortex [199]. At P1 *Prnp* was detected in the SVZ/E layer of the neocortex, in which the neurogenesis persists throughout the animal's adult life, suggesting a possible involvement of PrP^C in the cellular proliferation control along development [87]. However, when the proliferative rate of cells is very high (at E14.5) PrP^C is not expressed in the BrdUrd positive cells, hence suggesting that PrP^C might not be directly involved in cell proliferation (Fig. 12 G).

In the developmental neocortex the mRNA expression of PrP^C seemed to parallel the time course of neuronal cellular differentiation, since at P1 we described a *Prnp* signal through the cortical layers 6-2, while at P7 the signal still spanned all the neocortex but was higher in the uppermost than in the inner layers (Fig. 12).

During early postnatal brain development we found a strong PrP^C signals in the hippocampus, both at protein (Fig. 10) and at mRNA levels (Fig.13). Since in this layered structure the strongest IR was observed in the *stratum lacunosum molecolare* — a synapse-rich region where hippocampal interneurons [200] and afferent neuronal inputs [201] make connections — we might argue an involvement of PrP^C in synapse development and activity. Indeed the lack of PrP^C has been related to a hippocampal synapatic impairment [76]. Central synapses have also been described as primary dysfunctional victims in prion diseases, before neurodegeneration occurs [202,203]. The strong developmental regulation and expression of PrP^C in the hippocampus and in the neocortex is intriguing, as it may account for the increased susceptibility of *Prnp* mice to epileptic seizures [118]. The lack of PrP^C may alter the physiological development of these brain structures, and in turn provoke changes in interneuronal connections and neural network properties.

In all the developmental stages analyzed we described a strong PrP^C signal in brain fiber bundles participating in the regulation of the thalamolimbic circuitry, such as the

fimbria/fornix, the *stria terminalis* and the *fasciculus restroflexus* (Fig. 10 and Fig. 11). This might reflect an active axonal transport of the PrP through these structures. In particular, PrP^C expression in the fimbria/fornix could be related to an axonal transport from the hippocampus PrP^C [72].

4.2. Mapping the PrP distribution in marsupials: Insights from comparing Op with mouse CNS

To date, little is known about PrP^C distribution in marsupial mammals for which no naturally occurring prion diseases have been reported. To extend our understanding of varying PrP^C expression profiles in different mammals we carried out a detailed expression analysis of PrP^C distribution along the neurodevelopment of the metatherian South American short-tailed Op (*Monodelphis domestica*).

4.2.1. Technical remarks about PrP^C detection in Op brain

The routine histological techniques might not be sensitive enough to map PrP^C expression in the Op brain. We tested different immunofluorescence protocols in combination with several monoclonal antibodies (Tsble 1), but none of them appeared to work (Fig. 15). We speculated that these technical difficulties experienced with the traditional immunohistochemical staining techniques might be due to a weak antibody affinity for Op PrP (OpPrP), possibly ascribable to epitope masking as a result of a different membrane environment. Alternatively, PrP^C signal might be masked by another molecule, which could make the binding of the antibody to the antigene inaccessible. To overcome these difficulties we decided to use the immunohistoblot technique described by Taraboulos et al. [182] to map the regional distribution of PrP^{Sc} in the brain of diseased SHa. The use of 0.1M sodium hydroxide enhanced the binding of PrP antibodies [204] thus allowing for the detection of a clear PrP^C signal in the cryostat sections of the freshly frozen Op brain tissues in this study.

4.2.2. Comparison of PrP^C distribution between marsupials and placental mammals

Our results showed that from the day of birth (P1) up to adulthood (P75) PrP^C was detectable by Western blotting in whole brain homogenates (Fig. 14 B) with the strongest PrP^C signal in the uppermost diglycosylated band (~37 kDa) and the weakest signal in the lowest non-glycosylated PrP^C band (~26 kDa). A change in PrP^C relative abundance was observed during Op brain development, corroborating previous evidence of a developmentally regulated expression of PrP^C. In the different brain regions under

consideration, PrP^C levels either remained at plateau or decreased slightly in adulthood (Fig. 14 C). Interestingly, after the time of weaning a tendency to an increase in PrP expression was observed in the olfactory bulbs. As postulated for placental mammals [186] this finding might be related to ongoing plasticity of the olfactory bulbs also in marsupials. However, no evidence is available yet to suggest that there is indeed plasticity in the olfactory bulbs of adult marsupials.

At P37 we observed a strong PrP^C immunoreactivity in the thalamus, a region which has a strong nonphotic influence on sleep and circadian rhythmicity [205]. This finding suggested an evolutionary conserved involvement of PrP^C in sleep homeostasis in the Op, in which a functioning circadian timing system exists [206-208].

Before weaning, PrP^C was detectable in the parenchyma of the hippocampus (Fig. 15 B). Interestingly, in different eutherian species, PrP^C preferentially localizes in specific hippocampal layers. In the adult Op (Figure 18C) and SHa [186] the strongest immunoreactive strata are the *oriens* and the *radiatum*, whereas $MoPrP^C$ specifically localizes in the *stratum lacunosum moleculare* (Fig. 19 A). These results seem to suggest a different regulatory role of PrP^C in the synaptic activity of different species. The lack of PrP^C in the nerve cell bodies was implied by the absence of signal in the pyramidal-cell layer and granule cell-layer of the dentate gyrus in both Mo and Op.

The most striking difference observed between the two species was the different localization of PrP^C in the white matter. The lower PrP^C signal in Op white matter structures argues for a lower expression of the protein by glial cells and neuronal axons. In P30 mice instead, a strong PrP^C immunoreactive signal was detectable in the *corpus callosum*, a specific eutherian structure enriched in myelinated axons and involved in interhemispheric communication [209].

4.2.3. Implications for TSE pathology

The different ability of prions to infect (or not infect) certain species is apparently encoded by their structural features, which result in different physio-pathological outcomes [210]. This strain-like behavior is known as the prion transmission barrier. However, under controlled laboratory conditions, prions are able to adapt and infect species previously believed to be TSE resistant, as was recently reported in rabbits infected by the murine ME7 prion strain using protein misfolding cyclic amplification (PMCA) [211]. Telling and his coworkers have recently developed a Tg mice line [Tg(EqPrP)SS251] expressing the equine PrP to study the susceptibility to TSEs in putatively resistant animals [212]. Their preliminary results suggest that these mice are resistant to all common prion strains, reinforcing the idea that prion resistance seems to be enciphered by PrP^C sequence. Structural studies on the recPrP of mammals for which no TSEs have been reported in natural conditions [e.g. horse, rabbit and the marsupial Tammar wallaby (*Macropus eugenii*)], postulated that resistance to prions might be due to some structural features in the globular domain of those mammalian PrP sequences [30,31,213]. The OpPrP sequence presents an outstandingly large number of amino acid substitutions at the N-terminal in the copper binding sites and, within the C-terminal domain, in epitopes (residues 163-174 and 221-230 in Mo numbering, Fig. 27) critical for prion conversion [8,33,36,37,214].

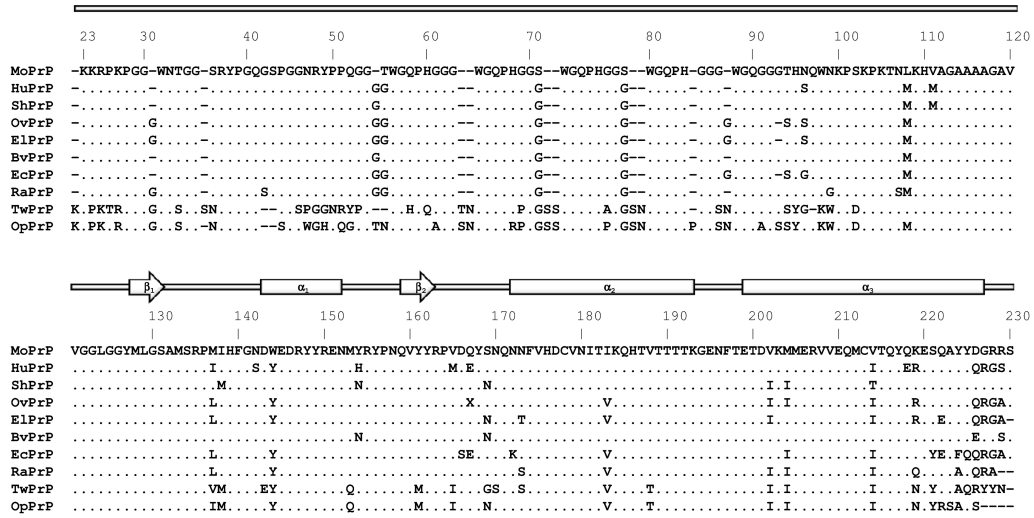

Figure 27. Comparison of amino acid sequences and secondary full-length PrP structure of selected mammalian species: mouse (MoPrP; *Mus musculus*, GenBank accession number: AAA39997), human (HuPrP; *Homo sapiens*, AAA60182), Syrian hamster (ShPrP; *Mesocricetus auratus*, AAA37091), sheep (OvPrP; *Ovis aries*, ABC61639), elk (ElPrP; *Cervus elaphus nelsoni*, AAB94788), bank vole (BvPrP; *Clethrionomys glareolus*, AAL57231), horse (EcPrP; *Equus caballus*, ABL86003), rabbit (RaPrP; *Oryctolagus cuniculus*, AAD01554), tammar wallaby (TwPrP; *Macropus eugenii*, AAT68002) and opossum (OpPrP; *Monodelphis domestica*, CBY05848).

Based on this sequence identity analysis, it is possible to argue that these amino acidic differences might have an impact on the ability of OpPrP to sustain prion conversion. On the other hand, if structural differences in mammalian PrP are important for understanding the molecular mechanisms of TSEs, the neuronal distribution of PrP^{C} in mammalian species that are putatively resistant to prion diseases should be considered.
It is noteworthy that PrP^{Sc} accumulates in the white matter areas of mouse and Syrian hamster brains, thus suggesting that glial cells may be the primary targets for prions [182,215]. Indeed, the infectious agent has been shown to spread from the needle track along white matter pathways towards the gray matter [216]. This hypothesis is strengthened by pathological studies in human brains of terminal CJD patients showing axonal damage, hence suggesting a transport of prions through white matter pathways [217].

Although prion diseases have not been reported in the Op so far, the differential expression profile might account for a different susceptibility to prions in general or to diverse prion strains in particular, as well as for a different pattern of PrP^{Sc} accumulation and propagation between placentals and marsupials. To gain more insights into this issue, serial automated PMCA (saPMCA) experiments were performed in collaboration with Prof. J. Castilla in Bilbao, using different scrapie inocula in adult Op brains. This preliminary experiment indicated that the only *inoculum* able to cross the Op barrier is the BSE adapted in sheep (Fig. 20). This result corroborates the idea that BSE in sheep is one of the most promiscuous and infectious inocula described to date [218]. It also seems to suggest putative difficulties in overcoming the species transmission barriers in infectivity *in vivo* experiments with the regular inocula.

4.3. Increased activation of the Reelin-signaling pathway in early postnatal mouse hippocampus lacking PrP^C

Our findings show that the hippocampus is one of the brain regions with the earliest expression of PrP^C along neural development. Interestingly, we showed that PrP^C has a specific localization in this layered structure among mammals. In the mouse it is mainly expressed in the *stratum lacunosum molecolare,* whereas in the Op it is located in the adjacent layers. Based on the overall pattern of findings discussed here, we hypothesized a connection between PrP^C and another protein specifically expressed in the *stratum lacunosum molecolare,* and this connection may be dysregulated in absence of PrP^C. To investigate this hypothesis, we examined the possible candidates to ascertain whether they share the same physiological functions as PrP^C in the hippocampus. Among all the putative candidates we decided to focus our attention on the extracellular matrix protein Reelin, as Schachner and coworkers [114] have shown a functional interaction of Reelin with PrP^C in the developing mouse brain. Reelin was expressed in the *stratum lacunosum moleculare* in the mouse hippocampus (Fig. 21-22) and its mRNA was detected in the same location also in the Op [181]. The lack of PrP^C knock-out Op did not allow us to make further speculations about the physiological role of PrP^C in the hippocampus of this animal model. To overcome these difficulties we targeted our analysis on the brains of PrP^C knock-out mice in which no PrP^C is expressed in the different hippocampal layers.

Reelin is a glycoprotein of the extracellular matrix involved in different neuronal cellular functions. In particular, it has been shown to regulate neural migration and synaptogenesis during development [219], it is a key component of synaptic plasticity [220] in adult brain, it increases NMDA receptors subunit activity [221] as well as the number of transmembrane proteins in synaptosomal membranes [161] and it influences neuronal cellular function via interactions with cell-surface receptors such as integrins [222]. The involvement in the proper homeostatic functioning of hippocampal circuits [223], the association with integrins [224] and the modulation of synaptic NMDA activity are also features associated with PrP^C [119]. *In vivo*, PrP^C and Reelin demonstrate similar regulation throughout brain development, with both peaking early in post-natal development. To gain more insights into a possible interaction between PrP^C and Reelin we tested whether the

absence of PrP^C may cause impairments in the signaling pathway triggered by Reelin in the early postnatal mice hippocampus.

Reelin is a huge secretory serine protease, which appears in Western blot as several protein bands, ranging from 410 to 330 kDa. In the extracellular and/or post-endoplasmic environment it appears as subjected to proteolytic cleavage at two sites, which generate smaller fragments [225]. Differently from what had been previously reported [114] we did not find a significant difference in the expression levels of the full length Reelin between PrP^C WT and knock-out mice (Fig. 23 A-B). Interestingly, in the brains of PrP(ΔSTE) mice overexpressing and favoring the secretory-GPI-anchored ^{Sec}PrP expression [226] and in PrP(KH>II) mice, overexpressing and favoring the C-transmembrane form of PrP (^{CTM}PrP) [227] there seemed to be less Reelin in the 460 kDa bands (Fig. 23 C). Using antibodies raised against the Reelin N-terminal we found that the expression of the isoforms at 140 kDa and 70 kDa increased in the hippocampus of PrP-deficient mice (Fig. 23 A-B). A higher expression of the truncated forms of Reelin concomitant with a decrease of PrP^C expression was also found in different constructs. This suggests that our findings do not depend on the mice genetic background (Fig. 23 C) and that the absence of PrP^C might be associated with an increased processing of Reelin, mediated by a metalloproteinase, probably belonging to the adamalysins and astacins [135]. Adamalysin and astacin activity or expression might be differently modulated by the presence PrP^C. The proteolytic processing of Reelin has been reported to be important from a functional point of view, and the full activity of Reelin might require degradation of the full-length precursor to generate smaller, more active isoforms [129]. There is controversy over which cleavage product activates the Reelin signal transduction cascade on target cells. In some studies, the so-called central Reelin fragment, consisting of repeats 3– 6, has been proved crucial for receptor activation [131], whereas others claim that a smaller fragment, repeats 5– 6, is also important [228].

These observations, together with the higher PrP^C expression in the brain of Reeler mice than in their WT counterparts (Fig. 23 D), seem to reinforce the hypothesis of a compensatory expression for these two proteins.

The effects of Reelin are mediated by the concomitant binding of a pair of homologous cell surface receptors designated as apolipoprotein E receptor 2 (ApoER2) and very low-density lipoprotein receptor (VLDLR). We did not observe any significant difference in the expression levels of either receptor in the early postnatal hippocampi of PrP^C WT and PrP^C knock-out brains (Fig. 24 A-B). Differently from VLDLR, ApoER2 and PrP^C are mainly associated with lipid rafts. The possibility that they may form a complex is supported by coimmunoprecipitation experiments (Fig. 24 C). The existence of a functional interaction of PrP^C and lipoprotein receptors is also supported by the ability of the recPrP to form complexes with both recombinant and native ApoE [229].

Reelin-signaling is relayed by the Dab1 adaptor protein, interacting with the cytoplasmic tail of receptors and it is phosphorylated by Fyn and Src tyrosine kinases (SFK) [148]. Our observation that in the hippocampus of PrP knock-out mice the levels of activated Dab1 are higher than in PrP^C WT mice is controversial. On the one hand, the activation of the fyn kinase seems to be reduced in PrP knock-out mice [89] but on the other, partial Reelin fragments, whose levels are enhanced in absence of PrP^C, have been shown to be efficient in Dab1 phosphorylation assay [131]. The observation that in primary neuronal cell cultures the increased intracellular ROS generation and oxidative stress induced by treatment with the fibrillar PrP fragment PrP (106–126) is responsible for Dab1 phosphorylation [193] seems to be consistent with our results and with the increased susceptibility to neuronal damage by oxidative stress in absence of PrP^C [65].

Activated Dab1 suppresses the activities of glycogen synthase kinase-3β (GSK-3β), a kinase known to phosphorylate tau at multiple sites, including some of those found in neurofibrillary tangles (NFTs) [230]. Specific biochemical assays of brain lysates have shown that the activity of GSK-3β increased significantly in Reeler mice and that it was considerably higher in mice lacking both Reln and ApoE. Thus, the observation that the expression of Reelin products seems to be different in absence of PrP^C, led us to hypothesize a different activation of GSK-3β. Microarray analyses using RNA isolated from the hippocampus of newborn PrP^C WT and PrP^C knock-out mice have shown that the GSK-3β gene was downregulated in *Prnp*$^{0/0}$ mice [196]. Interestingly we observed that in PrP^C WT mice the levels of activated GSK-3β normalized on total Gsk3β were higher than in PrP^C knock-out mice (Fig. 26 A-B). This seems to agree with an higher phosphorylation

of Dab1, probably due to an increased activation of the two lipoprotein receptors by partial Reelin fragments in absence of PrP^C. Unlike other protein kinases, GSK-3 is constitutively active under resting conditions and is inactivated by extracellular signals through phosphorylation of an N-terminal serine residue, Ser-9 in GSK-3β and Ser-21 in GSK-3α. Various kinases have been implicated in mediating serine phosphorylation and inactivation of GSK-3, including PI3-kinase (PI3K)-regulated Akt/PKB, protein kinase A and protein kinase C (PKC) [231] [232]. We might hypothesize that the elevated PI3K activity in brain lysates from WT mice, as compared to PrP knock-out mice [102] results in a major phosphorylation of Ser21 on GSK-3α and Ser9 on GSK-3β. The latter inhibits GSK-3 activity and in turn might explain the higher phosphorylation levels of tau observed during early postnatal development in absence of PrP^C [196].

In this work we explored a possible involvement of PrP^C in the Reelin-signaling pathway in the early postnatal mouse hippocampus. Both proteins share some common features in the context of their physiological role in the hippocampus. Our observations suggest an interesting scenario in which the absence of PrP^C may provoke impairment in the downstream signaling events promoted by Reelin. Our findings lead us to hypothesize a functional crosstalk between PrP^C and the Reelin-signaling complex. This may contribute to explain the phenotype described in the hippocampus of PrP^C knock-out mice, namely the enhanced neuronal excitability that might be linked to a role for Reelin in the regulation of the NMDA receptor.

Bibliography

1. Zahn R, Liu A, Luhrs T, Riek R, von Schroetter C, et al. (2000) NMR solution structure of the human prion protein. Proc Natl Acad Sci U S A 97: 145-150.
2. Riek R, Hornemann S, Wider G, Billeter M, Glockshuber R, et al. (1996) NMR structure of the mouse prion protein domain PrP(121-231). Nature 382: 180-182.
3. Riek R, Hornemann S, Wider G, Glockshuber R, Wuthrich K (1997) NMR characterization of the full-length recombinant murine prion protein, mPrP(23-231). FEBS Lett 413: 282-288.
4. Singh N, Das D, Singh A, Mohan ML (2010) Prion protein and metal interaction: physiological and pathological implications. Curr Issues Mol Biol 12: 99-107.
5. Vey M, Pilkuhn S, Wille H, Nixon R, DeArmond SJ, et al. (1996) Subcellular colocalization of the cellular and scrapie prion proteins in caveolae-like membranous domains. Proc Natl Acad Sci U S A 93: 14945-14949.
6. Shi Q, Dong XP (2011) (Ctm)PrP and ER stress: a neurotoxic mechanism of some special PrP mutants. Prion 5: 123-125.
7. Chen SG, Teplow DB, Parchi P, Teller JK, Gambetti P, et al. (1995) Truncated forms of the human prion protein in normal brain and in prion diseases. J Biol Chem 270: 19173-19180.
8. Kaneko K, Zulianello L, Scott M, Cooper CM, Wallace AC, et al. (1997) Evidence for protein X binding to a discontinuous epitope on the cellular prion protein during scrapie prion propagation. Proc Natl Acad Sci U S A 94: 10069-10074.
9. Marella M, Lehmann S, Grassi J, Chabry J (2002) Filipin prevents pathological prion protein accumulation by reducing endocytosis and inducing cellular PrP release. J Biol Chem 277: 25457-25464.
10. Peters PJ, Mironov A, Jr., Peretz D, van Donselaar E, Leclerc E, et al. (2003) Trafficking of prion proteins through a caveolae-mediated endosomal pathway. J Cell Biol 162: 703-717.
11. Shyng SL, Heuser JE, Harris DA (1994) A glycolipid-anchored prion protein is endocytosed via clathrin-coated pits. J Cell Biol 125: 1239-1250.

12. Taylor DR, Watt NT, Perera WS, Hooper NM (2005) Assigning functions to distinct regions of the N-terminus of the prion protein that are involved in its copper-stimulated, clathrin-dependent endocytosis. J Cell Sci 118: 5141-5153.
13. Sunyach C, Jen A, Deng J, Fitzgerald KT, Frobert Y, et al. (2003) The mechanism of internalization of glycosylphosphatidylinositol-anchored prion protein. EMBO J 22: 3591-3601.
14. Lysek DA, Calzolai L, Wuthrich K (2004) NMR assignment of the chicken prion protein fragments chPrP(128-242) and chPrP(25-242). J Biomol NMR 30: 97.
15. Wopfner F, Weidenhofer G, Schneider R, von Brunn A, Gilch S, et al. (1999) Analysis of 27 mammalian and 9 avian PrPs reveals high conservation of flexible regions of the prion protein. J Mol Biol 289: 1163-1178.
16. Kim HO, Snyder GP, Blazey TM, Race RE, Chesebro B, et al. (2008) Prion disease induced alterations in gene expression in spleen and brain prior to clinical symptoms. Adv Appl Bioinform Chem 1: 29-50.
17. Uversky VN (2009) Intrinsically disordered proteins and their environment: effects of strong denaturants, temperature, pH, counter ions, membranes, binding partners, osmolytes, and macromolecular crowding. Protein J 28: 305-325.
18. Uversky VN, Dunker AK (2010) Understanding protein non-folding. Biochim Biophys Acta 1804: 1231-1264.
19. Wang F, Yin S, Wang X, Zha L, Sy MS, et al. (2010) Role of the highly conserved middle region of prion protein (PrP) in PrP-lipid interaction. Biochemistry 49: 8169-8176.
20. Gabus C, Auxilien S, Pechoux C, Dormont D, Swietnicki W, et al. (2001) The prion protein has DNA strand transfer properties similar to retroviral nucleocapsid protein. J Mol Biol 307: 1011-1021.
21. Zanata SM, Lopes MH, Mercadante AF, Hajj GN, Chiarini LB, et al. (2002) Stress-inducible protein 1 is a cell surface ligand for cellular prion that triggers neuroprotection. EMBO J 21: 3307-3316.
22. Parkyn CJ, Vermeulen EG, Mootoosamy RC, Sunyach C, Jacobsen C, et al. (2008) LRP1 controls biosynthetic and endocytic trafficking of neuronal prion protein. J Cell Sci 121: 773-783.

23. Lauren J, Gimbel DA, Nygaard HB, Gilbert JW, Strittmatter SM (2009) Cellular prion protein mediates impairment of synaptic plasticity by amyloid-beta oligomers. Nature 457: 1128-1132.

24. Steele AD, Lindquist S, Aguzzi A (2007) The prion protein knockout mouse: a phenotype under challenge. Prion 1: 83-93.

25. Linden R, Martins VR, Prado MA, Cammarota M, Izquierdo I, et al. (2008) Physiology of the prion protein. Physiol Rev 88: 673-728.

26. Pastore A, Zagari A (2007) A structural overview of the vertebrate prion proteins. Prion 1: 185-197.

27. Donne DG, Viles JH, Groth D, Mehlhorn I, James TL, et al. (1997) Structure of the recombinant full-length hamster prion protein PrP(29-231): the N terminus is highly flexible. Proc Natl Acad Sci U S A 94: 13452-13457.

28. Gossert AD, Bonjour S, Lysek DA, Fiorito F, Wuthrich K (2005) Prion protein NMR structures of elk and of mouse/elk hybrids. Proc Natl Acad Sci U S A 102: 646-650.

29. Christen B, Perez DR, Hornemann S, Wuthrich K (2008) NMR structure of the bank vole prion protein at 20 degrees C contains a structured loop of residues 165-171. J Mol Biol 383: 306-312.

30. Christen B, Hornemann S, Damberger FF, Wuthrich K (2009) Prion protein NMR structure from tammar wallaby (Macropus eugenii) shows that the beta2-alpha2 loop is modulated by long-range sequence effects. J Mol Biol 389: 833-845.

31. Wen Y, Li J, Yao W, Xiong M, Hong J, et al. (2010) Unique structural characteristics of the rabbit prion protein. J Biol Chem 285: 31682-31693.

32. Perez DR, Damberger FF, Wuthrich K (2010) Horse prion protein NMR structure and comparisons with related variants of the mouse prion protein. J Mol Biol 400: 121-128.

33. Sigurdson CJ, Nilsson KP, Hornemann S, Manco G, Fernandez-Borges N, et al. (2010) A molecular switch controls interspecies prion disease transmission in mice. J Clin Invest 120: 2590-2599.

34. Biljan I, Ilc G, Giachin G, Plavec J, Legname G (2012) Structural Rearrangements at Physiological pH: Nuclear Magnetic Resonance Insights from the V210I Human Prion Protein Mutant. Biochemistry.

35. Biljan I, Giachin G, Ilc G, Zhukov I, Plavec J, et al. (2012) Structural basis for the protective effect of the human prion protein carrying the dominant-negative E219K polymorphism. Biochem J 446: 243-251.

36. Biljan I, Ilc G, Giachin G, Raspadori A, Zhukov I, et al. (2011) Toward the molecular basis of inherited prion diseases: NMR structure of the human prion protein with V210I mutation. J Mol Biol 412: 660-673.

37. Ilc G, Giachin G, Jaremko M, Jaremko L, Benetti F, et al. (2010) NMR structure of the human prion protein with the pathological Q212P mutation reveals unique structural features. PLoS One 5: e11715.

38. Locht C, Chesebro B, Race R, Keith JM (1986) Molecular cloning and complete sequence of prion protein cDNA from mouse brain infected with the scrapie agent. Proc Natl Acad Sci U S A 83: 6372-6376.

39. Bueler H, Aguzzi A, Sailer A, Greiner RA, Autenried P, et al. (1993) Mice devoid of PrP are resistant to scrapie. Cell 73: 1339-1347.

40. Weissmann C, Fischer M, Raeber A, Bueler H, Sailer A, et al. (1996) The use of transgenic mice in the investigation of transmissible spongiform encephalopathies. Int J Exp Pathol 77: 283-293.

41. Manson JC, Clarke AR, Hooper ML, Aitchison L, McConnell I, et al. (1994) 129/Ola mice carrying a null mutation in PrP that abolishes mRNA production are developmentally normal. Mol Neurobiol 8: 121-127.

42. Sakaguchi S, Katamine S, Nishida N, Moriuchi R, Shigematsu K, et al. (1996) Loss of cerebellar Purkinje cells in aged mice homozygous for a disrupted PrP gene. Nature 380: 528-531.

43. Rossi D, Cozzio A, Flechsig E, Klein MA, Rulicke T, et al. (2001) Onset of ataxia and Purkinje cell loss in PrP null mice inversely correlated with Dpl level in brain. EMBO J 20: 694-702.

44. Moore RC, Mastrangelo P, Bouzamondo E, Heinrich C, Legname G, et al. (2001) Doppel-induced cerebellar degeneration in transgenic mice. Proc Natl Acad Sci U S A 98: 15288-15293.

45. Nishida N, Tremblay P, Sugimoto T, Shigematsu K, Shirabe S, et al. (1999) A mouse prion protein transgene rescues mice deficient for the prion protein gene from purkinje cell degeneration and demyelination. Lab Invest 79: 689-697.

46. Behrens A, Aguzzi A (2002) Small is not beautiful: antagonizing functions for the prion protein PrP(C) and its homologue Dpl. Trends Neurosci 25: 150-154.

47. Telling GC, Haga T, Torchia M, Tremblay P, DeArmond SJ, et al. (1996) Interactions between wild-type and mutant prion proteins modulate neurodegeneration in transgenic mice. Genes Dev 10: 1736-1750.

48. Shmerling D, Hegyi I, Fischer M, Blattler T, Brandner S, et al. (1998) Expression of amino-terminally truncated PrP in the mouse leading to ataxia and specific cerebellar lesions. Cell 93: 203-214.

49. Radovanovic I, Braun N, Giger OT, Mertz K, Miele G, et al. (2005) Truncated prion protein and Doppel are myelinotoxic in the absence of oligodendrocytic PrPC. J Neurosci 25: 4879-4888.

50. Baumann F, Tolnay M, Brabeck C, Pahnke J, Kloz U, et al. (2007) Lethal recessive myelin toxicity of prion protein lacking its central domain. EMBO J 26: 538-547.

51. Li A, Barmada SJ, Roth KA, Harris DA (2007) N-terminally deleted forms of the prion protein activate both Bax-dependent and Bax-independent neurotoxic pathways. J Neurosci 27: 852-859.

52. Colby DW, Prusiner SB (2011) Prions. Cold Spring Harb Perspect Biol 3: a006833.

53. Stolp HB, Ek CJ, Johansson PA, Dziegielewska KM, Bethge N, et al. (2009) Factors involved in inflammation-induced developmental white matter damage. Neurosci Lett 451: 232-236.

54. Saunders NR, Kitchener P, Knott GW, Nicholls JG, Potter A, et al. (1998) Development of walking, swimming and neuronal connections after complete spinal cord transection in the neonatal opossum, Monodelphis domestica. J Neurosci 18: 339-355.

55. Smith KK (2001) Early development of the neural plate, neural crest and facial region of marsupials. J Anat 199: 121-131.

56. Mikkelsen TS, Wakefield MJ, Aken B, Amemiya CT, Chang JL, et al. (2007) Genome of the marsupial Monodelphis domestica reveals innovation in non-coding sequences. Nature 447: 167-177.

57. Samollow PB (2008) The opossum genome: insights and opportunities from an alternative mammal. Genome Res 18: 1199-1215.

58. Keyte AL, Smith KK (2008) Basic Maintenance and Breeding of the Opossum Monodelphis domestica. CSH Protoc 2008: pdb prot5073.

59. Aguzzi A, Baumann F, Bremer J (2008) The prion's elusive reason for being. Annu Rev Neurosci 31: 439-477.

60. Roucou X, LeBlanc AC (2005) Cellular prion protein neuroprotective function: implications in prion diseases. J Mol Med (Berl) 83: 3-11.

61. Bounhar Y, Zhang Y, Goodyer CG, LeBlanc A (2001) Prion protein protects human neurons against Bax-mediated apoptosis. J Biol Chem 276: 39145-39149.

62. Shyu WC, Lin SZ, Chiang MF, Ding DC, Li KW, et al. (2005) Overexpression of PrPC by adenovirus-mediated gene targeting reduces ischemic injury in a stroke rat model. J Neurosci 25: 8967-8977.

63. Spudich A, Frigg R, Kilic E, Kilic U, Oesch B, et al. (2005) Aggravation of ischemic brain injury by prion protein deficiency: role of ERK-1/-2 and STAT-1. Neurobiol Dis 20: 442-449.

64. White AR, Collins SJ, Maher F, Jobling MF, Stewart LR, et al. (1999) Prion protein-deficient neurons reveal lower glutathione reductase activity and increased susceptibility to hydrogen peroxide toxicity. Am J Pathol 155: 1723-1730.

65. Brown DR, Schulz-Schaeffer WJ, Schmidt B, Kretzschmar HA (1997) Prion protein-deficient cells show altered response to oxidative stress due to decreased SOD-1 activity. Exp Neurol 146: 104-112.

66. Brown DR, Wong BS, Hafiz F, Clive C, Haswell SJ, et al. (1999) Normal prion protein has an activity like that of superoxide dismutase. Biochem J 344 Pt 1: 1-5.

67. Waggoner DJ, Drisaldi B, Bartnikas TB, Casareno RL, Prohaska JR, et al. (2000) Brain copper content and cuproenzyme activity do not vary with prion protein expression level. J Biol Chem 275: 7455-7458.

68. Hutter G, Heppner FL, Aguzzi A (2003) No superoxide dismutase activity of cellular prion protein in vivo. Biol Chem 384: 1279-1285.

69. Choi SI, Ju WK, Choi EK, Kim J, Lea HZ, et al. (1998) Mitochondrial dysfunction induced by oxidative stress in the brains of hamsters infected with the 263 K scrapie agent. Acta Neuropathol 96: 279-286.

70. Miele G, Jeffrey M, Turnbull D, Manson J, Clinton M (2002) Ablation of cellular prion protein expression affects mitochondrial numbers and morphology. Biochem Biophys Res Commun 291: 372-377.

71. Herms J, Tings T, Gall S, Madlung A, Giese A, et al. (1999) Evidence of presynaptic location and function of the prion protein. J Neurosci 19: 8866-8875.

72. Moya KL, Sales N, Hassig R, Creminon C, Grassi J, et al. (2000) Immunolocalization of the cellular prion protein in normal brain. Microsc Res Tech 50: 58-65.

73. Grigoriev V, Escaig-Haye F, Streichenberger N, Kopp N, Langeveld J, et al. (1999) Submicroscopic immunodetection of PrP in the brain of a patient with a new-variant of Creutzfeldt-Jakob disease. Neurosci Lett 264: 57-60.

74. Ferrer I, Rivera R, Blanco R, Marti E (1999) Expression of proteins linked to exocytosis and neurotransmission in patients with Creutzfeldt-Jakob disease. Neurobiol Dis 6: 92-100.

75. Bouzamondo-Bernstein E, Hopkins SD, Spilman P, Uyehara-Lock J, Deering C, et al. (2004) The neurodegeneration sequence in prion diseases: evidence from functional, morphological and ultrastructural studies of the GABAergic system. J Neuropathol Exp Neurol 63: 882-899.

76. Collinge J, Whittington MA, Sidle KC, Smith CJ, Palmer MS, et al. (1994) Prion protein is necessary for normal synaptic function. Nature 370: 295-297.

77. Huber R, Deboer T, Tobler I (1999) Prion protein: a role in sleep regulation? J Sleep Res 8 Suppl 1: 30-36.

78. Criado JR, Sanchez-Alavez M, Conti B, Giacchino JL, Wills DN, et al. (2005) Mice devoid of prion protein have cognitive deficits that are rescued by reconstitution of PrP in neurons. Neurobiol Dis 19: 255-265.

79. Gohel C, Grigoriev V, Escaig-Haye F, Lasmezas CI, Deslys JP, et al. (1999) Ultrastructural localization of cellular prion protein (PrPc) at the neuromuscular junction. J Neurosci Res 55: 261-267.

80. Re L, Rossini F, Re F, Bordicchia M, Mercanti A, et al. (2006) Prion protein potentiates acetylcholine release at the neuromuscular junction. Pharmacol Res 53: 62-68.

81. Rieger R, Edenhofer F, Lasmezas CI, Weiss S (1997) The human 37-kDa laminin receptor precursor interacts with the prion protein in eukaryotic cells. Nat Med 3: 1383-1388.

82. Graner E, Mercadante AF, Zanata SM, Forlenza OV, Cabral AL, et al. (2000) Cellular prion protein binds laminin and mediates neuritogenesis. Brain Res Mol Brain Res 76: 85-92.

83. Gauczynski S, Peyrin JM, Haik S, Leucht C, Hundt C, et al. (2001) The 37-kDa/67-kDa laminin receptor acts as the cell-surface receptor for the cellular prion protein. EMBO J 20: 5863-5875.

84. Schmitt-Ulms G, Legname G, Baldwin MA, Ball HL, Bradon N, et al. (2001) Binding of neural cell adhesion molecules (N-CAMs) to the cellular prion protein. J Mol Biol 314: 1209-1225.

85. Lopes MH, Hajj GN, Muras AG, Mancini GL, Castro RM, et al. (2005) Interaction of cellular prion and stress-inducible protein 1 promotes neuritogenesis and neuroprotection by distinct signaling pathways. J Neurosci 25: 11330-11339.

86. Chen S, Mange A, Dong L, Lehmann S, Schachner M (2003) Prion protein as trans-interacting partner for neurons is involved in neurite outgrowth and neuronal survival. Mol Cell Neurosci 22: 227-233.

87. Steele AD, Emsley JG, Ozdinler PH, Lindquist S, Macklis JD (2006) Prion protein (PrPc) positively regulates neural precursor proliferation during developmental and adult mammalian neurogenesis. Proc Natl Acad Sci U S A 103: 3416-3421.

88. Mouillet-Richard S, Schneider B, Pradines E, Pietri M, Ermonval M, et al. (2007) Cellular prion protein signaling in serotonergic neuronal cells. Ann N Y Acad Sci 1096: 106-119.

89. Santuccione A, Sytnyk V, Leshchyns'ka I, Schachner M (2005) Prion protein recruits its neuronal receptor NCAM to lipid rafts to activate p59fyn and to enhance neurite outgrowth. J Cell Biol 169: 341-354.

90. He Q, Meiri KF (2002) Isolation and characterization of detergent-resistant microdomains responsive to NCAM-mediated signaling from growth cones. Mol Cell Neurosci 19: 18-31.

91. Taylor DR, Hooper NM (2006) The prion protein and lipid rafts. Mol Membr Biol 23: 89-99.

92. Chiarini LB, Freitas AR, Zanata SM, Brentani RR, Martins VR, et al. (2002) Cellular prion protein transduces neuroprotective signals. EMBO J 21: 3317-3326.

93. Sunyach C, Checler F (2005) Combined pharmacological, mutational and cell biology approaches indicate that p53-dependent caspase 3 activation triggered by cellular prion is dependent on its endocytosis. J Neurochem 92: 1399-1407.

94. Kanaani J, Prusiner SB, Diacovo J, Baekkeskov S, Legname G (2005) Recombinant prion protein induces rapid polarization and development of synapses in embryonic rat hippocampal neurons in vitro. J Neurochem 95: 1373-1386.

95. Mouillet-Richard S, Pietri M, Schneider B, Vidal C, Mutel V, et al. (2005) Modulation of serotonergic receptor signaling and cross-talk by prion protein. J Biol Chem 280: 4592-4601.

96. Cooper DM, Crossthwaite AJ (2006) Higher-order organization and regulation of adenylyl cyclases. Trends Pharmacol Sci 27: 426-431.

97. Schneider B, Mutel V, Pietri M, Ermonval M, Mouillet-Richard S, et al. (2003) NADPH oxidase and extracellular regulated kinases 1/2 are targets of prion protein signaling in neuronal and nonneuronal cells. Proc Natl Acad Sci U S A 100: 13326-13331.

98. Krebs B, Dorner-Ciossek C, Schmalzbauer R, Vassallo N, Herms J, et al. (2006) Prion protein induced signaling cascades in monocytes. Biochem Biophys Res Commun 340: 13-22.

99. Mouillet-Richard S, Ermonval M, Chebassier C, Laplanche JL, Lehmann S, et al. (2000) Signal transduction through prion protein. Science 289: 1925-1928.

100. Botto L, Masserini M, Cassetti A, Palestini P (2004) Immunoseparation of Prion protein-enriched domains from other detergent-resistant membrane fractions, isolated from neuronal cells. FEBS Lett 557: 143-147.

101. Mazzoni IE, Ledebur HC, Jr., Paramithiotis E, Cashman N (2005) Lymphoid signal transduction mechanisms linked to cellular prion protein. Biochem Cell Biol 83: 644-653.

102. Vassallo N, Herms J, Behrens C, Krebs B, Saeki K, et al. (2005) Activation of phosphatidylinositol 3-kinase by cellular prion protein and its role in cell survival. Biochem Biophys Res Commun 332: 75-82.

103. Weise J, Sandau R, Schwarting S, Crome O, Wrede A, et al. (2006) Deletion of cellular prion protein results in reduced Akt activation, enhanced postischemic caspase-3 activation, and exacerbation of ischemic brain injury. Stroke 37: 1296-1300.

104. Simons K, Ikonen E (1997) Functional rafts in cell membranes. Nature 387: 569-572.

105. Mayor S, Maxfield FR (1995) Insolubility and redistribution of GPI-anchored proteins at the cell surface after detergent treatment. Mol Biol Cell 6: 929-944.

106. Naslavsky N, Shmeeda H, Friedlander G, Yanai A, Futerman AH, et al. (1999) Sphingolipid depletion increases formation of the scrapie prion protein in neuroblastoma cells infected with prions. J Biol Chem 274: 20763-20771.

107. Taraboulos A, Scott M, Semenov A, Avrahami D, Laszlo L, et al. (1995) Cholesterol depletion and modification of COOH-terminal targeting sequence of the prion protein inhibit formation of the scrapie isoform. J Cell Biol 129: 121-132.

108. Ivanova L, Barmada S, Kummer T, Harris DA (2001) Mutant prion proteins are partially retained in the endoplasmic reticulum. J Biol Chem 276: 42409-42421.

109. Magalhaes AC, Silva JA, Lee KS, Martins VR, Prado VF, et al. (2002) Endocytic intermediates involved with the intracellular trafficking of a fluorescent cellular prion protein. J Biol Chem 277: 33311-33318.

110. Brown DR, Qin K, Herms JW, Madlung A, Manson J, et al. (1997) The cellular prion protein binds copper in vivo. Nature 390: 684-687.

111. Lee KS, Magalhaes AC, Zanata SM, Brentani RR, Martins VR, et al. (2001) Internalization of mammalian fluorescent cellular prion protein and N-terminal deletion mutants in living cells. J Neurochem 79: 79-87.

112. Graner E, Mercadante AF, Zanata SM, Martins VR, Jay DG, et al. (2000) Laminin-induced PC-12 cell differentiation is inhibited following laser inactivation of cellular prion protein. FEBS Lett 482: 257-260.

113. Biasini E, Turnbaugh JA, Unterberger U, Harris DA (2012) Prion protein at the crossroads of physiology and disease. Trends Neurosci 35: 92-103.

114. Devanathan V, Jakovcevski I, Santuccione A, Li S, Lee HJ, et al. (2010) Cellular form of prion protein inhibits Reelin-mediated shedding of Caspr from the neuronal cell surface to potentiate Caspr-mediated inhibition of neurite outgrowth. J Neurosci 30: 9292-9305.

115. Malaga-Trillo E, Solis GP, Schrock Y, Geiss C, Luncz L, et al. (2009) Regulation of embryonic cell adhesion by the prion protein. PLoS Biol 7: e55.

116. Mallucci GR, Ratte S, Asante EA, Linehan J, Gowland I, et al. (2002) Post-natal knockout of prion protein alters hippocampal CA1 properties, but does not result in neurodegeneration. EMBO J 21: 202-210.

117. Herms JW, Tings T, Dunker S, Kretzschmar HA (2001) Prion protein affects Ca2+-activated K+ currents in cerebellar purkinje cells. Neurobiol Dis 8: 324-330.

118. Walz R, Amaral OB, Rockenbach IC, Roesler R, Izquierdo I, et al. (1999) Increased sensitivity to seizures in mice lacking cellular prion protein. Epilepsia 40: 1679-1682.

119. Khosravani H, Zhang Y, Tsutsui S, Hameed S, Altier C, et al. (2008) Prion protein attenuates excitotoxicity by inhibiting NMDA receptors. J Cell Biol 181: 551-565.

120. Rangel A, Burgaya F, Gavin R, Soriano E, Aguzzi A, et al. (2007) Enhanced susceptibility of Prnp-deficient mice to kainate-induced seizures, neuronal apoptosis, and death: Role of AMPA/kainate receptors. J Neurosci Res 85: 2741-2755.

121. Beraldo FH, Arantes CP, Santos TG, Machado CF, Roffe M, et al. (2011) Metabotropic glutamate receptors transduce signals for neurite outgrowth after binding of the prion protein to laminin gamma1 chain. FASEB J 25: 265-279.

122. Solomon IH, Huettner JE, Harris DA (2010) Neurotoxic mutants of the prion protein induce spontaneous ionic currents in cultured cells. J Biol Chem 285: 26719-26726.

123. Solomon IH, Khatri N, Biasini E, Massignan T, Huettner JE, et al. (2011) An N-terminal polybasic domain and cell surface localization are required for mutant prion protein toxicity. J Biol Chem 286: 14724-14736.

124. Peles E, Salzer JL (2000) Molecular domains of myelinated axons. Curr Opin Neurobiol 10: 558-565.

125. Lambert de Rouvroit C, Goffinet AM (1998) The reeler mouse as a model of brain development. Adv Anat Embryol Cell Biol 150: 1-106.

126. Rice DS, Nusinowitz S, Azimi AM, Martinez A, Soriano E, et al. (2001) The reelin pathway modulates the structure and function of retinal synaptic circuitry. Neuron 31: 929-941.

127. Hong SE, Shugart YY, Huang DT, Shahwan SA, Grant PE, et al. (2000) Autosomal recessive lissencephaly with cerebellar hypoplasia is associated with human RELN mutations. Nat Genet 26: 93-96.

128. DeSilva U, D'Arcangelo G, Braden VV, Chen J, Miao GG, et al. (1997) The human reelin gene: isolation, sequencing, and mapping on chromosome 7. Genome Res 7: 157-164.

129. Smalheiser NR, Costa E, Guidotti A, Impagnatiello F, Auta J, et al. (2000) Expression of reelin in adult mammalian blood, liver, pituitary pars intermedia, and adrenal chromaffin cells. Proc Natl Acad Sci U S A 97: 1281-1286.

130. Lugli G, Krueger JM, Davis JM, Persico AM, Keller F, et al. (2003) Methodological factors influencing measurement and processing of plasma reelin in humans. BMC Biochem 4: 9.

131. Quattrocchi CC, Wannenes F, Persico AM, Ciafre SA, D'Arcangelo G, et al. (2002) Reelin is a serine protease of the extracellular matrix. J Biol Chem 277: 303-309.

132. Dityatev A, Schachner M (2003) Extracellular matrix molecules and synaptic plasticity. Nat Rev Neurosci 4: 456-468.

133. Jossin Y, Ignatova N, Hiesberger T, Herz J, Lambert de Rouvroit C, et al. (2004) The central fragment of Reelin, generated by proteolytic processing in vivo, is critical to its function during cortical plate development. J Neurosci 24: 514-521.

134. Nogi T, Yasui N, Hattori M, Iwasaki K, Takagi J (2006) Structure of a signaling-competent reelin fragment revealed by X-ray crystallography and electron tomography. EMBO J 25: 3675-3683.

135. Lambert de Rouvroit C, de Bergeyck V, Cortvrindt C, Bar I, Eeckhout Y, et al. (1999) Reelin, the extracellular matrix protein deficient in reeler mutant mice, is processed by a metalloproteinase. Exp Neurol 156: 214-217.

136. D'Arcangelo G, Nakajima K, Miyata T, Ogawa M, Mikoshiba K, et al. (1997) Reelin is a secreted glycoprotein recognized by the CR-50 monoclonal antibody. J Neurosci 17: 23-31.

137. Utsunomiya-Tate N, Kubo K, Tate S, Kainosho M, Katayama E, et al. (2000) Reelin molecules assemble together to form a large protein complex, which is inhibited by the function-blocking CR-50 antibody. Proc Natl Acad Sci U S A 97: 9729-9734.

138. Katsuyama Y, Terashima T (2009) Developmental anatomy of reeler mutant mouse. Dev Growth Differ 51: 271-286.

139. D'Arcangelo G, Curran T (1998) Reeler: new tales on an old mutant mouse. Bioessays 20: 235-244.

140. Weiss KH, Johanssen C, Tielsch A, Herz J, Deller T, et al. (2003) Malformation of the radial glial scaffold in the dentate gyrus of reeler mice, scrambler mice, and ApoER2/VLDLR-deficient mice. J Comp Neurol 460: 56-65.

141. Zhao S, Chai X, Frotscher M (2007) Balance between neurogenesis and gliogenesis in the adult hippocampus: role for reelin. Dev Neurosci 29: 84-90.

142. Alcantara S, Ruiz M, D'Arcangelo G, Ezan F, de Lecea L, et al. (1998) Regional and cellular patterns of reelin mRNA expression in the forebrain of the developing and adult mouse. J Neurosci 18: 7779-7799.

143. Angevine JB, Jr., Sidman RL (1961) Autoradiographic study of cell migration during histogenesis of cerebral cortex in the mouse. Nature 192: 766-768.

144. Caviness VS, Jr., Sidman RL (1973) Retrohippocampal, hippocampal and related structures of the forebrain in the reeler mutant mouse. J Comp Neurol 147: 235-254.

145. Caviness VS, Jr., Sidman RL (1973) Time of origin or corresponding cell classes in the cerebral cortex of normal and reeler mutant mice: an autoradiographic analysis. J Comp Neurol 148: 141-151.

146. Hiesberger T, Trommsdorff M, Howell BW, Goffinet A, Mumby MC, et al. (1999) Direct binding of Reelin to VLDL receptor and ApoE receptor 2 induces tyrosine phosphorylation of disabled-1 and modulates tau phosphorylation. Neuron 24: 481-489.

147. Trommsdorff M, Gotthardt M, Hiesberger T, Shelton J, Stockinger W, et al. (1999) Reeler/Disabled-like disruption of neuronal migration in knockout mice lacking the VLDL receptor and ApoE receptor 2. Cell 97: 689-701.

148. Herz J, Chen Y (2006) Reelin, lipoprotein receptors and synaptic plasticity. Nat Rev Neurosci 7: 850-859.

149. Ballif BA, Arnaud L, Cooper JA (2003) Tyrosine phosphorylation of Disabled-1 is essential for Reelin-stimulated activation of Akt and Src family kinases. Brain Res Mol Brain Res 117: 152-159.

150. Bock HH, Herz J (2003) Reelin activates SRC family tyrosine kinases in neurons. Curr Biol 13: 18-26.

151. Assadi AH, Zhang G, Beffert U, McNeil RS, Renfro AL, et al. (2003) Interaction of reelin signaling and Lis1 in brain development. Nat Genet 35: 270-276.

152. Bock HH, Jossin Y, Liu P, Forster E, May P, et al. (2003) Phosphatidylinositol 3-kinase interacts with the adaptor protein Dab1 in response to Reelin signaling and is required for normal cortical lamination. J Biol Chem 278: 38772-38779.

153. Beffert U, Morfini G, Bock HH, Reyna H, Brady ST, et al. (2002) Reelin-mediated signaling locally regulates protein kinase B/Akt and glycogen synthase kinase 3beta. J Biol Chem 277: 49958-49964.

154. Arnaud L, Ballif BA, Cooper JA (2003) Regulation of protein tyrosine kinase signaling by substrate degradation during brain development. Mol Cell Biol 23: 9293-9302.

155. Morimura T, Hattori M, Ogawa M, Mikoshiba K (2005) Disabled1 regulates the intracellular trafficking of reelin receptors. J Biol Chem 280: 16901-16908.

156. Bock HH, Jossin Y, May P, Bergner O, Herz J (2004) Apolipoprotein E receptors are required for reelin-induced proteasomal degradation of the neuronal adaptor protein Disabled-1. J Biol Chem 279: 33471-33479.

157. Rice DS, Curran T (2001) Role of the reelin signaling pathway in central nervous system development. Annu Rev Neurosci 24: 1005-1039.

158. Lavdas AA, Grigoriou M, Pachnis V, Parnavelas JG (1999) The medial ganglionic eminence gives rise to a population of early neurons in the developing cerebral cortex. J Neurosci 19: 7881-7888.

159. Weeber EJ, Beffert U, Jones C, Christian JM, Forster E, et al. (2002) Reelin and ApoE receptors cooperate to enhance hippocampal synaptic plasticity and learning. J Biol Chem 277: 39944-39952.

160. Chen Y, Beffert U, Ertunc M, Tang TS, Kavalali ET, et al. (2005) Reelin modulates NMDA receptor activity in cortical neurons. J Neurosci 25: 8209-8216.

161. Beffert U, Weeber EJ, Durudas A, Qiu S, Masiulis I, et al. (2005) Modulation of synaptic plasticity and memory by Reelin involves differential splicing of the lipoprotein receptor Apoer2. Neuron 47: 567-579.

162. Stockinger W, Brandes C, Fasching D, Hermann M, Gotthardt M, et al. (2000) The reelin receptor ApoER2 recruits JNK-interacting proteins-1 and -2. J Biol Chem 275: 25625-25632.

163. Ovadia G, Shifman S (2011) The genetic variation of RELN expression in schizophrenia and bipolar disorder. PLoS One 6: e19955.

164. Haas CA, Dudeck O, Kirsch M, Huszka C, Kann G, et al. (2002) Role for reelin in the development of granule cell dispersion in temporal lobe epilepsy. J Neurosci 22: 5797-5802.

165. Villeda SA, Akopians AL, Babayan AH, Basbaum AI, Phelps PE (2006) Absence of Reelin results in altered nociception and aberrant neuronal positioning in the dorsal spinal cord. Neuroscience 139: 1385-1396.

166. Kocherhans S, Madhusudan A, Doehner J, Breu KS, Nitsch RM, et al. (2010) Reduced Reelin expression accelerates amyloid-beta plaque formation and tau pathology in transgenic Alzheimer's disease mice. J Neurosci 30: 9228-9240.

167. Aguzzi A, Sigurdson C, Heikenwaelder M (2008) Molecular mechanisms of prion pathogenesis. Annu Rev Pathol 3: 11-40.

168. Collinge J, Clarke AR (2007) A general model of prion strains and their pathogenicity. Science 318: 930-936.

169. Balducci C, Beeg M, Stravalaci M, Bastone A, Sclip A, et al. (2010) Synthetic amyloid-beta oligomers impair long-term memory independently of cellular prion protein. Proc Natl Acad Sci U S A 107: 2295-2300.

170. Calella AM, Farinelli M, Nuvolone M, Mirante O, Moos R, et al. (2010) Prion protein and Abeta-related synaptic toxicity impairment. EMBO Mol Med 2: 306-314.

171. Cisse M, Sanchez PE, Kim DH, Ho K, Yu GQ, et al. (2011) Ablation of cellular prion protein does not ameliorate abnormal neural network activity or cognitive dysfunction in the J20 line of human amyloid precursor protein transgenic mice. J Neurosci 31: 10427-10431.

172. Brandner S, Isenmann S, Raeber A, Fischer M, Sailer A, et al. (1996) Normal host prion protein necessary for scrapie-induced neurotoxicity. Nature 379: 339-343.

173. Aguzzi A, Calella AM (2009) Prions: protein aggregation and infectious diseases. Physiol Rev 89: 1105-1152.

174. You H, Tsutsui S, Hameed S, Kannanayakal TJ, Chen L, et al. (2012) Abeta neurotoxicity depends on interactions between copper ions, prion protein, and N-methyl-D-aspartate receptors. Proc Natl Acad Sci U S A 109: 1737-1742.

175. Hegde RS, Mastrianni JA, Scott MR, DeFea KA, Tremblay P, et al. (1998) A transmembrane form of the prion protein in neurodegenerative disease. Science 279: 827-834.

176. Chakrabarti O, Hegde RS (2009) Functional depletion of mahogunin by cytosolically exposed prion protein contributes to neurodegeneration. Cell 137: 1136-1147.

177. Peretz D, Williamson RA, Kaneko K, Vergara J, Leclerc E, et al. (2001) Antibodies inhibit prion propagation and clear cell cultures of prion infectivity. Nature 412: 739-743.

178. Safar JG, DeArmond SJ, Kociuba K, Deering C, Didorenko S, et al. (2005) Prion clearance in bigenic mice. J Gen Virol 86: 2913-2923.

179. Mallucci G, Dickinson A, Linehan J, Klohn PC, Brandner S, et al. (2003) Depleting neuronal PrP in prion infection prevents disease and reverses spongiosis. Science 302: 871-874.

180. Lledo PM, Tremblay P, DeArmond SJ, Prusiner SB, Nicoll RA (1996) Mice deficient for prion protein exhibit normal neuronal excitability and synaptic transmission in the hippocampus. Proc Natl Acad Sci U S A 93: 2403-2407.

181. Puzzolo E, Mallamaci A (2010) Cortico-cerebral histogenesis in the opossum Monodelphis domestica: generation of a hexalaminar neocortex in the absence of a basal proliferative compartment. Neural Dev 5: 8.

182. Taraboulos A, Jendroska K, Serban D, Yang SL, DeArmond SJ, et al. (1992) Regional mapping of prion proteins in brain. Proc Natl Acad Sci U S A 89: 7620-7624.

183. Deng JB, Yu DM, Li MS (2006) Formation of the entorhino-hippocampal pathway: a tracing study in vitro and in vivo. Neurosci Bull 22: 305-314.

184. Lee Y, Davis M (1997) Role of the hippocampus, the bed nucleus of the stria terminalis, and the amygdala in the excitatory effect of corticotropin-releasing hormone on the acoustic startle reflex. J Neurosci 17: 6434-6446.

185. Guillery RW, Harting JK (2003) Structure and connections of the thalamic reticular nucleus: Advancing views over half a century. J Comp Neurol 463: 360-371.

186. Sales N, Hassig R, Rodolfo K, Di Giamberardino L, Traiffort E, et al. (2002) Developmental expression of the cellular prion protein in elongating axons. Eur J Neurosci 15: 1163-1177.

187. Mihrshahi R (2006) The corpus callosum as an evolutionary innovation. J Exp Zool B Mol Dev Evol 306: 8-17.

188. Romay-Tallon R, Dopeso-Reyes IG, Lussier AL, Kalynchuk LE, Caruncho HJ (2010) The coexpression of reelin and neuronal nitric oxide synthase in a subpopulation of dentate gyrus neurons is downregulated in heterozygous reeler mice. Neural Plast 2010: 130429.

189. Beffert U, Durudas A, Weeber EJ, Stolt PC, Giehl KM, et al. (2006) Functional dissection of Reelin signaling by site-directed disruption of Disabled-1 adaptor binding to apolipoprotein E receptor 2: distinct roles in development and synaptic plasticity. J Neurosci 26: 2041-2052.

190. Bueler H, Fischer M, Lang Y, Bluethmann H, Lipp HP, et al. (1992) Normal development and behaviour of mice lacking the neuronal cell-surface PrP protein. Nature 356: 577-582.

191. Duit S, Mayer H, Blake SM, Schneider WJ, Nimpf J (2010) Differential functions of ApoER2 and very low density lipoprotein receptor in Reelin signaling depend on differential sorting of the receptors. J Biol Chem 285: 4896-4908.

192. Howell BW, Herrick TM, Hildebrand JD, Zhang Y, Cooper JA (2000) Dab1 tyrosine phosphorylation sites relay positional signals during mouse brain development. Curr Biol 10: 877-885.

193. Gavin R, Urena J, Rangel A, Pastrana MA, Requena JR, et al. (2008) Fibrillar prion peptide PrP(106-126) treatment induces Dab1 phosphorylation and impairs APP processing and Abeta production in cortical neurons. Neurobiol Dis 30: 243-254.

194. Hughes K, Nikolakaki E, Plyte SE, Totty NF, Woodgett JR (1993) Modulation of the glycogen synthase kinase-3 family by tyrosine phosphorylation. EMBO J 12: 803-808.

195. Wang QM, Fiol CJ, DePaoli-Roach AA, Roach PJ (1994) Glycogen synthase kinase-3 beta is a dual specificity kinase differentially regulated by tyrosine and serine/threonine phosphorylation. J Biol Chem 269: 14566-14574.

196. Benvegnu S, Roncaglia P, Agostini F, Casalone C, Corona C, et al. (2011) Developmental influence of the cellular prion protein on the gene expression profile in mouse hippocampus. Physiol Genomics 43: 711-725.

197. Perez M, Rojo AI, Wandosell F, Diaz-Nido J, Avila J (2003) Prion peptide induces neuronal cell death through a pathway involving glycogen synthase kinase 3. Biochem J 372: 129-136.

198. Rogers JT, Weeber EJ (2008) Reelin and apoE actions on signal transduction, synaptic function and memory formation. Neuron Glia Biol 4: 259-270.

199. Meyer G, Soria JM, Martinez-Galan JR, Martin-Clemente B, Fairen A (1998) Different origins and developmental histories of transient neurons in the marginal zone of the fetal and neonatal rat cortex. J Comp Neurol 397: 493-518.

200. Bertrand S, Lacaille JC (2001) Unitary synaptic currents between lacunosum-moleculare interneurones and pyramidal cells in rat hippocampus. J Physiol 532: 369-384.

201. Deng PY, Porter JE, Shin HS, Lei S (2006) Thyrotropin-releasing hormone increases GABA release in rat hippocampus. J Physiol 577: 497-511.

202. Jeffrey M, McGovern G, Goodsir CM, Brown KL, Bruce ME (2000) Sites of prion protein accumulation in scrapie-infected mouse spleen revealed by immuno-electron microscopy. J Pathol 191: 323-332.

203. Cunningham C, Deacon R, Wells H, Boche D, Waters S, et al. (2003) Synaptic changes characterize early behavioural signs in the ME7 model of murine prion disease. Eur J Neurosci 17: 2147-2155.

204. Prusiner SB, DeArmond SJ (1994) Prion diseases and neurodegeneration. Annu Rev Neurosci 17: 311-339.

205. Jan JE, Reiter RJ, Wasdell MB, Bax M (2009) The role of the thalamus in sleep, pineal melatonin production, and circadian rhythm sleep disorders. J Pineal Res 46: 1-7.

206. Gambetti P, Parchi P, Petersen RB, Chen SG, Lugaresi E (1995) Fatal familial insomnia and familial Creutzfeldt-Jakob disease: clinical, pathological and molecular features. Brain Pathol 5: 43-51.

207. Montagna P, Cortelli P, Gambetti P, Lugaresi E (1995) Fatal familial insomnia: sleep, neuroendocrine and vegetative alterations. Adv Neuroimmunol 5: 13-21.

208. Rivkees SA, Fox CA, Jacobson CD, Reppert SM (1988) Anatomic and functional development of the suprachiasmatic nuclei in the gray short-tailed opossum. J Neurosci 8: 4269-4276.

209. Filley CM (2010) White matter: organization and functional relevance. Neuropsychol Rev 20: 158-173.

210. Legname G, Nguyen HO, Baskakov IV, Cohen FE, Dearmond SJ, et al. (2005) Strain-specified characteristics of mouse synthetic prions. Proc Natl Acad Sci U S A 102: 2168-2173.

211. Chianini F, Fernandez-Borges N, Vidal E, Gibbard L, Pintado B, et al. (2012) Rabbits are not resistant to prion infection. Proc Natl Acad Sci U S A 109: 5080-5085.

212. Telling GC (2012) Chronic wasting disease transmission and pathogenesis in cervid and non-cervid species. In: Chernoff YO, editor. Prion 2012. Amsterdam, The Netherlands: Landes Bioscience. pp. 7.

213. Perez DR, Damberger FF, Wuthrich K (2010) Erratum to "Horse Prion Protein NMR Structure and Comparisons with Related Variants of the Mouse Prion Protein" [J. Mol. Biol. 400/2 (2010) 121-128]. J Mol Biol.

214. Rossetti G, Giachin G, Legname G, Carloni P (2010) Structural facets of disease-linked human prion protein mutants: a molecular dynamic study. Proteins 78: 3270-3280.

215. Moser M, Colello RJ, Pott U, Oesch B (1995) Developmental expression of the prion protein gene in glial cells. Neuron 14: 509-517.

216. Kordek R, Hainfellner JA, Liberski PP, Budka H (1999) Deposition of the prion protein (PrP) during the evolution of experimental Creutzfeldt-Jakob disease. Acta Neuropathol 98: 597-602.

217. Lee H, Cohen OS, Rosenmann H, Hoffmann C, Kingsley PB, et al. (2012) Cerebral White Matter Disruption in Creutzfeldt-Jakob Disease. AJNR Am J Neuroradiol.

218. Fernandez-Borges N, de Castro J, Castilla J (2009) In vitro studies of the transmission barrier. Prion 3: 220-223.

219. Borrell V, Del Rio JA, Alcantara S, Derer M, Martinez A, et al. (1999) Reelin regulates the development and synaptogenesis of the layer-specific entorhino-hippocampal connections. J Neurosci 19: 1345-1358.

220. Sinagra M, Verrier D, Frankova D, Korwek KM, Blahos J, et al. (2005) Reelin, very-low-density lipoprotein receptor, and apolipoprotein E receptor 2 control somatic NMDA receptor composition during hippocampal maturation in vitro. J Neurosci 25: 6127-6136.

221. Qiu S, Weeber EJ (2007) Reelin signaling facilitates maturation of CA1 glutamatergic synapses. J Neurophysiol 97: 2312-2321.

222. Vasudevan A, Ho MS, Weiergraber M, Nischt R, Schneider T, et al. (2010) Basement membrane protein nidogen-1 shapes hippocampal synaptic plasticity and excitability. Hippocampus 20: 608-620.

223. Rangel A, Madronal N, Gruart A, Gavin R, Llorens F, et al. (2009) Regulation of GABA(A) and glutamate receptor expression, synaptic facilitation and long-term potentiation in the hippocampus of prion mutant mice. PLoS One 4: e7592.

224. Loubet D, Dakowski C, Pietri M, Pradines E, Bernard S, et al. (2012) Neuritogenesis: the prion protein controls beta1 integrin signaling activity. FASEB J 26: 678-690.

225. Kohno S, Kohno T, Nakano Y, Suzuki K, Ishii M, et al. (2009) Mechanism and significance of specific proteolytic cleavage of Reelin. Biochem Biophys Res Commun 380: 93-97.

226. Lin DT, Jodoin J, Baril M, Goodyer CG, Leblanc AC (2008) Cytosolic prion protein is the predominant anti-Bax prion protein form: exclusion of transmembrane and secreted prion protein forms in the anti-Bax function. Biochim Biophys Acta 1783: 2001-2012.

227. Gu Y, Luo X, Basu S, Fujioka H, Singh N (2006) Cell-specific metabolism and pathogenesis of transmembrane prion protein. Mol Cell Biol 26: 2697-2715.

228. Yasui N, Nogi T, Kitao T, Nakano Y, Hattori M, et al. (2007) Structure of a receptor-binding fragment of reelin and mutational analysis reveal a recognition mechanism similar to endocytic receptors. Proc Natl Acad Sci U S A 104: 9988-9993.

229. Gao C, Lei YJ, Han J, Shi Q, Chen L, et al. (2006) Recombinant neural protein PrP can bind with both recombinant and native apolipoprotein E in vitro. Acta Biochim Biophys Sin (Shanghai) 38: 593-601.

230. Ohkubo N, Lee YD, Morishima A, Terashima T, Kikkawa S, et al. (2003) Apolipoprotein E and Reelin ligands modulate tau phosphorylation through an apolipoprotein E receptor/disabled-1/glycogen synthase kinase-3beta cascade. FASEB J 17: 295-297.

231. Cross DA, Alessi DR, Cohen P, Andjelkovich M, Hemmings BA (1995) Inhibition of glycogen synthase kinase-3 by insulin mediated by protein kinase B. Nature 378: 785-789.

232. Fang X, Yu SX, Lu Y, Bast RC, Jr., Woodgett JR, et al. (2000) Phosphorylation and inactivation of glycogen synthase kinase 3 by protein kinase A. Proc Natl Acad Sci U S A 97: 11960-11965.

Neurodevelopmental Expression and Localization of the Cellular Prion Protein in the Central Nervous System of the Mouse

Stefano Benvegnù,[1,2] Ilaria Poggiolini,[1,2] and Giuseppe Legname[1,2]*

[1]Scuola Internazionale Superiore di Studi Avanzati-International School for Advanced Studies (SISSA-ISAS), Neurobiology Sector, I-34151 Trieste, Italy

[2]Italian Institute of Technology, SISSA-ISAS Unit, I-34151 Trieste, Italy

ABSTRACT

Transmissible spongiform encephalopathies (TSEs) are neurodegenerative disorders caused by PrP^{Sc}, or prion, an abnormally folded form of the cellular prion protein (PrP^{C}). The abundant expression of PrP^{C} in the central nervous system (CNS) is a requirement for prion replication, yet despite years of intensive research the physiological function of PrP^{C} still remains unclear. Several routes of investigation point out a potential role for PrP^{C} in axon growth and neuronal development. Thus, we undertook a detailed analysis of the spatial and temporal expression of PrP^{C} during mouse CNS development. Our findings show regional differences of the expression of PrP, with some specific white matter structures showing the earliest and highest expression of PrP^{C}. Indeed, all these regions are part of the thalamolimbic neurocircuitry, suggesting a potential role of PrP^{C} in the development and functioning of this specific brain system. J. Comp. Neurol. 518:1879–1891, 2010.

INDEXING TERMS: cellular prion protein; PrP^{C}; *Prnp* gene; infectious isoform of PrP; PrP^{Sc}; neurodevelopment; limbic system; hippocampal fimbria; fornix; stria terminalis; fasciculus retroflexus; stratum lacunosum moleculare; neural circuit

Prions are the proteinaceous infective particles causative of transmissible spongiform encephalopathies (TSEs) or prion diseases, fatal neurodegenerative disorders including Creutzfeldt–Jakob disease (CJD), fatal familial insomnia (FFI), and kuru in humans; bovine spongiform encephalopathy (BSE) and scrapie in cows and sheep, respectively; and the recently emerging chronic wasting disease (CWD) in deer. According to the protein-only hypothesis (Prusiner, 1982), prions are composed exclusively of PrP^{Sc}, an abnormally folded form of the cellular prion protein (PrP^{C}). PrP^{C} is a ubiquitous sialoglycoprotein mainly expressed in the brain, particularly in neurons, and anchored at the cell membrane surface with a glycosylphosphatidylinositol (GPI) moiety.

Despite the striking evidence of an association of PrP^{C} pathological conversion with the etiology of prion diseases, its physiological function is at present unknown. Several putative functions of PrP^{C} have been postulated, including synaptic activity (Herms et al., 1999), maintenance of myelinated sheet (Radovanovic et al., 2005), neuroprotective functions (Bounhar et al., 2001), and neurogenesis and differentiation (Steele et al., 2006). Moreover, PrP^{C} is able to stimulate neuritogenesis, rapid polarization, and development of synapses in cultured neurons (Kanaani et al., 2005; Santuccione et al., 2005). All these features hint at PrP acting as a growth factor, possibly involved in central nervous system (CNS) development. Indeed, PrP expression was shown to be developmentally regulated (Mobley et al., 1988; Lazarini et al., 1991; Manson et al., 1992; Sales et al., 2002; Tremblay et al., 2007).

Here, by combining in situ hybridization and immunohistochemical techniques, we analyzed the spatiotemporal expression of PrP^{C} during mouse CNS development. For this purpose we took advantage of the PrP-specific monovalent recombinant antibody antigen-binding fragment (Fab) D18 (Peretz et al., 2001). Our findings reveal

Grant sponsor: Italian Institute of Technology, SISSA-ISAS Unit; European Community's Seventh Framework Programme; Grant number: FP7/2007-2013 under grant agreement no. 222887; Grant sponsor: PRIORITY project.

*CORRESPONDENCE TO: Giuseppe Legname, SISSA, S.S.14 Km. 163,5 – 34149 Trieste TS, Italy. E-mail: legname@sissa.it

Received August 17, 2009; Revised December 23, 2009; Accepted January 28, 2010

DOI 10.1002/cne.22357

Published online February 16, 2010 in Wiley InterScience (www.interscience.wiley.com)

regional differences in the expression of PrP^C, with the earliest expression of the protein in the hippocampus, thalamic, and hypothalamic regions. In particular, specific white matter fiber tracts (i.e., the hippocampal fimbria, the stria terminalis, and the fasciculus retroflexus) show the highest expression of the mature protein. All these white matter fibers are part of the thalamolimbic system, an integrated brain neurocircuitry that regulates circadian, autonomic, and hormonal functions, as well as stress response behaviors. Thus, the high neurodevelopmental expression of PrP^C in these specific brain structures suggests a potential implication for PrP^C in the correct development and functioning of the thalamolimbic system. The localization of PrP^C in nonneuronal cell types will also be discussed.

MATERIALS AND METHODS

Animals

All experiments were carried out in accordance with European regulations (European Community Council Directive, November 24, 1986 (86/609/EEC)) and were approved by the local veterinary service authority. C57/B6 wildtype, B6/129 *Prnp*$^{-/-}$ (Bueler et al., 1992), FVB wildtype, and FVB *Prnp*$^{-/-}$ (Lledo et al., 1996) mice were used in these experiments. Embryonic and newborn animals were sacrificed and brains immediately collected and washed several times in cold phosphate-buffered saline (PBS) 1× pH 7.4 glucose 0.6% w/v. Then brains were fixed by complete immersion in freshly prepared PBS 1× paraformaldehyde (PFA) 4% with very gentle shaking overnight at 4°C. The day after, the samples were washed in PBS 1× and cryopreserved by complete immersion in PBS 1× sucrose 30% with gentle shaking overnight at 4°C. Then brains were washed several times in PBS 1× to remove excess glucose, included in OCT, and stored at −80°C. Two-week-old and older animals were deeply anesthetized, then perfused with PBS 1× and PBS 1× PFA 4%. After perfusion, animals were decapitated and brains were collected, fixed, and cryopreserved as previously described.

Immunohistochemistry

Ten-micrometer-thick brain serial sections were cut with a cryostat and mounted onto Superfrost Plus coated slides (Menzel-Gläser, Madison, WI). Slides were thawed at room temperature (RT), then washed with Tris-buffered saline (TBS) + Triton X-100 0.3% (TBS+T). Sections then were blocked with blocking solution: TBS+T + normal goat serum (NGS) 10% and bovine serum albumin (BSA) 5% for 1 hour at RT. Slides were then incubated with primary antibodies diluted in blocking solution for 2 hours at RT with gentle shaking. After washing the appropriate secondary antibodies, diluted in blocking solution, were added for 1 hour at RT with gentle shaking. Slides then were extensively washed with TBS+T, mounted with Vectashield (Vector Laboratories, Burlingame, CA), and analyzed under Leica fluorescence microscope. All data are representative of at least three independent experiments. Staining was performed on both FVB and C57/B6 genetic backgrounds. As control, age-matched FVB *Prnp*$^{-/-}$ and B6/129 *Prnp*$^{-/-}$ mice were used. The same exposure times were used for acquisition of images from both wild-type and *Prnp* knockout brain slices. Images were not modified other than to balance brightness and contrast with GIMP software, v. 2.6.7.

Antibodies

Recombinant anti-PrP^C humanized (HuM) Fab D18 was purchased from InPro Biotechnology (South San Francisco, CA; ABR-0D18) and used to a final concentration of 1 μg/mL. HuM-D18 is a recombinant Fab with human constant moiety, first raised by immunizing *Prnp*$^{-/-}$ mice against the protease-resistant core of Syrian hamster (SHa) PrP^{Sc} (Peretz et al., 1997). It showed high affinity for the region spanning the residues 133–152 incorporated in the first alpha-helix of PrP^C (Williamson et al., 1998), and proved to have a large accessibility to its specific epitope and to bind the largest fraction of the cell-surface PrP^C population, as revealed by cross-competition experiments (Leclerc et al., 2003). Moreover, it was able to inhibit prion propagation and clear cell cultures of prion infectivity (Peretz et al., 2001).

Anti-neurofilament 200 antibody was purchased from Sigma (St. Louis, MO; N-4142) and used at dilution 1:800. This antibody is developed in rabbit using purified neurofilament 200 from bovine spinal cord as the immunogen. It localizes only the 200-kDa neurofilament polypeptide in immunoblotting from mouse brain homogenate.

In situ hybridization

Twenty-μm-thick cryosections were cut and collected on slides (Menzel Gläser SuperFrost Plus) and then stored at −80°C. Sections were dried at RT for 2 hours and fixed in 4% PFA in PBS 1× at room temperature for 10 minutes, washed in PBS 1×, treated with 18 mg/mL Proteinase K (Roche, Nutley, NJ) at 30°C for 15 minutes, washed in glycine 4 mg/mL, PBS 1×, and fixed once more in 4% PFA for 10 minutes, washed, incubated in 0.1 M thriethanolamine pH 8.0 with acetic anhydride (0.03%), and washed again. Slides were then dried at RT and hybridized overnight at 55°C with 1.5 μg/mL digoxigenin (DIG)-labeled probe in hybridization solution: 50% formamide, salts 10× pH 7.2 (NaCl 3M, Tris HCl 0.1M, NaH_2PO_4 0.1M, 2% Ficoll 400 (Sigma), 2% polyvinyl pyrrolidone (Sigma)), DTT

2M (Sigma) in 10 mM sodium acetate pH 5.2, polyadenilic acid (Sigma) 10 mg/mL, ribonucleic acid (Sigma) 9.2 mg/mL, transfer type x–SA (Sigma) 7 mg/mL, 10% dextran sulfate (Sigma).

After hybridization, slides were washed in 5× SSC-βmercaptoethanol at RT for 30 minutes. Then they were washed in 50% formamide-1× SSC-βmercaptoethanol at 65°C for 30 minutes, several times in the NTE solution (5M NaCl, 1M Tris-HCl pH 8.0, 0.5 M EDTA pH 8.0) at RT, then in 2× SSC and 0.2× SSC. Slides were put in a humidified chamber with buffer B1 (1M Tris-HCl pH 7.5, 5 M NaCl), blocked in HI-FBS (heat-inactivated fetal bovine serum)-B1 (10÷90) for 60 minutes. Each slide was treated with 1:1,000 anti-DIG (Roche) in HI-FBS-B1, covered with a parafilm coverslip, and incubated overnight at 4°C.

Chromogenic-stained slides were washed several times with buffer B1 and with buffer B2 (0.1 M Tris-HCl pH 7.5, 0.1 M NaCl, 50 mM $MgCl_2$ pH 9.5) and stained with NBT 3.5 μL (Roche)-BCIP 3.5 μL (Roche) in 4 mL B2. After 10 minutes the reaction was observed under the microscope and stopped when the transcript signal level was detectable. Slides were then washed several times in buffer B1, then in PBS 1×. Slides were mounted with one 20 μL drop of PBS 1× 30% glycerol solution and a glass coverslip, sealed with enamel, and stored at 4°C.

In situ probes cloning and synthesis

Primer sequences were designed in order to clone the complete 765-basepairs-long coding sequence (CDS) of mouse (*Mus musculus*) *Prnp* gene in pGEM–T vector (Promega, Madison, WI): 5′-TCATCCCACGATCAGGAA GATGA-3′; 5′-ATGGCGAACCTTGGCTACTG-3′. Sense and antisense probes were transcribed in vitro with SP6 and T7 RNA Polymerase (Promega) in the presence of DIG-UTP RNA Labeling Mix (Roche), then stored at −80°C. The efficiency of labeling was checked and confirmed by Northern blot assay, which revealed a single band at the expected basepairs number.

RESULTS

Prnp gene expression detected throughout the developmental mouse brain

To investigate *Prnp* gene expression, PrP mRNA expression was analyzed in several regions of the mouse brain during pre- and postnatal development. In situ hybridizations were performed on 20-μm-thick coronal cryosections of mouse brains. *Prnp* gene expression in the brain was analyzed in 14.5- and 16.5-day-old embryos (E14.5, E16.5), in 1- (P1) and 7- (P7) day-old mice, and in adult mice. As negative control, sections from *Prnp* null mice were hybridized with the PrP riboprobes (data not shown).

Between E14.5 and E16.5 noticeable labeling was detected in brain regions known to have a highly active cellular proliferation, such as the ventricular zone (VZ) of the neocortex of the lateral ventricles (Fig. 1A,B) and the neuroepithelia of the third ventricle (IIIv) (Fig. 1I–L). In addition, *Prnp* signal was detected underneath the marginal zone (MZ) in the superficial cortical plate (CP), where newborn neurons were. At P1 the signal spanned the entire CP (Fig. 1C,D), whereas at P7 it was mainly restricted to the superficial CP, where the youngest neurons were (Fig. 1E,F). At P7 it was possible to observe a decrease of the signal in the subventricular/ependymal zone (SVZ/E) and in the subplate zone (SP), while it increased in the outer layers of the cortex (layers 6-2) (Fig. 1E,F).

At P7 it was possible to observe strong *Prnp* gene expression in other brain areas, such as the CA1 and the DG fields of the hippocampus (Fig. 2).

Moreover, during postnatal development and in the adult the expression pattern of PrP mRNA was constantly detectable in the olfactory bulbs. Hybridization signals were found in the mitral cells layer (Mi), along the wall of the olfactory bulb ventricle, and in the glomerular layer (GL) at P7 (Fig. 3A,B); this expression pattern remained constant during adult life (data not shown). These results are in agreement with previous descriptions (Le Pichon and Firestein, 2008). As expected, a signal was also detected in the frontal cortex.

By E16.5, intense expression was also found in non-neuronal tissue, such as the choroid plexus (ChP) of the ventricles, both at the mRNA and protein level (Fig. 3C–F). Specifically, PrP^C immunoreactivity was detected in the apical surface of the epithelial cells, on the side facing the ventricle (Fig. 3F).

Dynamics of PrP^C expression in the developmental mouse brain

The overall distribution of PrP^C in the developmental mouse brain was also examined by immunohistochemistry technique. The dynamics of PrP^C expression during prenatal and postnatal development were examined in coronal and longitudinal brain sections of E14.5, E18.5, P1, P4, P7, P9, and adult mice. The hippocampus was the region with the earliest and highest PrP^C immunoreactivity. Starting from E18.5 to adult life the hippocampus was labeled by Fab D18 in all parenchyma, with a net increase in PrP^C immunoreactivity in the stratum lacunosum moleculare (str l m) (Fig. 4A,B). This layer of the hippocampus contains a high number of synapses from hippocampal internal interneurons and from external inputs,

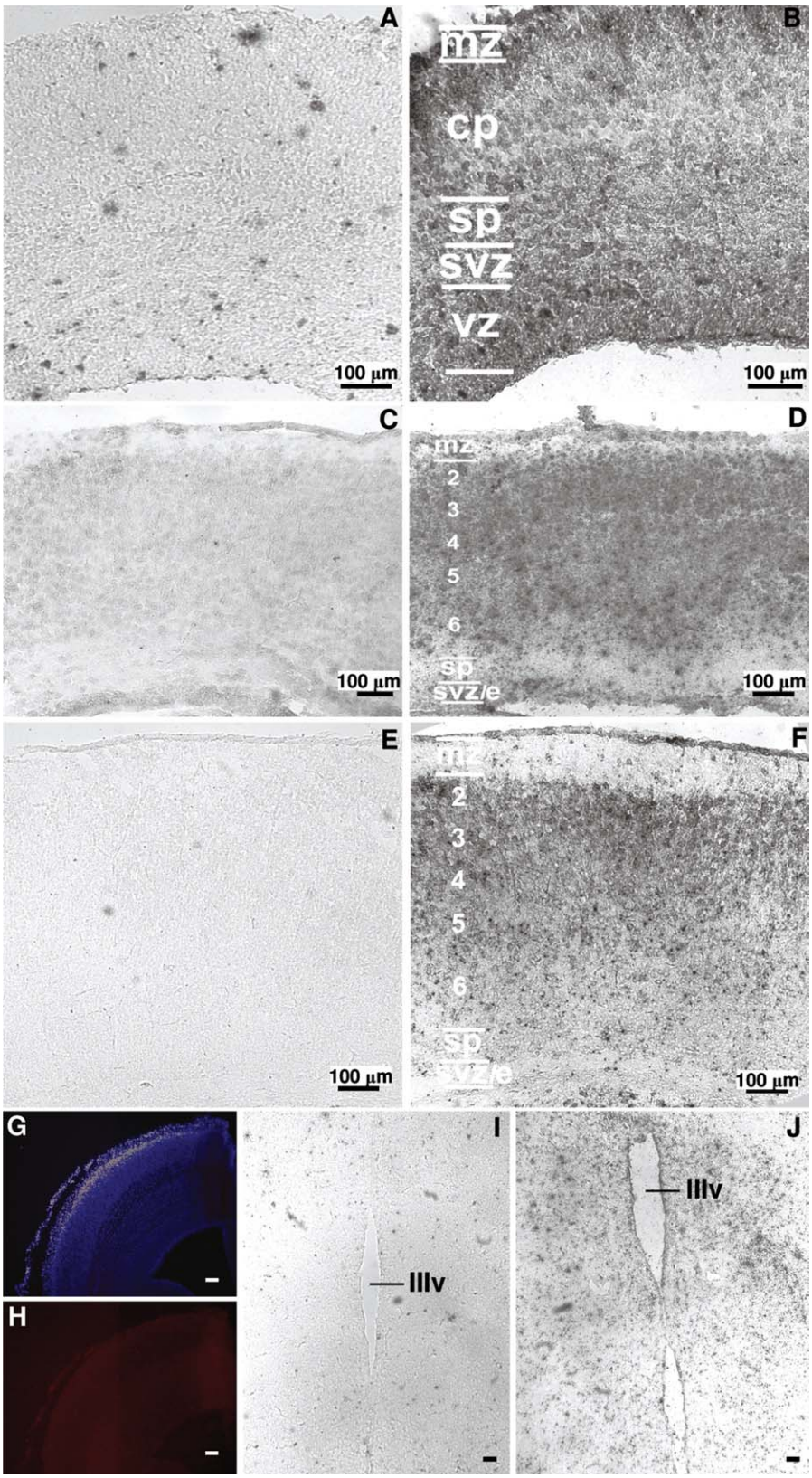
A
100 μm
B
mz
cp
sp
svz
vz
100 μm
C
100 μm
D
mz
2
3
4
5
6
sp
svz/e
100 μm
E
100 μm
F
mz
2
3
4
5
6
sp
svz/e
100 μm
G
H
I
IIIv
J
IIIv

Figure 1

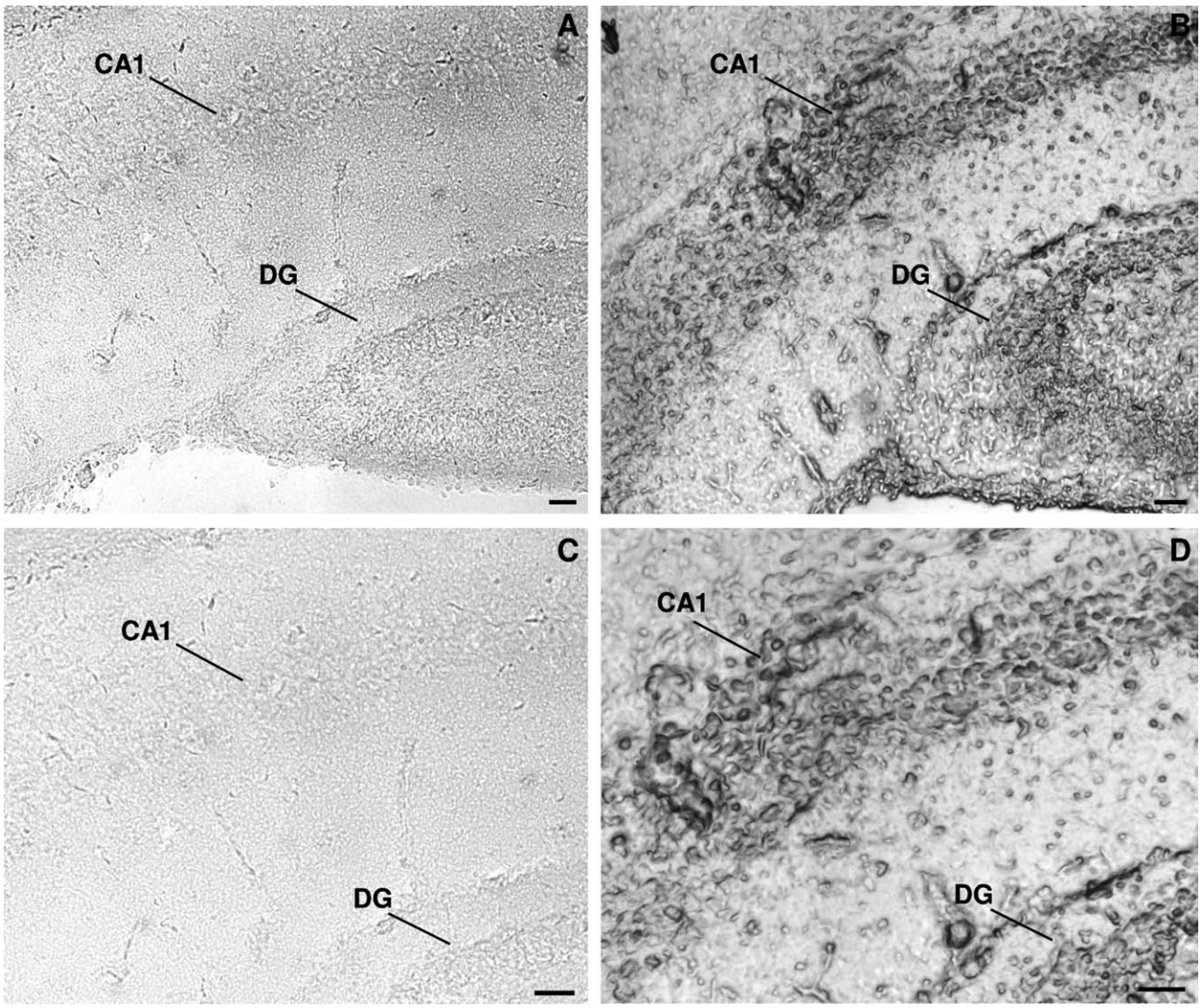

Figure 2. Expression of *Prnp* in the postnatal hippocampus. A–D: In situ hybridization of P7 hippocampal coronal section. **A,B:** *Prnp* signal was detected in the CA1 and in the DG cells in the hippocampus (B); no signal was detected with the control probe (A). **C,D:** Higher magnification of the CA1 pyramidal cells, indicating a clear perinuclear staining of *Prnp* expression (D). No signal was detected when using the negative sense probe (C). Scale bars = 50 μm.

such as the enthorinal cortex (Deng et al., 2006). Strong PrP^C immunoreactivity was also observed in the fimbria (Fi) of the hippocampus (Fig. 4C–L). In this structure, PrP^C-immunoreactivity was first observed at E18.5 and progressively increased during development (Fig. 4E–H). Next to the fimbria of the hippocampus, the stria

Figure 1. *Prnp* shows a patterned developmental expression in mouse brain. **A,B:** In situ hybridization of E14.5 brain coronal section. A: No positive cell was detected in the neocortex area using negative sense probe. B: Positive antisense probe shows that *Prnp* was detected in the ventricular zone (VZ). In addition, *Prnp* signal seems to be underneath the marginal zone (MZ) and in the superficial cortical plate (CP). Less intense signal was detected in the subventricular zone (SVZ) and in the subplate zone (SP). **C,D:** In situ hybridization of P1 brain coronal section. The antisense probe (D) shows signal for *Prnp* spanning the entire CP (layer 6-2). Negative control sense probe shows specificity of the signal in (C). **E,F:** Expression pattern of *Prnp* gene in the cortex layers of P7 postnatal stage. The positive signal of *Prnp* (F) is mainly concentrated to the superficial CP, whereas it progressively decreases in the subventricular/ependymal zone (SVZ/E) and in the subplate zone (SP). No signal was detected with the negative probe (E). **G,H:** Immunohistochemical staining of E14.5 mouse brain shows no expression of the mature PrP^C in the neocortex. PrP^C (in H) and nuclei (blue, in G) were stained, and no PrP^C immunoreactivity was detected. **I,J:** The expression of *Prnp* was detected in the neuroepithelia of the third ventricle (IIIv) at E14.5 using antisense probe (J), whereas no signal was detected using negative sense probe (I). Scale bars = 100 μm in G,H; 25 μm in I,J.

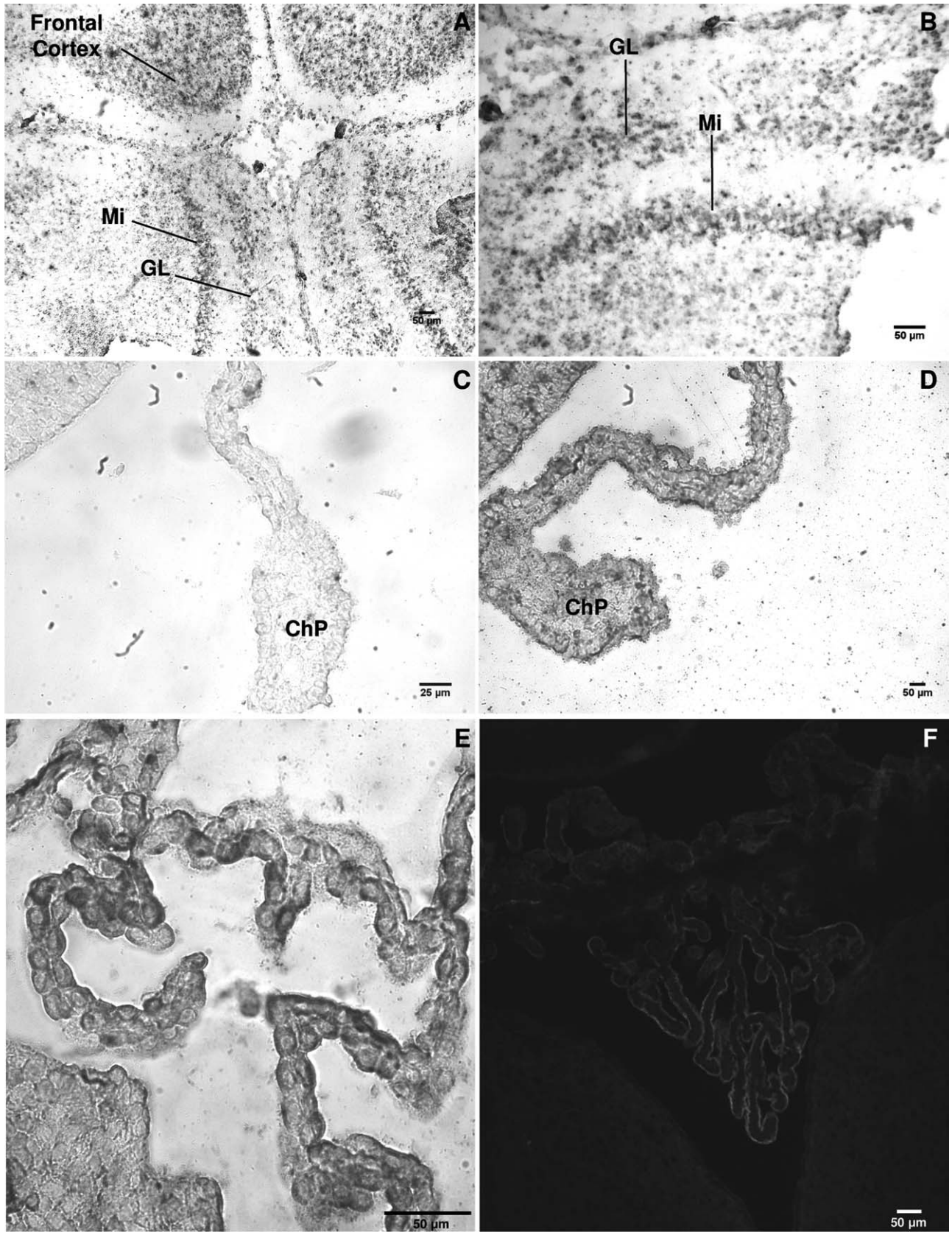
Frontal Cortex
A
Mi
GL
50 µm
B
GL
Mi
50 µm
C
ChP
25 µm
D
ChP
50 µm
E
50 µm
F
50 µm

Figure 3

terminalis (St) also showed a high level of PrP^C immunoreactivity (Fig. 4C–L), and paralleled the developmental expression of PrP^C of the fimbria (Fig. 4E–H). The stria terminalis is the main nervous output of the amygdala up to thalamic nuclei (Lee and Davis, 1997). The immunostaining clearly highlighted that PrP^C expression in these white matter fiber bundles is very high and well defined (Fig. 4I–L).

The thalamus was another region showing basal PrP^C expression during neurodevelopment (Fig. 5). Within the thalamus the fornix, the anatomical continuation of the hippocampal fimbria, showed an intense and definite PrP^C-immunoreactivity (Fig. 5A). The specificity of PrP^C expression for particular brain white matter tracts could be appreciated by the complete lack of PrP^C staining of the mammillothalamic tract (Fig. 5A–C). Moreover, the fasciculus retroflexus (Fr) specifically showed a high staining for the mature protein during development (Fig. 5D–H). As for the fimbria of the hippocampus and the stria terminalis, PrP^C immunoreactivity was first observed at E18.5 and progressively increased during development both for the fornix (Fig. 5I–M) and for the fasciculus retroflexus (Fig. 5N–P).

However, we did not observe any dramatic alterations in the size or in the morphology of any of these structures in *Prnp*$^{-/-}$ animals.

DISCUSSION

In the present study we describe a restricted PrP^C expression in specific brain areas during prenatal and postnatal brain development. By in situ hybridization we could identify *Prnp* gene expression at E14.5 in the VZ, which is known to be a proliferative brain area, in the superficial CP, underneath the MZ where newborn neurons are, and in the neuroepithelia of the third ventricle (Fig. 1). The developing choroid plexus epithelium of the ventricular zone is known to contain multipotent neural stem cells (Tramontin et al., 2003). The MZ is the outermost layer of the cerebral cortex. Cells of the MZ are known to play key roles during development such as orchestrating the development of the cortical layers and contributing to the GABAergic interneurons in the cerebral cortex (Meyer et al., 1998). MZ cells have also been shown to guide cortical afferents to their targets (Marin-Padilla, 1978; McConnell et al., 1989) and develop a transient neuronal circuit of crucial importance for setting up the mature circuitry among CP neurons (Friauf and Shatz, 1991; Ghosh and Shatz, 1992; Schwartz et al., 1998).

In the neocortex of P1 mouse, *Prnp* gene expression was detected in the SVZ/E, located adjacent to the VZ along the lateral ventricle wall. Importantly, neurogenesis persists in this part of the brain throughout the animal's adult life.

The expression pattern of *Prnp* in the VZ and SVZ/E suggests that the *Prnp* gene could be involved in the cellular proliferation control along development. Indeed, one report suggests that PrP^C positively regulates neuronal precursor proliferation in the SVZ/E during development and adult neurogenesis (Steele et al., 2006).

At P1 *Prnp* gene is expressed throughout the cortical layers 6-2. At P7 the signal could still be detected in the cortical layers 6-2, with the strongest signal in layer 2 and progressively decreasing down to layer 6 (Fig. 1). Premature neural cells proliferate in the ventricular side and migrate toward the cortical layers in the developing cerebral cortex. Neuronal precursors generated in the ventricular/ependymal zone migrate outwards along the glial processes to form the CP at the outer surface of the brain. Since the *Prnp* expression pattern during neurodevelopment seems to parallel such a time course of neuronal differentiation, it is possible to argue that *Prnp* expression could be implicated in neuronal proliferation and maturation: *Prnp* signal detected in neurons of layers 2 to 6 at P7 could be due to the same neurons that were previously described to express PrP mRNA in the VZ and in the SVZ/E zones at E14.5 and at P1. However, since PrP^C immunoreactivity in the cortical layers was not observed during prenatal development, it is possible to hypothesize that in the cortex PrP mRNA is not translated in PrP^C, or, if translated, the protein is quickly degraded during this developmental stage.

During brain early postnatal development we found PrP^C strongly expressed in the hippocampus. Differently from the cortex, in the hippocampus we revealed the expression of PrP^C concomitantly with the presence of *Prnp* mRNA (Figs. 2, 4). Indeed, among all brain areas the hippocampus exhibited the earliest and the highest PrP^C expression. Our results show that, within hippocampus, the stratum lacunosum-moleculare (str l m) revealed the highest PrP^C expression. As this is a synapse-rich region

Figure 3. *Prnp* is expressed in the olfactory bulb and in the choroid plexus during development and in adult life. **A:** At P7 the expression of *Prnp* is widespread in the olfactory bulb, with an increased expression in mitral cells layer (Mi) and in the glomerular layer (GL). **B:** Higher magnification of the different layers. C–F: PrP is expressed also by the choroid plexus. **C–E:** Epithelial cells of the choroid plexus show an intense *Prnp* signal starting at E16.5 (D) until adult life (E). No signal is detected using the control probe (C). **F:** At P7 PrP^C is detected in the epithelial cells of the choroid plexus, specifically at the apical surface of the cells toward the ventricle.

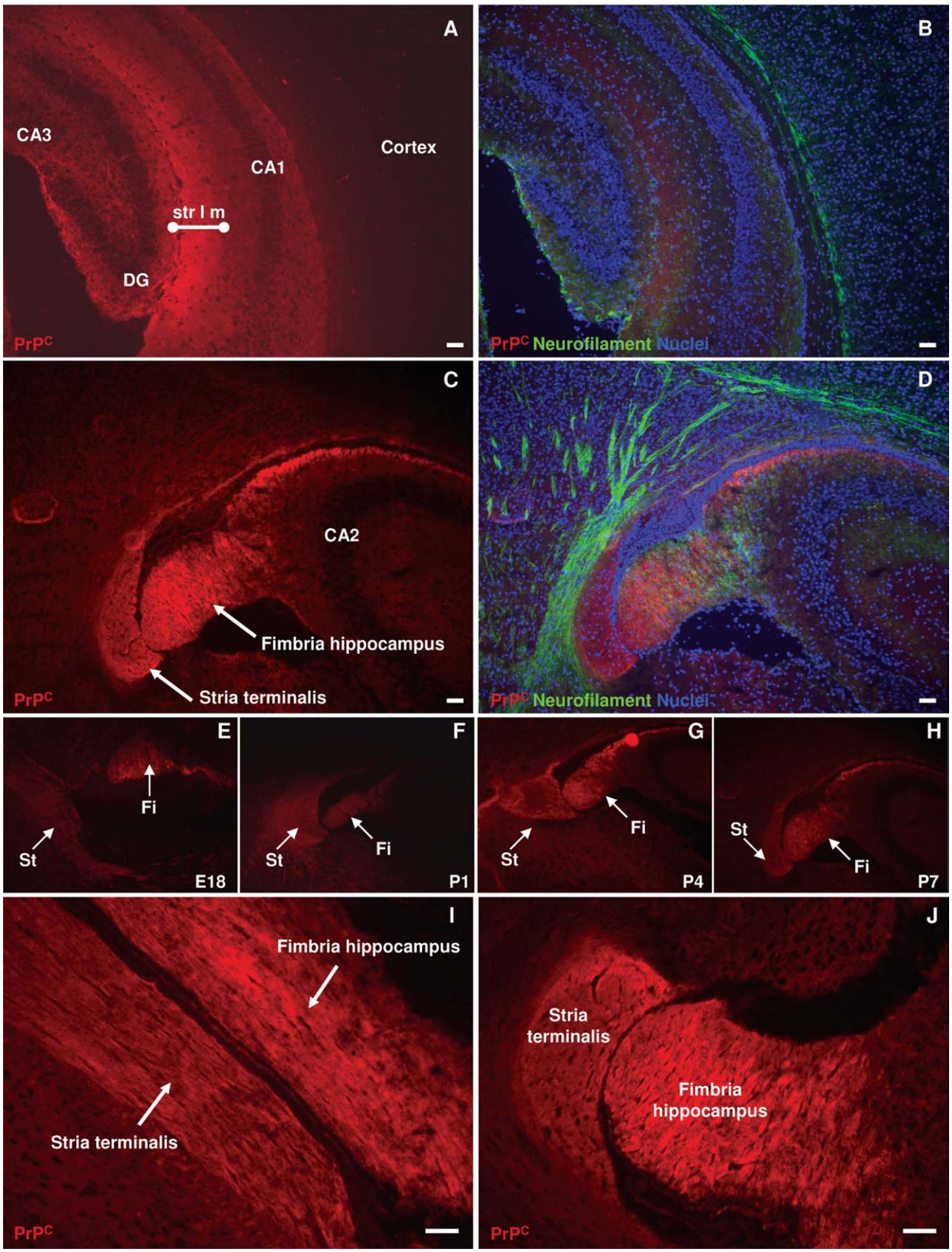
A
CA3
CA1
Cortex
str l m
DG
PrPC
B
PrPC Neurofilament Nuclei
C
CA2
Fimbria hippocampus
Stria terminalis
PrPC
D
PrPC Neurofilament Nuclei
E
Fi
St
E18
F
St
Fi
P1
G
Fi
St
P4
H
St
Fi
P7
I
Fimbria hippocampus
Stria terminalis
PrPC
J
Stria terminalis
Fimbria hippocampus
PrPC

Figure 4

where hippocampal interneurons (Bertrand and Lacaille, 2001) and afferent neuronal inputs (Deng et al., 2006) make connections (Fig. 6), we can infer that the relatively high expression of PrP^C in this region could possibly be necessary to the correct development of synapses and, in turn, to a correct synaptic activity. Several studies suggest that the synaptic compartment could be the critical site of functional PrP^C expression (Herms et al., 1999; Carleton et al., 2001), and that loss of PrP^C function, such as in *Prnp*$^{-/-}$ mice, may interfere with the correct, physiological connections between neurons. Indeed, many of the abnormalities identified in *Prnp*$^{-/-}$ mice are related to a hippocampal synaptic dysfunction (Collinge et al., 1994; Carleton et al., 2001; Curtis et al., 2003; Maglio et al., 2004; but also see Lledo et al., 1996). Interestingly, some reports point to central synapses as primary dysfunctional victims also in prion diseases, before neurodegeneration occurs (Jeffrey et al., 2000; Cunningham et al., 2003).

Another phenotype of *Prnp*$^{-/-}$ mice is their increased susceptibility to epileptic seizures (Walz et al., 1999). The core of many forms of seizures are large and synchronized bursts of activity originated, among all the brain structures, peculiarly in the hippocampus and the neocortex (McCormick and Contreras, 2001). Indeed, increasing evidence suggests that an altered neurodevelopment, leading to either brain malformations or injuries, may be involved in the generation of epilepsy (Hermann et al., 2008). Our finding of a strong developmental regulation and expression of PrP^C in the hippocampus and in the neocortex is intriguing, as it may account for the increased susceptibility of *Prnp*$^{-/-}$ mice to epileptic seizures. The lack of PrP^C, in fact, may alter the physiological development of these brain structures, and in turn provoke changes in interneuronal connections and neural network properties.

Strong PrP^C immunoreactivity was also observed in brain structure involved in the regulation of the thalamolimbic system, such as the fimbria/fornix, the fasciculus retroflexus, and the stria terminalis (Fig. 4, 5). The thalamolimbic system is involved in the regulation of circadian, autonomic, and hormonal functions, as well as stress response behaviors (Herman et al., 2003, 2005; Saper, 2006; Ulrich-Lai and Herman, 2009). The fimbria/fornix provides the major afferent and efferent projections of the hippocampus to basal forebrain (Olton et al., 1978); the fasciculus retroflexus connects the habenular nucleus to the interpeduncular nucleus and it is known to be integrated in the processing of various subsystems involved in the sleep–wake mechanisms (Valjakka et al., 1998); the stria terminalis is a limbic forebrain structure that receives heavy projections from, among other areas, the basolateral amygdala, and projects in turn to hypothalamic and brainstem target areas that mediate many of the autonomic and behavioral responses to aversive or threatening stimuli (Walker et al., 2003) (Fig. 6). Thus, the high developmental expression of PrP^C in brain fiber bundles participating in the regulation of the thalamolimbic circuitry may reveal a potential role for PrP^C in the correct development, structuring, and functioning of this complex neural system. Interestingly, the lack of PrP^C in *Prnp*$^{-/-}$ mice was proved to be responsible for alterations that can be related to incorrect performance of this neural system. These alterations include altered circadian activity rhythms and sleep activities (Tobler et al., 1996), deficits in hippocampal-dependent spatial learning (Criado et al., 2005), altered stress response and neuroendocrine stress functions (Sanchez-Alavez et al., 2007), altered fear-induced behavior (Lobao-Soares et al., 2008), and disregulation of the hypothalamic-pituitary-adrenal axis, the "stress" axis (Sanchez-Alavez et al., 2008). Intriguingly, pathological alterations that can be related to a dysfunction of the thalamolimbic system have been described also in some cases of prion diseases, such as corticosteroid disturbance (Gayrard et al., 2000; Voigtlander et al., 2006). Moreover, patients suffering the genetic prion disease FFI show predominant sleep, neuroendocrine, and autonomic dysfunction (Montagna et al., 2003). Hence, the absence of PrP^C in *Prnp*$^{-/-}$ mice, or its possibly altered physiological functioning in certain cases of prion diseases, gives rise to pathological alterations associated with incorrect neural information processing by brain structures contributing to the regulation of the thalamolimbic neurocircuitry.

In summary, we have identified PrP^C expression to be highly regulated during neurodevelopment, and in

Figure 4. PrP^C expression in the hippocampus during development. **A,B:** At P7 PrP^C (in red; A) is detected throughout the hippocampus, and in particular at high levels in the stratum lacunosum-molecolare (str l m), a synapse-dense region. No signal for PrP^C is yet detected in the cortex. A merged image is shown in B (PrP^C, in red; neurofilament, in green; nuclei signals in blue). **C–H:** PrP^C is specifically and highly expressed by the fimbria of the hippocampus and the stria terminalis at P7 (C,D). The fimbria of the hippocampus (Fi) and the stria terminalis (St) express high level of PrP^C also at embryonic stages (E18.5), and progressively increase the level of expression during postnatal development: P1 (F), P4 (G), and P7 (H). **I,J:** Higher magnification of longitudinal (I) and coronal (J) section of the fimbria of the hippocampus and the stria terminalis, highlighting the net boundaries of PrP^C-expression between other brain regions and these structures. Scale bars = 50 μm.

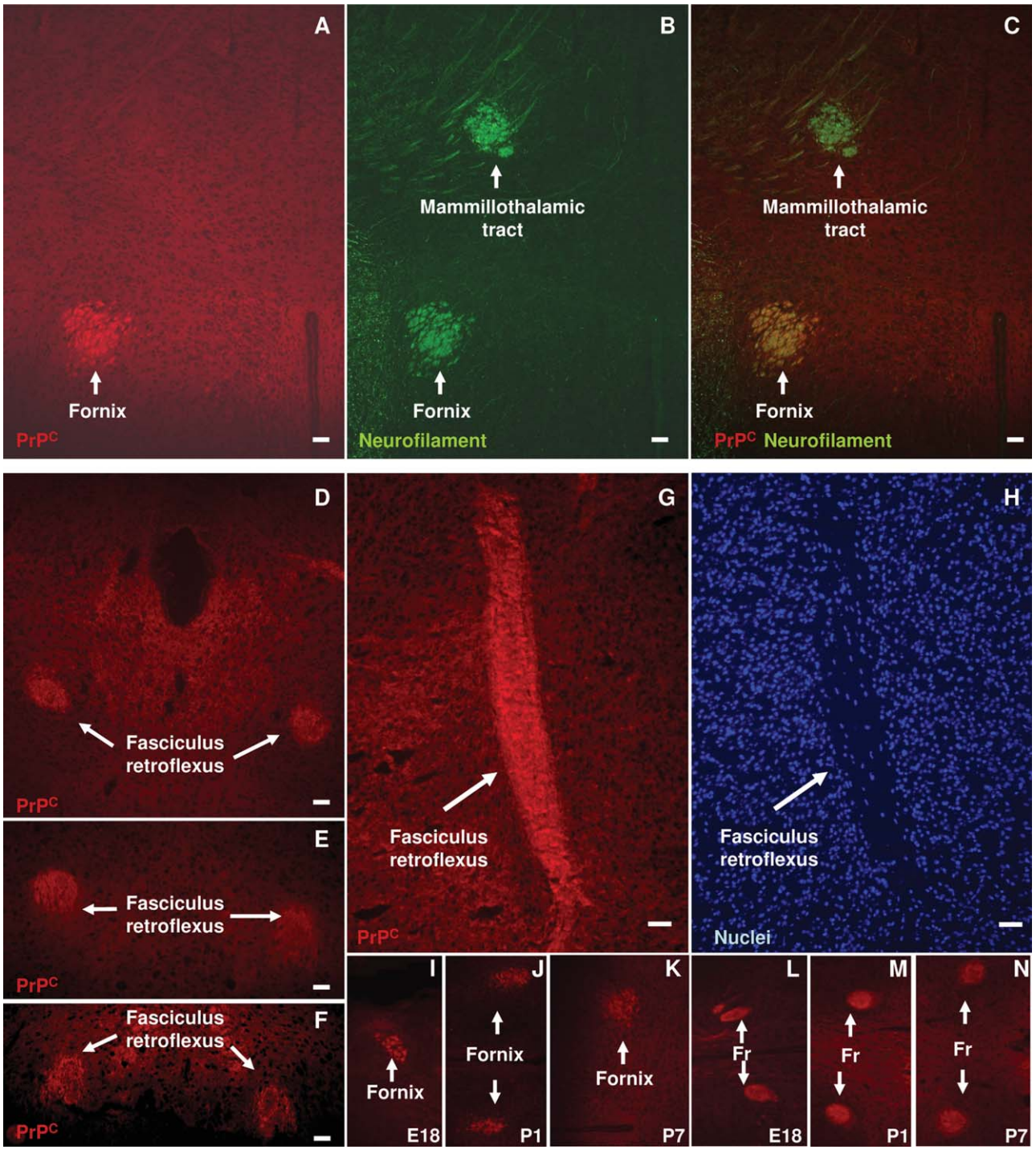

Figure 5. Thalamic expression of PrP^C during development. Immunohistochemical staining for PrP^C (in red; A,C,D–G,I–N) and neurofilament (in green; B,C). A merged image is shown in (C). **A–C:** At P7 PrP^C is detected in the thalamus, with abundant and specific expression in fornix (A). The specificity of PrP^C expression by this structure is highlighted by the counterstaining of neurofilaments, which labels both the mammillothalamic tract and the fornix (B). Only the fornix shows colocalization of PrP^C and neurofilament signals (in yellow; C). **D–H:** P7: PrP^C expression is detected also specifically in the fasciculus retroflexus (or habenulointerpeduncular tract). The fasciculus retroflexus express PrP^C all along its length, with clear boundaries, highlighted by coronal (D–F) or longitudinal (G) PrP^C staining. Counterstaining of nuclei (in blue; H) underlines the low number of nuclei in this white matter structure. **I–N:** Developmental PrP^C expression by the fornix and the fasciculus retroflexus (Fr). Both these structures show a progressively increasing level of expression of the protein during development, starting from E18.5 (fornix and Fr, respectively; I,L), to P1 (respectively, J,M), until P7 (respectively, K,N). Scale bars = 50 μm.

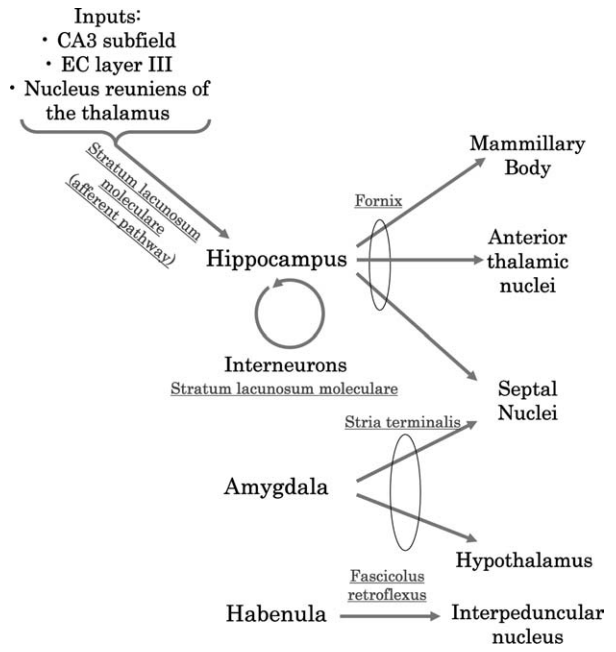

Figure 6. Brain limbic system circuits expressing PrP^C during development. Gray lines indicate the neural connections (i.e., the hippocampal fimbria, the stria terminalis, and the fasciculus retroflexus) and the synapses-rich region (i.e., stratum lacunosum-moleculare of the hippocampus) expressing high levels of PrP^C in neurodevelopment.

particular we have described a high level of expression of PrP^C in specific nerve fiber bundles involved in the thalamolimbic system regulation. The high developmental expression of PrP^C in these white matter tracts might reflect an active axonal transport of the prion protein through these fiber bundles; indeed, PrP^C can be transported along axons (Borchelt et al., 1994; Moya et al., 2004), and in particular, in the case of the fimbria/fornix, PrP^C expression in these tracts could be due to axonal transport from the hippocampus.

This strong developmental regulation and the main synaptic localization of PrP^C in adult neurons (Herms et al., 1999; Moya et al., 2000) could implicate PrP^C in the correct structuring and functioning of specific brain circuits. The lack of PrP^C, such as in *Prnp*$^{-/-}$ animals, could be more detrimental for brain regions requiring high levels of expression of the protein during development than in regions with a lower physiological expression. In turn, these regions would not be able to form and/or operate properly, and when challenged by the proper external stimulus they would respond with a nonphysiological nervous output, if compared to wildtype situations. In this perspective, this may also be true for the aberrant function of PrP^C once converted into PrP^{Sc}.

Despite PrP^C synaptic localization (Moya et al., 2000), in adult mice it can also be localized in other parts of the neurons plasma membrane, including dendritic, somatic, and axonal membranes (Mironov et al., 2003). These findings point to a broader physiological role for PrP^C in adult life than simply a synaptic one. Indeed, besides synapse formation and function, PrP^C was shown to influence several cellular processes in the nervous system, e.g., neuronal survival, intercellular contacts, and signaling, and maintenance of myelin fibers (reviewed in Aguzzi et al., 2008). Our data can indeed support the hypothesis for distinct temporal functions for PrP^C as being supposedly involved in circuit formation and refinement during neuronal development, and in other functions in adult life once the correct neuronal circuits have been formed.

ACKNOWLEDGMENTS

The authors thank Gabriella Furlan for editing and proofreading the article.

LITERATURE CITED

Aguzzi A, Baumann F, Bremer J. 2008. The prion's elusive reason for being. Annu Rev Neurosci 31:439–477.

Bertrand S, Lacaille JC. 2001. Unitary synaptic currents between lacunosum-moleculare interneurones and pyramidal cells in rat hippocampus. J Physiol 532(Pt 2):369–384.

Borchelt DR, Koliatsos VE, Guarnieri M, Pardo CA, Sisodia SS, Price DL. 1994. Rapid anterograde axonal transport of the cellular prion glycoprotein in the peripheral and central nervous systems. J Biol Chem 269:14711–14714.

Bounhar Y, Zhang Y, Goodyer CG, LeBlanc A. 2001. Prion protein protects human neurons against Bax-mediated apoptosis. J Biol Chem 276:39145–39149.

Bueler H, Fischer M, Lang Y, Bluethmann H, Lipp HP, DeArmond SJ, Prusiner SB, Aguet M, Weissmann C. 1992. Normal development and behaviour of mice lacking the neuronal cell-surface PrP protein. Nature 356:577–582.

Carleton A, Tremblay P, Vincent JD, Lledo PM. 2001. Dose-dependent, prion protein (PrP)-mediated facilitation of excitatory synaptic transmission in the mouse hippocampus. Pflugers Arch 442:223–229.

Collinge J, Whittington MA, Sidle KC, Smith CJ, Palmer MS, Clarke AR, Jefferys JG. 1994. Prion protein is necessary for normal synaptic function. Nature 370:295–297.

Criado JR, Sanchez-Alavez M, Conti B, Giacchino JL, Wills DN, Henriksen SJ, Race R, Manson JC, Chesebro B, Oldstone MB. 2005. Mice devoid of prion protein have cognitive deficits that are rescued by reconstitution of PrP in neurons. Neurobiol Dis 19:255–265.

Cunningham C, Deacon R, Wells H, Boche D, Waters S, Diniz CP, Scott H, Rawlins JN, Perry VH. 2003. Synaptic changes characterize early behavioural signs in the ME7 model of murine prion disease. Eur J Neurosci 17:2147–2155.

Curtis J, Errington M, Bliss T, Voss K, MacLeod N. 2003. Age-dependent loss of PTP and LTP in the hippocampus of PrP-null mice. Neurobiol Dis 13:55–62.

Deng JB, Yu DM, Li MS. 2006. Formation of the entorhino-hippocampal pathway: a tracing study in vitro and in vivo. Neurosci Bull 22:305–314.

Friauf E, Shatz CJ. 1991. Changing patterns of synaptic input to subplate and cortical plate during development of visual cortex. J Neurophysiol 66:2059–2071.

Gayrard V, Picard-Hagen N, Grino M, Sauze N, Grandjean C, Galea J, Andreoletti O, Schelcher F, Toutain PL. 2000.

Major hypercorticism is an endocrine feature of ewes with naturally occurring scrapie. Endocrinology 141:988–994.
Ghosh A, Shatz CJ. 1992. Involvement of subplate neurons in the formation of ocular dominance columns. Science 255: 1441–1443.
Herman JP, Figueiredo H, Mueller NK, Ulrich-Lai Y, Ostrander MM, Choi DC, Cullinan WE. 2003. Central mechanisms of stress integration: hierarchical circuitry controlling hypothalamo-pituitary-adrenocortical responsiveness. Front Neuroendocrinol 24:151–180.
Herman JP, Ostrander MM, Mueller NK, Figueiredo H. 2005. Limbic system mechanisms of stress regulation: hypothalamo-pituitary-adrenocortical axis. Prog Neuropsychopharmacol Biol Psychiatry 29:1201–1213.
Hermann B, Seidenberg M, Jones J. 2008. The neurobehavioural comorbidities of epilepsy: can a natural history be developed? Lancet Neurol 7:151–160.
Herms J, Tings T, Gall S, Madlung A, Giese A, Siebert H, Schurmann P, Windl O, Brose N, Kretzschmar H. 1999. Evidence of presynaptic location and function of the prion protein. J Neurosci 19:8866–8875.
Jeffrey M, Halliday WG, Bell J, Johnston AR, MacLeod NK, Ingham C, Sayers AR, Brown DA, Fraser JR. 2000. Synapse loss associated with abnormal PrP precedes neuronal degeneration in the scrapie-infected murine hippocampus. Neuropathol Appl Neurobiol 26:41–54.
Kanaani J, Prusiner SB, Diacovo J, Baekkeskov S, Legname G. 2005. Recombinant prion protein induces rapid polarization and development of synapses in embryonic rat hippocampal neurons in vitro. J Neurochem 95:1373–1386.
Lazarini F, Deslys JP, Dormont D. 1991. Regulation of the glial fibrillary acidic protein, beta actin and prion protein mRNAs during brain development in mouse. Brain Res Mol Brain Res 10:343–346.
Le Pichon CE, Firestein S. 2008. Expression and localization of the prion protein PrP(C) in the olfactory system of the mouse. J Comp Neurol 508:487–499.
Leclerc E, Peretz D, Ball H, Solforosi L, Legname G, Safar J, Serban A, Prusiner SB, Burton DR, Williamson RA. 2003. Conformation of PrP(C) on the cell surface as probed by antibodies. J Mol Biol 326:475–483.
Lee Y, Davis M. 1997. Role of the hippocampus, the bed nucleus of the stria terminalis, and the amygdala in the excitatory effect of corticotropin-releasing hormone on the acoustic startle reflex. J Neurosci 17:6434–6446.
Lledo PM, Tremblay P, DeArmond SJ, Prusiner SB, Nicoll RA. 1996. Mice deficient for prion protein exhibit normal neuronal excitability and synaptic transmission in the hippocampus. Proc Natl Acad Sci U S A 93:2403–2407.
Lobao-Soares B, Walz R, Prediger RD, Freitas RL, Calvo F, Bianchin MM, Leite JP, Landemberger MC, Coimbra NC. 2008. Cellular prion protein modulates defensive attention and innate fear-induced behaviour evoked in transgenic mice submitted to an agonistic encounter with the tropical coral snake Oxyrhopus guibei. Behav Brain Res 194: 129–137.
Maglio LE, Perez MF, Martins VR, Brentani RR, Ramirez OA. 2004. Hippocampal synaptic plasticity in mice devoid of cellular prion protein. Brain Res Mol Brain Res 131:58–64.
Manson J, West JD, Thomson V, McBride P, Kaufman MH, Hope J. 1992. The prion protein gene: a role in mouse embryogenesis? Development 115:117–122.
Marin-Padilla M. 1978. Dual origin of the mammalian neocortex and evolution of the cortical plate. Anat Embryol (Berl) 152:109–126.
McConnell SK, Ghosh A, Shatz CJ. 1989. Subplate neurons pioneer the first axon pathway from the cerebral cortex. Science 245:978–982.
McCormick DA, Contreras D. 2001. On the cellular and network bases of epileptic seizures. Annu Rev Physiol 63: 815–846.
Meyer G, Soria JM, Martinez-Galan JR, Martin-Clemente B, Fairen A. 1998. Different origins and developmental histories of transient neurons in the marginal zone of the fetal and neonatal rat cortex. J Comp Neurol 397:493–518.
Mironov A Jr, Latawiec D, Wille H, Bouzamondo-Bernstein E, Legname G, Williamson RA, Burton D, DeArmond SJ, Prusiner SB, Peters PJ. 2003. Cytosolic prion protein in neurons. J Neurosci 23:7183–7193.
Mobley WC, Neve RL, Prusiner SB, McKinley MP. 1988. Nerve growth factor increases mRNA levels for the prion protein and the beta-amyloid protein precursor in developing hamster brain. Proc Natl Acad Sci U S A 85:9811–9815.
Montagna P, Gambetti P, Cortelli P, Lugaresi E. 2003. Familial and sporadic fatal insomnia. Lancet Neurol 2:167–176.
Moya KL, Sales N, Hassig R, Creminon C, Grassi J, Di Giamberardino L. 2000. Immunolocalization of the cellular prion protein in normal brain. Microsc Res Tech 50:58–65.
Moya KL, Hassig R, Creminon C, Laffont I, Di Giamberardino L. 2004. Enhanced detection and retrograde axonal transport of PrPc in peripheral nerve. J Neurochem 88: 155–160.
Olton DS, Walker JA, Gage FH. 1978. Hippocampal connections and spatial discrimination. Brain Res 139:295–308.
Peretz D, Williamson RA, Matsunaga Y, Serban H, Pinilla C, Bastidas RB, Rozenshteyn R, James TL, Houghten RA, Cohen FE, Prusiner SB, Burton DR. 1997. A conformational transition at the N terminus of the prion protein features in formation of the scrapie isoform. J Mol Biol 273: 614–622.
Peretz D, Williamson RA, Kaneko K, Vergara J, Leclerc E, Schmitt-Ulms G, Mehlhorn IR, Legname G, Wormald MR, Rudd PM, Dwek RA, Burton DR, Prusiner SB. 2001. Antibodies inhibit prion propagation and clear cell cultures of prion infectivity. Nature 412:739–743.
Prusiner SB. 1982. Novel proteinaceous infectious particles cause scrapie. Science 216:136–144.
Radovanovic I, Braun N, Giger OT, Mertz K, Miele G, Prinz M, Navarro B, Aguzzi A. 2005. Truncated prion protein and Doppel are myelinotoxic in the absence of oligodendrocytic PrPC. J Neurosci 25:4879–4888.
Sales N, Hassig R, Rodolfo K, Di Giamberardino L, Traiffort E, Ruat M, Fretier P, Moya KL. 2002. Developmental expression of the cellular prion protein in elongating axons. Eur J Neurosci 15:1163–1177.
Sanchez-Alavez M, Conti B, Moroncini G, Criado JR. 2007. Contributions of neuronal prion protein on sleep recovery and stress response following sleep deprivation. Brain Res 1158:71–80.
Sanchez-Alavez M, Criado JR, Klein I, Moroncini G, Conti B. 2008. Hypothalamic-pituitary-adrenal axis disregulation in PrPC-null mice. Neuroreport 19:1473–1477.
Santuccione A, Sytnyk V, Leshchyns'ka I, Schachner M. 2005. Prion protein recruits its neuronal receptor NCAM to lipid rafts to activate p59fyn and to enhance neurite outgrowth. J Cell Biol 169:341–354.
Saper CB. 2006. Staying awake for dinner: hypothalamic integration of sleep, feeding, and circadian rhythms. Prog Brain Res 153:243–252.
Schwartz TH, Rabinowitz D, Unni V, Kumar VS, Smetters DK, Tsiola A, Yuste R. 1998. Networks of coactive neurons in developing layer 1. Neuron 20:541–552.
Steele AD, Emsley JG, Ozdinler PH, Lindquist S, Macklis JD. 2006. Prion protein (PrPc) positively regulates neural precursor proliferation during developmental and adult

mammalian neurogenesis. Proc Natl Acad Sci U S A 103: 3416–3421.

Tobler I, Gaus SE, Deboer T, Achermann P, Fischer M, Rulicke T, Moser M, Oesch B, McBride PA, Manson JC. 1996. Altered circadian activity rhythms and sleep in mice devoid of prion protein. Nature 380:639–642.

Tramontin AD, Garcia-Verdugo JM, Lim DA, Alvarez-Buylla A. 2003. Postnatal development of radial glia and the ventricular zone (VZ): a continuum of the neural stem cell compartment. Cereb Cortex 13:580–587.

Tremblay P, Bouzamondo-Bernstein E, Heinrich C, Prusiner SB, DeArmond SJ. 2007. Developmental expression of PrP in the post-implantation embryo. Brain Res 1139:60–67.

Ulrich-Lai YM, Herman JP. 2009. Neural regulation of endocrine and autonomic stress responses. Nat Rev Neurosci 10:397–409.

Valjakka A, Vartiainen J, Tuomisto L, Tuomisto JT, Olkkonen H, Airaksinen MM. 1998. The fasciculus retroflexus controls the integrity of REM sleep by supporting the generation of hippocampal theta rhythm and rapid eye movements in rats. Brain Res Bull 47:171–184.

Voigtlander T, Unterberger U, Touma C, Palme R, Polster B, Strohschneider M, Dorner S, Budka H. 2006. Prominent corticosteroid disturbance in experimental prion disease. Eur J Neurosci 23:2723–2730.

Walker DL, Toufexis DJ, Davis M. 2003. Role of the bed nucleus of the stria terminalis versus the amygdala in fear, stress, and anxiety. Eur J Pharmacol 463:199–216.

Walz R, Amaral OB, Rockenbach IC, Roesler R, Izquierdo I, Cavalheiro EA, Martins VR, Brentani RR. 1999. Increased sensitivity to seizures in mice lacking cellular prion protein. Epilepsia 40:1679–1682.

Williamson RA, Peretz D, Pinilla C, Ball H, Bastidas RB, Rozenshteyn R, Houghten RA, Prusiner SB, Burton DR. 1998. Mapping the prion protein using recombinant antibodies. J Virol 72:9413–9418.

OPEN ACCESS Freely available online

PLOS ONE

Mapping the Prion Protein Distribution in Marsupials: Insights from Comparing Opossum with Mouse CNS

Ilaria Poggiolini[1], **Giuseppe Legname**[1,2]*

1 Department of Neuroscience, Laboratory of Prion Biology, Scuola Internazionale Superiore di Studi Avanzati (SISSA), Trieste, Italy, **2** ELETTRA Laboratory, Sincrotrone Trieste S.C.p.A., Basovizza, Trieste, Italy

Abstract

The cellular form of the prion protein (PrP^C) is a sialoglycoprotein widely expressed in the central nervous system (CNS) of mammalian species during neurodevelopment and in adulthood. The location of the protein in the CNS may play a role in the susceptibility of a species to fatal prion diseases, which are also known as the transmissible spongiform encephalopathies (TSEs). To date, little is known about PrP^C distribution in marsupial mammals, for which no naturally occurring prion diseases have been reported. To extend our understanding of varying PrP^C expression profiles in different mammals we carried out a detailed expression analysis of PrP^C distribution along the neurodevelopment of the metatherian South American short-tailed opossum (*Monodelphis domestica*). We detected lower levels of PrP^C in white matter fiber bundles of opossum CNS compared to mouse CNS. This result is consistent with a possible role for PrP^C in the distinct neurodevelopment and neurocircuitry found in marsupials compared to other mammalian species.

Citation: Poggiolini I, Legname G (2012) Mapping the Prion Protein Distribution in Marsupials: Insights from Comparing Opossum with Mouse CNS. PLoS ONE 7(11): e50370. doi:10.1371/journal.pone.0050370

Editor: Anthony E. Kincaid, Creighton University, United States of America

Received June 19, 2012; **Accepted** October 18, 2012; **Published** November 29, 2012

Funding: The authors have no support or funding to report.

Competing Interests: The authors have declared that no competing interests exist.

* E-mail: legname@sissa.it

Introduction

The cellular form of the prion protein (PrP^C) is a cell-surface glycosylphosphatidylinositol-anchored glycopolypeptide abundantly expressed in the central nervous system (CNS), with expression levels varying among different cell types and brain regions [1]. The distribution pattern of PrP^C has already been investigated in deep detail in the CNS of several placental mammalian organisms, including mouse (Mo) [2–6], hamster [7], cattle [8], sheep [9] and primates [10,11]. Additional studies, along the same lines of research, have reported the pattern of PrP^C distribution also in avian [12] and fish [13]. The earliest expression of the protein in mammals has been observed in the hippocampus, thalamus and hypothalamus and the highest levels of PrP^C expression have been noted in specific white matter fiber tracts [6].

Structurally, mature PrP^C expressed by a wide variety of mammalian species shares a similar fold: while the N-terminus is largely unstructured, the C-terminus possesses well-defined secondary and tertiary structures [14,15]. The N-terminus features an evolutionarily conserved motif denoted as the octapeptide-repeat region (residues from 51 to 90 in Mo numbering, Figure 1). The octapeptide-repeat region is able to coordinate the binding of copper ions, thus implicating a possible role of PrP^C in copper homeostasis [16].

The sequence identity of PrP^C among mammals suggests an important physiological role [17]. However, the function of the protein has not been fully clarified, mostly due to the fact that PrP^C-null mice ($Prnp^{0/0}$) do not show remarkable phenotypic abnormalities [18,19]. Putative PrP^C functions are based on its localization. In particular, the highest expression of the protein in the hippocampus and, within this brain region, in the *stratum lacunosum-moleculare*, suggests a role for PrP^C in synaptic structure, function and maintenance [6]. Additionally, the large number of PrP^C-interacting molecules identified thus far [20] implies that PrP^C may be a dynamic cell surface platform for the assembly of signaling modules.

Defining the function of PrP^C is also a prerequisite for understanding TSEs, or prion diseases, as they are attributed to the posttranslational conversion of PrP^C into a misfolded, pathogenic form denoted prion or PrP^{Sc} [21]. This group of rare neurodegenerative maladies, affecting humans and animals alike, can be sporadic, genetic or iatrogenic. They include Creutzfeldt-Jakob disease (CJD), fatal familial insomnia and Gerstmann-Sträussler-Scheinker syndrome in humans, scrapie in sheep and goats, bovine spongiform encephalopathy in cattle, and chronic wasting disease in cervids.

A still controversial aspect in TSEs is the different ability of prions to infect some mammalian species and not others. So far no naturally occurring TSEs have been reported in rabbit, horse or any marsupial species. A possible explanation for this argues that the PrP^C primary sequence, together with local structural variations within the C-terminus globular domain, might account for prion resistance in different mammals [22]. However, little is known about the regional distribution of PrP^C in the CNS of mammalian species that seem resistant to TSEs. Differences in PrP^C expression in mammalian species, for which no naturally occurring TSEs occur, may shed light on different susceptibility to these maladies.

To gain insights into this neglected issue we analyzed PrP^C distribution along the neurodevelopment of the metatherian mammal South American short-tailed opossum (*Monodelphis domestica*) (hereafter Op). This animal model is used in develop-

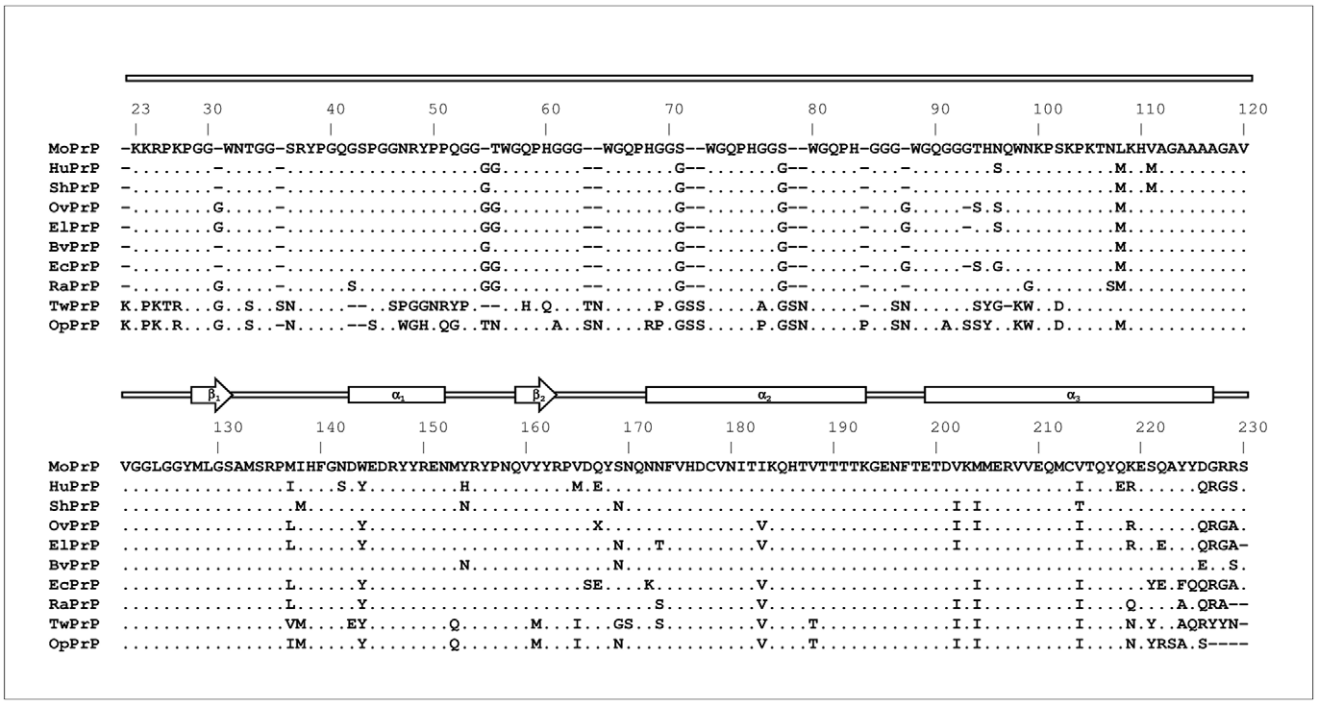

Figure 1. Comparison of amino acid sequences and secondary full-length prion protein structure of selected mammalian species: mouse (MoPrP; *Mus musculus*, GenBank accession number: AAA39997), human (HuPrP; *Homo sapiens*, AAA60182), Syrian hamster (ShPrP; *Mesocricetus auratus*, AAA37091), sheep (OvPrP; *Ovis aries*, ABC61639), elk (ElPrP; *Cervus elaphus nelsoni*, AAB94788), bank vole (BvPrP; *Clethrionomys glareolus*, AAL57231), horse (EcPrP; *Equus caballus*, ABL86003), rabbit (RaPrP; *Oryctolagus cuniculus*, AAD01554), tammar wallaby (TwPrP; *Macropus eugenii*, AAT68002) and opossum (OpPrP; *Monodelphis domestica*, CBY05848).
doi:10.1371/journal.pone.0050370.g001

mental studies mainly because of the rudimental stage of development of the newborn pups, which resemble 11- or 12-day Mo embryos [23,24]. In the newborn Op pup the CNS is still at an embryonic stage [23], because its development is completed during postnatal life.

The Op genome sequencing has provided an important tool for comparison with Eutherians, such as human and Mo, and has contributed to our knowledge about the evolution of Amniota [25,26]. Because of its evolutionary position between avian and eutherian genomes, Op represents an invaluable model for evolutionary comparison. Ultimately, its small size, ease of care and the non-seasonal breeding make Op a suitable laboratory animal model [27,28].

The assignment and characterization of Op prion protein (PrP) gene has revealed that OpPrP and MoPrP share approximately 70% sequence identity [29]. Sequence variations are most prominently localized on the N-terminus copper binding sites region: while MoPrP contains one nonapeptide, and four octarepeats of identical sequence, OpPrP features five different decarepeats, which are able to bind copper ions [30,31]. Additionally, the region from residue 91 to 110 (in MoPrP numbering), which also binds copper, is less conserved in OpPrP (Figure 1).

In this work, the expression profile of OpPrP was characterized at different postnatal developmental stages of Op CNS using Western blotting and histoblot techniques. To compare OpPrP and MoPrP distribution in CNS, we examined the expression of PrP^C in postnatal 30-day-old (P30) mice – which resemble young adult Op in the overall development – under the same experimental conditions.

The most striking difference between the two mammals concerned the lower PrP^C detection in the Op white matter structures. The different organization pattern observed might offer insights into the role of PrP^C in neurodevelopment and in neurocircuitry formation in Op and other mammals [32]. Ultimately, it might also expand our current knowledge of PrP^C function in mammals.

Materials and Methods

Animals

All experiments were carried out in accordance with European regulations [European Community Council Directive, November 24, 1986 (86/609/EEC)] and were approved by the local veterinary service authority. FVB wild-type, and FVB $Prnp^{0/0}$ mice [33] were used in these experiments. Animals were obtained from the colony maintained at the animal house facility of the University of Trieste, Italy. Animals were staged by systematic daily inspection of the colony for newborn litters. P0 corresponds to the day of birth [34]. Each experiment was performed at least in triplicate. Mice and Op pups were decapitated. Mice (at P30) and Op adults (at P45, P50, and P75) were killed by cervical dislocation. For histoblotting, brains were rapidly harvested, immediately covered in powdered dry ice and included in the embedding medium OCT (Optimal Cutting Temperature).

Histology

CNS specimens were fixed in 4% paraformaldehyde-PBS overnight at 4°C, cryoprotected in 30% sucrose/PBS and cut coronally at 20 μm. Cryosections were mounted on Fischer SuperFrost Plus slides and subsequently processed for histology.

Histoblots

The histoblot technique was performed according to the protocol described by Taraboulos et al. [35] with a few modifications. Briefly, uncoated microscope slides (Menzel-Glaser, Madison, WI) carrying 20 µm-thick brain serial coronal sections were pressed onto a nitrocellulose membrane wetted in lysis buffer (0.5% sodium deoxycholate, 0.5% Nonidet P-40, 100 mM NaCl, 10 mM EDTA, 10 mM Tris-HCl, pH 8.0), incubated for one hour at room temperature in 0.1 M NaOH and rinsed 3 times for 1 minute in TBST 1X (50 mM Tris-HCl, 150 mM NaCl, 0.1% Tween20, pH 7.4). Blots were blocked for 90 minutes in 5% non-fat dry milk-TBST 1X. They were incubated overnight at 4°C with the primary antibody anti-PrP^C humanized Fab D18 [36] purchased from InPro Biotechnology (South San Francisco, CA; ABR-0D18) and used at a final concentration of 1 µg/mL. This antibody shows high affinity for the region encompassing residues 133 to 152 (in Mo numbering), which is highly conserved in different mammals (Figure 1). Membranes were extensively washed in TBST 1X and incubated for one hour with secondary antibody diluted in blocking mix. The signal was achieved using SIGMAFAST^{TM} 3,3′-Diaminobenzidine tablets (Sigma) according to the protocols of the supplier. All data are representative of at least three independent experiments.

Nissl staining

Twenty-micrometer fixed frozen cryostat sections, mounted on slides, were air-dried for 60 minutes, stained in 0.1% cressyl violet (Sigma) at 40°C for 7 minutes and then rinsed in distilled water. Slides were soaked in 95% ethyl alcohol for 5 minutes and dehydrated in 100% alcohol for 5 minutes. Before mounting on glass slides (Sigma) with resin medium (Eukitt, Bio-Optica) slides were cleared twice in xylene for 5 minutes.

Western blotting analysis

Total brains or different brain regions were dissected using a stereomicroscope (Nikon SMZ 800) and immediately frozen in liquid nitrogen. Tissues were homogenized in RIPA buffer (150 mM NaCl, NP-40 1%, sodium deoxycholate 0.5%, SDS 0.1%, 50 mM Tris, pH 8.0) with Glass/Teflon Potter Elvehjem homogenizers and spun at 1000 g at 4°C for 5 minutes. The total protein amount was determined using the BCA Protein Assay Kit (Thermo Scientific Pierce). Fifty µg of total protein was then electrophoresed through 10%–SDS polyacrylamide gels and transferred to nitrocellulose membranes. Membranes were probed with monoclonal antibody Fab D18 and developed by enhanced chemiluminescence (Amersham ECL Western Blotting Systems, GE Healthcare). Band intensity was quantified using the UVI Soft software (UVITEC, Cambridge).

Results

PrP^C expression in the Op brain is developmentally regulated

PrP^C protein extracts from adult knockout PrP ($MoPrP^{-/-}$), wild-type PrP ($MoPrP^{+/+}$) mice and adult Op were compared using Western blotting (Figure 2A). The expected di- (~37 kDa), mono- (~30 kDa) and un- (~27 kDa) glycosylated forms were detected by Fab D18 monoclonal antibody both in $MoPrP^{+/+}$ and Op lanes. The absence of signal in the lane loaded with $MoPrP^{-/-}$ sample showed the specificity of the antibody. Although all the lanes were loaded with the same amount of total protein, the lower intensity of Op PrP signal compared to $MoPrP^{+/+}$ signal might be due to a lower affinity of the antibody for the Op PrP than for $MoPrP^{+/+}$. Alternatively, these results might indicate a lower PrP^C expression in adult Op than in Mo. Figure 2B shows the PrP^C pattern observed by immunoblotting from P1 to P45. A predominance of the diglycosylated form of the protein at ~37 kDa and of the monoglycosylated form of the protein at ~30 kDa was observed. A minor band corresponding to the non-glycosylated form of the protein was detected at ~27 kDa. This expression pattern resembles those observed in eutherian Syrian hamster (SHa) and Mo brains [37].

The PrP^C expression from P10 to P70 was also evaluated in the thalamus, olfactory bulbs, cortex and hippocampus (Figure 2C). In all these regions an increase in PrP^C expression was observed until P50. In adulthood the expression of PrP^C decreased slightly or remained at plateau. Like in SHa [7], a tendency to an increase in PrP^C signal was observed in the olfactory bulbs at P75.

Regional expression of PrP^C

Since PrP^C was not detected by immunofluorescence staining performed following well-established protocols described in the literature, we investigated the regional distribution of PrP^C in the Op brain at P15, P20, P37 and P70 by histoblot (see Materials and Methods) [35]. After the completion of cortico-cerebral neurogenesis [34], at P15 and at P20 strong PrP^C immunoreactivity was detected in the hippocampus, in the thalamus and in the neocortex. In the hippocampus, a signal was observed in the parenchyma, but not in the pyramidal layer of the Ammon's Horn (CA1-CA3) nor in the granule cell layer of the dentate gyrus (DG) (Figure 3A–B). At P37 (Figure 4A and B) a dense PrP^C signal was identified in gray matter structures such as thalamus, cortex and hippocampus. In the latter, PrP^C immunostaining was deep in the *stratum radiatum* and in the *stratum oriens*. As observed at P20, the signal was virtually absent in the pyramidal cells of the CA and in the granule cells of the DG. In the hilar region, immunoreactivity (IR) was minimal. IR was observed around the dorsal and the lateral parts of the thalamus (Figure 4A), encompassing structures involved in the communication between cortex and thalamus [38].

The PrP^C signal was also evaluated at P70, after the time of weaning [23]. A low IR was observed in white matter areas such as the internal and external capsules (Figure 5B). As observed at P37, in the P70 hippocampus the strongest IR was present in the *oriens* and *radiatum* strata. A less intense signal was detected in the *stratum lacunosum-moleculare* (Figure 5C). The expression pattern profile observed in adult Op hippocampus is similar to that in SHa [7].

PrP^C immunolocalization in Mo brain coronal sections

Histoblots of P30 $MoPrP^{+/+}$ brain coronal sections were immunostained to measure differences in PrP^C localization between Op and Mo (Figure 6A and B). The lack of IR in P30 $MoPrP^{-/-}$ coronal sections (Figure 6C and D) confirmed the specificity of the D18 signal. Ponceau staining was performed to ensure the presence of the section on the nitrocellulose membrane.

The pattern of PrP^C distribution in P30 $MoPrP^{+/+}$ was detected in many structures throughout the brain (Figure 6A and B). At P30 strong IR was found in the alveus, a thalamo-limbic structure of fornix fibers surrounding the *stratum oriens* that contains the axons of pyramidal neurons. As previously reported [6], a well-defined PrP^C signal was present in the *stratum lacunosum-moleculare* (Figure 6A). Strong labeling of the white matter fiber bundles was particularly evident at the level of the *corpus callosum* – the major interhemispheric fiber bundle in eutherians – and in the anterior commissure, also involved in interhemispheric communication [39]. Within the limbic system, a signal was detected in

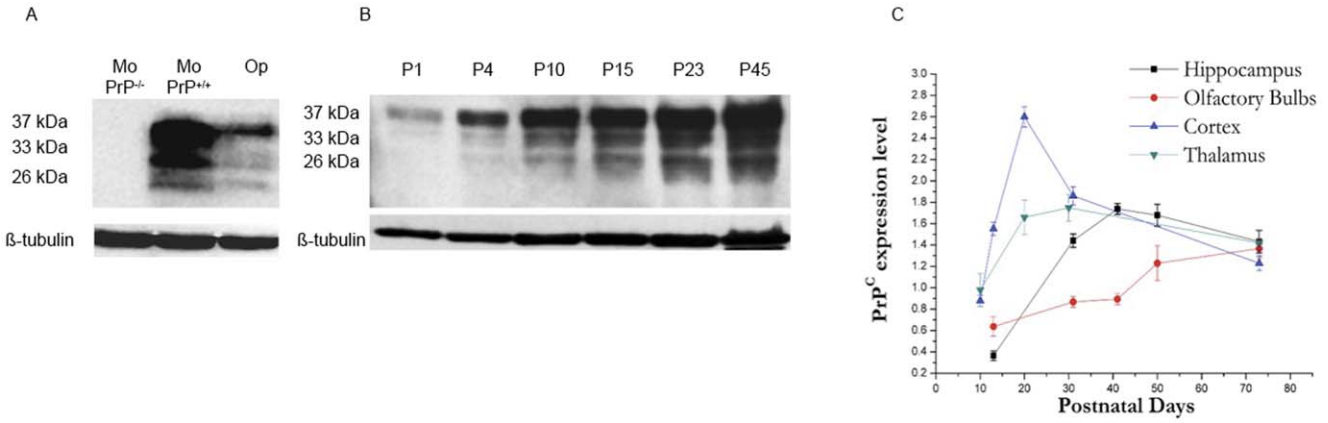

Figure 2. Confirmation of antibody specificity and developmental expression of PrP^C in opossum CNS. (A) Western blotting of Op, $MoPrP^{+/+}$ and $MoPrP^{-/-}$ whole brain homogenates confirmed the specificity of the PrP^C signal. The blot was then reprobed with β-tubulin antibody to demonstrate equal loading of samples (50 μg per lane). (B) Western blotting analysis of equal amounts of total brain homogenate (50 μg per lane) at different developmental stages showed a major electrophoretic band at 37 kDa, which corresponds to the diglycosylated form of the protein. β-tubulin was used as loading control. (C) Western blotting of indicated brain regions at different developmental stages showed a relevant change in PrP^C expression during postnatal development. Each data point represents the mean absorbance ±SEM of 3 females from different litters. All the absorbance values were normalized against β-actin.
doi:10.1371/journal.pone.0050370.g002

the hippocampal fimbria, in its continuation, the fornix and in the hippocampus. In the neocortex (NCx), staining was detected in a region adjacent to the ependymal layer.

Discussion

Over the last twenty years, the expression of PrP^C in the CNS of placental mammals, such as Mo and SHa, has been intensively investigated. Here we described a restricted PrP^C expression during Op brain development. Our data appear to corroborate current evidence of a developmentally regulated expression of PrP^C in all mammals. The direct comparison between Op and $MoPrP^C$ expression in CNS showed striking differences in distinct brain regions, such as white matter structures and hippocampus, thus suggesting possible functional implications for the role of PrP^C in marsupials.

Technical remarks about PrP^C detection in Op brain

The routine histological techniques might not be sensitive enough to map PrP^C expression in the Op brain. We tested different immunofluorescence protocols in combination with several monoclonal antibodies, but none of them appeared to work (data not shown). We speculated that these technical difficulties experienced with the traditional immunohistochemical staining techniques might be due to a weak antibody affinity for OpPrP, possibly ascribable to epitope masking as a result of a different membrane environment. Alternatively, PrP^C signal might be masked by another molecule, which could make the binding of the antibody to the antigene inaccessible.

To overcome these difficulties we decided to use the immunohistoblot technique described by Taraboulos et al. [35] to map the regional distribution of PrP^{Sc} in the brain of diseased

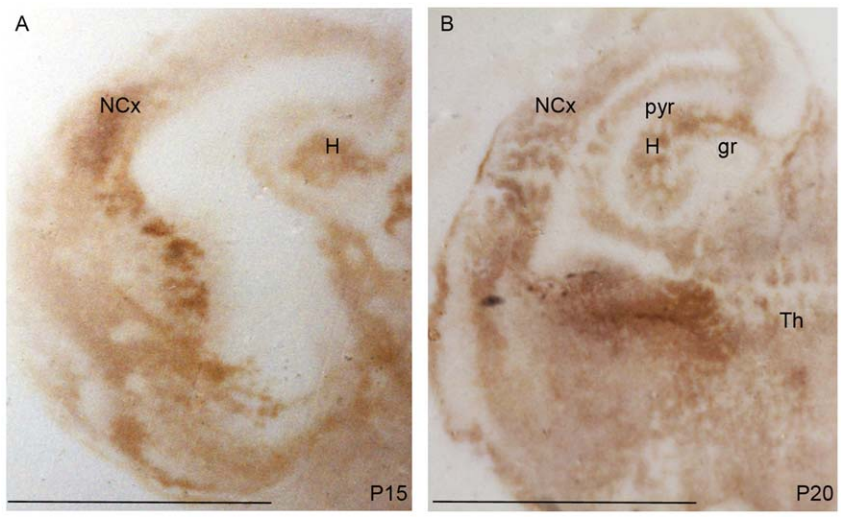

Figure 3. PrP^C expression in histoblots of P15 and P20 opossum brains. (A–B) In coronal sections of P15 and P20 a PrP^C signal was detected in the thalamus (Th), in the neocortex (NCx) and in the hippocampus (H). The pyramidal cell layer (pyr) and the granule cell layer (gr) of the hippocampus were not stained by PrP^C (Bars: A–B 4 mm).
doi:10.1371/journal.pone.0050370.g003

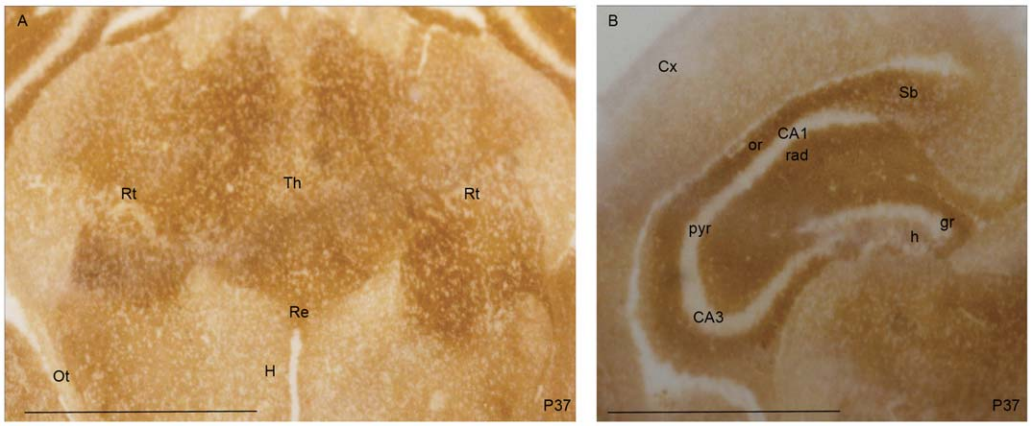

Figure 4. PrP^C distribution in a P37 opossum brain. (A–B) Coronal sections in the caudal diencephalon from a P37 opossum were stained for PrP^C in the thalamus (Th) and in the parenchyma of the hippocampus. (A) In the ventral thalamus, a strong IR was observed in the reticular nucleus (Rt) and in the nucleus reuniens (Re). No IR was observed in the optic tract (Ot). In the hypothalamic area (H) the immunoreactivity was lower than in the thalamus. (B) A strong PrP^C signal was observed in the *stratum oriens* (or) and in the *stratum radiatum* (rad) of the hippocampus. A low PrP^C immunoreactivity was observed in the hilar region (h), while the pyramidal (pyr) and granule (gr) cell layers of the CA1-CA3 and DG were devoid of immunostaining (Bars: 1 mm).
doi:10.1371/journal.pone.0050370.g004

SHa. The use of 0.1 M sodium hydroxide enhanced the binding of PrP antibodies [40] thus allowing for the detection of a clear PrP^C signal in the cryostat sections of the freshly frozen Op brain tissues in this study.

Comparison of PrP^C distribution between marsupials and placental mammals

Our results showed that from the day of birth (P1) up to adulthood (P75) PrP^C was detectable by Western blotting in whole brain homogenates (Figure 2B) with the strongest PrP^C signal in the uppermost diglycosylated band (~37 kDa) and the weakest signal in the lowest non-glycosylated PrP^C band (~26 kDa). A change in PrP^C relative abundance was observed during Op brain development, corroborating previous evidence of a developmentally regulated expression of PrP^C. In the different brain regions under consideration, PrP^C levels either remained at plateau or decreased slightly in adulthood (Figure 2C). Interestingly, after the time of weaning a tendency to an increase in PrP expression was observed in the olfactory bulbs. As postulated for placental mammals [7] this finding might be related to ongoing plasticity of the olfactory bulbs also in marsupials. However, no evidence is available yet to suggest that there is indeed plasticity in the olfactory bulbs of adult marsupials.

At P37 we observed a strong PrP^C immunoreactivity in the thalamus, a region which has a strong nonphotic influence on sleep and circadian rhythmicity [41]. This finding suggested an evolutionary conserved involvement of PrP^C in sleep homeostasis in the Op, in which a functioning circadian timing system exists [42–44].

Before weaning, PrP^C was detectable in the parenchyma of the hippocampus (Figure 3B). Interestingly, in different eutherian species, PrP^C preferentially localizes in specific hippocampal layers. In the adult Op (Figure 5C) and SHa [7] the strongest immunoreactive strata are the *oriens* and the *radiatum*, whereas MoPrP^C specifically localizes in the *stratum lacunosum-moleculare* (Figure 6A). These results seem to suggest a different regulatory role of PrP^C in the synaptic activity of different species. The lack of PrP^C in the nerve cell bodies was implied by the absence of signal

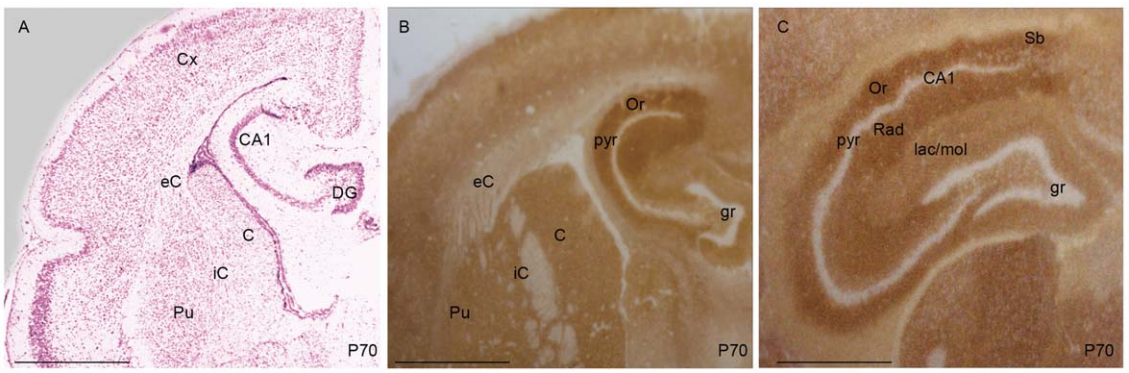

Figure 5. Coronal sections of opossum brain at P70 (A–C). In (A) the coronal section was Nissl-stained. In the adult opossum (B) a strong signal was predominantly present in the hippocampus. Marginal signal was also detected in the caudate nucleus (C), in the internal capsule (iC) and in the putamen (Pu). A very residual signal was observed in the external capsule (eC). In (C) the specific distribution of PrP^C in the different hippocampal layers was analyzed. Staining in the *lacunosum* and *moleculare* (lac/mol) was lower than in the *oriens* (Or) and the *radiatum* (Rad). PrP^C immunoreactivity was also observed in the *subiculum* (Sb) the main output of the hippocampus. (Bars: 0.5 mm).
doi:10.1371/journal.pone.0050370.g005

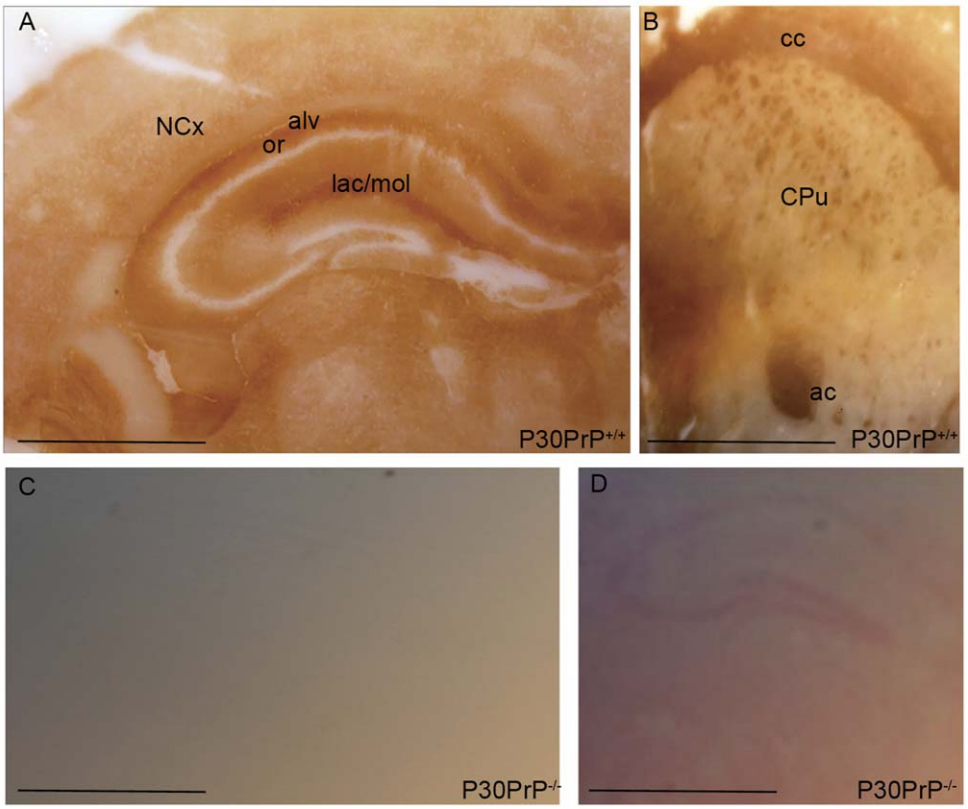

Figure 6. Localization of PrP^C in P30 $MoPrP^{+/+}$ brain and control of signal specificity. (A) At P30 a well-defined signal was present in the hippocampal *stratum lacunosum-moleculare* layer (lac/mol) and in the alveus (alv) lying just deep to the *stratum oriens* layer (or). (B) In the septum-caudatum, PrP^C signal was detected predominantly in white matter fiber bundles, such as the anterior commissure (ac) and the *corpus callosum* (cc). The dark dots observed in the caudate-putamen (CPu) are fiber fascicles cut on end. (C) At P30, the lack of IR in $MoPrP^{-/-}$ coronal section confirmed the signal specificity. (D) The presence of the brain section on the nitrocellulose membrane was confirmed by Ponceau staining. (Bars: A–D 0.5 mm).
doi:10.1371/journal.pone.0050370.g006

in the pyramidal cell layer and granule cell layer of the dentate gyrus in both Mo and Op.

The most striking difference observed between the two species was the different localization of PrP^C in the white matter. The lower PrP^C signal in Op white matter structures argues for a lower expression of the protein by glial cells and neuronal axons. In P30 mice instead, a strong PrP^C immunoreactive signal was detectable in the *corpus callosum*, a specific eutherian structure enriched in myelinated axons and involved in interhemispheric communication [45].

Implications for TSE pathology

The different ability of prions to infect certain species is apparently encoded by their structural features, which result in different physio-pathological outcomes [46]. Indeed some species may result resistant to prion infection. This strain-like behavior is known as the prion transmission barrier. However, under controlled laboratory conditions, prions are able to adapt and infect species previously believed to be TSE resistant, as was recently reported in rabbits infected by the murine ME7 prion strain using protein misfolding cyclic amplification (PMCA) techniques [47].

Structural studies on the recombinant PrP of mammals for which no TSEs have been reported in natural conditions [e.g. horse, rabbit and the marsupial Tammar wallaby (*Macropus eugenii*)], postulated that resistance to prions might be due to some structural features in the globular domain of those mammalian PrP sequences [48–50]. The OpPrP sequence presents an outstandingly large number of amino acid substitutions at the N-terminus in the copper binding sites and, within the C-terminus domain, in epitopes (residues 163–174 and 221–230 in Mo numbering, Figure 1) critical for prion conversion [22,51–54]. Based on this sequence identity analysis, it is possible to argue that these amino acidic differences might have an impact on the ability of OpPrP to sustain prion conversion. On the other hand, if structural differences in mammalian PrP are important for understanding the molecular mechanisms of TSEs, the neuronal distribution of PrP^C in mammalian species that are putatively resistant to prion diseases should be considered.

It is noteworthy that PrP^{Sc} accumulates in the white matter areas of Mo and SHa brains, thus suggesting that glial cells may be the primary targets for prions [35,55]. Indeed, the infectious agent has been shown to spread from the needle track along white matter pathways towards the gray matter [56]. This hypothesis is strengthened by pathological studies in human brains of terminal CJD patients showing axonal damage, hence suggesting a transport of prions through white matter pathways [57].

Although prion diseases have not been reported in the Op so far, the differential expression profile might account for a different susceptibility to prions in general or to diverse prion strains in particular, as well as for a different pattern of PrP^{Sc} accumulation and propagation between placentals and marsupials. To understand the biological and neurological significance of our observa-

tions, it would be of interest to attempt specific prion infectivity experiments in this mammalian model.

Acknowledgments

The authors thank Prof. A. Mallamaci and Prof. J. Nicholls for their critical observations and invaluable comments on this manuscript. The authors thankfully acknowledge Dr. G. Giachin for supplying precious information and suggestions. We acknowledge Dr. M. Righi for his technical assistance in brain dissections, Mr. A. Tomicich for the image acquisitions and Mr. S. Guarino for animal handling.

Author Contributions

Conceived and designed the experiments: IP GL. Performed the experiments: IP. Analyzed the data: IP GL. Contributed reagents/materials/analysis tools: GL. Wrote the paper: IP GL.

References

1. Linden R, Martins VR, Prado MA, Cammarota M, Izquierdo I, et al. (2008) Physiology of the prion protein. Physiol Rev 88: 673–728.
2. Manson J, West JD, Thomson V, McBride P, Kaufman MH, et al. (1992) The prion protein gene: a role in mouse embryogenesis? Development 115: 117–122.
3. Liu T, Zwingman T, Li R, Pan T, Wong BS, et al. (2001) Differential expression of cellular prion protein in mouse brain as detected with multiple anti-PrP monoclonal antibodies. Brain Res 896: 118–129.
4. Ford MJ, Burton LJ, Li H, Graham CH, Frobert Y, et al. (2002) A marked disparity between the expression of prion protein and its message by neurones of the CNS. Neuroscience 111: 533–551.
5. Bailly Y, Haeberle AM, Blanquet-Grossard F, Chasserot-Golaz S, Grant N, et al. (2004) Prion protein (PrPc) immunocytochemistry and expression of the green fluorescent protein reporter gene under control of the bovine PrP gene promoter in the mouse brain. J Comp Neurol 473: 244–269.
6. Benvegnu S, Poggiolini I, Legname G (2010) Neurodevelopmental expression and localization of the cellular prion protein in the central nervous system of the mouse. J Comp Neurol 518: 1879–1891.
7. Sales N, Hassig R, Rodolfo K, Di Giamberardino L, Traiffort E, et al. (2002) Developmental expression of the cellular prion protein in elongating axons. Eur J Neurosci 15: 1163–1177.
8. Velayos JL, Irujo A, Cuadrado-Tejedor M, Paternain B, Moleres FJ, et al. (2010) [Cellular prion protein in the central nervous system of mammals. Anatomo-clinical associations]. Neurologia 25: 228–233.
9. Thumdee P, Ponsuksili S, Murani E, Nganvongpanit K, Gehrig B, et al. (2007) Expression of the prion protein gene (PRNP) and cellular prion protein (PrPc) in cattle and sheep fetuses and maternal tissues during pregnancy. Gene Expr 13: 283–297.
10. Sales N, Rodolfo K, Hassig R, Faucheux B, Di Giamberardino L, et al. (1998) Cellular prion protein localization in rodent and primate brain. Eur J Neurosci 10: 2464–2471.
11. Laffont-Proust I, Fonta C, Renaud L, Hassig R, Moya KL (2007) Developmental changes in cellular prion protein in primate visual cortex. J Comp Neurol 504: 646–658.
12. Atoji Y, Ishiguro N (2009) Distribution of the cellular prion protein in the central nervous system of the chicken. J Chem Neuroanat 38: 292–301.
13. Malaga-Trillo E, Solis GP, Schrock Y, Geiss C, Luncz L, et al. (2009) Regulation of embryonic cell adhesion by the prion protein. PLoS Biol 7: e55.
14. Surewicz WK, Apostol MI (2011) Prion protein and its conformational conversion: a structural perspective. Top Curr Chem 305: 135–167.
15. Legname G, Giachin G, Benetti F (2012) Structural Studies of Prion Proteins and Prions. Non-fibrillar Amyloidogenic Protein Assemblies – Common Cytotoxins Underlying Degenerative Diseases. In: Rahimi F, Bitan G, editors: Springer Netherlands. 289–317.
16. Viles JH, Klewpatinond M, Nadal RC (2008) Copper and the structural biology of the prion protein. Biochem Soc Trans 36: 1288–1292.
17. Wopfner F, Weidenhofer G, Schneider R, von Brunn A, Gilch S, et al. (1999) Analysis of 27 mammalian and 9 avian PrPs reveals high conservation of flexible regions of the prion protein. J Mol Biol 289: 1163–1178.
18. Bueler H, Fischer M, Lang Y, Bluethmann H, Lipp HP, et al. (1992) Normal development and behaviour of mice lacking the neuronal cell-surface PrP protein. Nature 356: 577–582.
19. Manson JC, Clarke AR, Hooper ML, Aitchison L, McConnell I, et al. (1994) 129/Ola mice carrying a null mutation in PrP that abolishes mRNA production are developmentally normal. Mol Neurobiol 8: 121–127.
20. Aguzzi A, Baumann F, Bremer J (2008) The prion's elusive reason for being. Annu Rev Neurosci 31: 439–477.
21. Colby DW, Prusiner SB (2011) Prions. Cold Spring Harb Perspect Biol 3: a006833.
22. Sigurdson CJ, Nilsson KP, Hornemann S, Manco G, Fernandez-Borges N, et al. (2010) A molecular switch controls interspecies prion disease transmission in mice. J Clin Invest 120: 2590–2599.
23. Saunders NR, Adam E, Reader M, Mollgard K (1989) Monodelphis domestica (grey short-tailed opossum): an accessible model for studies of early neocortical development. Anat Embryol (Berl) 180: 227–236.
24. Smith KK (2001) Early development of the neural plate, neural crest and facial region of marsupials. J Anat 199: 121–131.
25. Gentles AJ, Wakefield MJ, Kohany O, Gu W, Batzer MA, et al. (2007) Evolutionary dynamics of transposable elements in the short-tailed opossum Monodelphis domestica. Genome Res 17: 992–1004.
26. Samollow PB (2008) The opossum genome: insights and opportunities from an alternative mammal. Genome Res 18: 1199–1215.
27. Keyte AL, Smith KK (2008) Basic Maintenance and Breeding of the Opossum Monodelphis domestica. CSH Protoc 2008: pdb prot5073.
28. Keyte AL, Smith KK (2008) Opossum (Monodelphis domestica): A Marsupial Development Model. CSH Protoc 2008: pdb emo104.
29. Premzl M, Delbridge M, Gready JE, Wilson P, Johnson M, et al. (2005) The prion protein gene: identifying regulatory signals using marsupial sequence. Gene 349: 121–134.
30. Gustiananda M, Haris PI, Milburn PJ, Gready JE (2002) Copper-induced conformational change in a marsupial prion protein repeat peptide probed using FTIR spectroscopy. FEBS Lett 512: 38–42.
31. Vagliasindi LI, Arena G, Bonomo RP, Pappalardo G, Tabbi G (2011) Copper complex species within a fragment of the N-terminal repeat region in opossum PrP protein. Dalton Trans 40: 2441–2450.
32. Karlen SJ, Krubitzer L (2006) Phenotypic diversity is the cornerstone of evolution: variation in cortical field size within short-tailed opossums. J Comp Neurol 499: 990–999.
33. Lledo PM, Tremblay P, DeArmond SJ, Prusiner SB, Nicoll RA (1996) Mice deficient for prion protein exhibit normal neuronal excitability and synaptic transmission in the hippocampus. Proc Natl Acad Sci U S A 93: 2403–2407.
34. Puzzolo E, Mallamaci A (2010) Cortico-cerebral histogenesis in the opossum Monodelphis domestica: generation of a hexalaminar neocortex in the absence of a basal proliferative compartment. Neural Dev 5: 8.
35. Taraboulos A, Jendroska K, Serban D, Yang SL, DeArmond SJ, et al. (1992) Regional mapping of prion proteins in brain. Proc Natl Acad Sci U S A 89: 7620–7624.
36. Peretz D, Williamson RA, Kaneko K, Vergara J, Leclerc E, et al. (2001) Antibodies inhibit prion propagation and clear cell cultures of prion infectivity. Nature 412: 739–743.
37. Russelakis-Carneiro M, Saborio GP, Anderes L, Soto C (2002) Changes in the glycosylation pattern of prion protein in murine scrapie. Implications for the mechanism of neurodegeneration in prion diseases. J Biol Chem 277: 36872–36877.
38. Guillery RW, Harting JK (2003) Structure and connections of the thalamic reticular nucleus: Advancing views over half a century. J Comp Neurol 463: 360–371.
39. Mihrshahi R (2006) The corpus callosum as an evolutionary innovation. J Exp Zool B Mol Dev Evol 306: 8–17.
40. Prusiner SB, DeArmond SJ (1994) Prion diseases and neurodegeneration. Annu Rev Neurosci 17: 311–339.
41. Jan JE, Reiter RJ, Wasdell MB, Bax M (2009) The role of the thalamus in sleep, pineal melatonin production, and circadian rhythm sleep disorders. J Pineal Res 46: 1–7.
42. Gambetti P, Parchi P, Petersen RB, Chen SG, Lugaresi E (1995) Fatal familial insomnia and familial Creutzfeldt-Jakob disease: clinical, pathological and molecular features. Brain Pathol 5: 43–51.
43. Montagna P, Cortelli P, Gambetti P, Lugaresi E (1995) Fatal familial insomnia: sleep, neuroendocrine and vegetative alterations. Adv Neuroimmunol 5: 13–21.
44. Rivkees SA, Fox CA, Jacobson CD, Reppert SM (1988) Anatomic and functional development of the suprachiasmatic nuclei in the gray short-tailed opossum. J Neurosci 8: 4269–4276.
45. Filley CM (2010) White matter: organization and functional relevance. Neuropsychol Rev 20: 158–173.
46. Legname G, Nguyen HOB, Baskakov IV, Cohen FE, DeArmond SJ, et al. (2005) Strain-specified characteristics of mouse synthetic prions. Proceedings of the National Academy of Sciences of the United States of America 102: 2168–2173.
47. Chianini F, Fernandez-Borges N, Vidal E, Gibbard L, Pintado B, et al. (2012) Rabbits are not resistant to prion infection. Proc Natl Acad Sci U S A 109: 5080–5085.
48. Wen Y, Li J, Yao W, Xiong M, Hong J, et al. (2010) Unique structural characteristics of the rabbit prion protein. J Biol Chem 285: 31682–31693.
49. Christen B, Hornemann S, Damberger FF, Wuthrich K (2009) Prion protein NMR structure from tammar wallaby (Macropus eugenii) shows that the beta2-alpha2 loop is modulated by long-range sequence effects. J Mol Biol 389: 833–845.
50. Perez DR, Damberger FF, Wuthrich K (2010) Horse prion protein NMR structure and comparisons with related variants of the mouse prion protein. J Mol Biol 400: 121–128.

51. Kaneko K, Zulianello L, Scott M, Cooper CM, Wallace AC, et al. (1997) Evidence for protein X binding to a discontinuous epitope on the cellular prion protein during scrapie prion propagation. Proc Natl Acad Sci U S A 94: 10069–10074.
52. Ilc G, Giachin G, Jaremko M, Jaremko L, Benetti F, et al. (2010) NMR structure of the human prion protein with the pathological Q212P mutation reveals unique structural features. PLoS One 5: e11715.
53. Biljan I, Ilc G, Giachin G, Raspadori A, Zhukov I, et al. (2011) Toward the molecular basis of inherited prion diseases: NMR structure of the human prion protein with V210I mutation. J Mol Biol 412: 660–673.
54. Rossetti G, Giachin G, Legname G, Carloni P (2010) Structural facets of disease-linked human prion protein mutants: a molecular dynamic study. Proteins 78: 3270–3280.
55. Moser M, Colello RJ, Pott U, Oesch B (1995) Developmental expression of the prion protein gene in glial cells. Neuron 14: 509–517.
56. Kordek R, Hainfellner JA, Liberski PP, Budka H (1999) Deposition of the prion protein (PrP) during the evolution of experimental Creutzfeldt-Jakob disease. Acta Neuropathol 98: 597–602.
57. Lee H, Cohen OS, Rosenmann H, Hoffmann C, Kingsley PB, et al. (2012) Cerebral White Matter Disruption in Creutzfeldt-Jakob Disease. AJNR Am J Neuroradiol.